Titre: Title:	Numerical solution of thermo-convective problems using spline integration
Auteur: Author:	Pu Wang
Date:	1991
Type:	Mémoire ou thèse / Dissertation or Thesis
Référence: Citation:	Wang, P. (1991). Numerical solution of thermo-convective problems using spline integration [Thèse de doctorat, Polytechnique Montréal]. PolyPublie. https://publications.polymtl.ca/57969/

Document en libre accès dans PolyPublie
Open Access document in PolyPublie

URL de PolyPublie: PolyPublie URL:	https://publications.polymtl.ca/57969/
Directeurs de recherche: Advisors:	
Programme: Program:	Non spécifié

UNIVERSITE DE MONTREAL

NUMERICAL SOLUTION OF THERMO-CONVECTIVE

PROBLEMS USING SPLINE INTEGRATION

par

Pu WANG

DEPARTEMENT DE GENIE CIVIL

ECOLE POLYTECHNIQUE

THESE PRESENTEE EN VUE DE L'OBTENTION

DU GRADE DE PHILOSOPHIAE DOCTOR (Ph.D.)

Juillet, 1991

UNIVERSITE DE MONTREAL

ECOLE POLYTECHNIQUE

Cette thèse intitulée:

NUMERICAL SOLUTION OF THERMO-CONVECTIVE

PROBLEMS USING SPLINE INTEGRATION

présentée par: Pu WANG

en vue de l'obtention du grade de: Philosophiae Doctor (Ph.D.)

a été dûment acceptée par le jury d'examen constitué de:

M.   T. Hung Nguyen   Ph.D., président

M.   R. Kahawita   Ph.D. direcdeur de recherche

M.   D. Long Nguyen   D.Sc. co-directeur

M.   P. Oosthuizen   Ph.D. membre

M.   M. Prud'homme   Ph.D. membre

SOMMAIRE

Cette thèse est consacrée aux études numériques de la convection naturelle laminaire autour d'un cylindre horizontal soumis à diverses conditions aux limites en utilisant une méthode de splines au pas fractionnaire proposée par l'auteur en 1987.

Le contenu de cette thèse consiste en trois articles publiés dans des revues spécialisées avec comité de lecture, soit:

(i) *Numerical Computation of the Natural Convection Flow about a Horizontal Cylinder using Splines*, **Numerical Heat Transfer**, Vol. 17, Part A, pp.191–215 (1990).

(ii) *Transient Laminar Natural Convection from Horizontal Cylinder*, **Int. J. Heat and Mass Transfer**, Vol. 34 ,pp.1429–1442 (1991).

(iii) *Transient Natural Convection with Density Inversion from a Horizontal Cylinder*, à paraître dans **Physics of Fluids A.**

Ces trois articles sont présentés dans les Chapitres II, III et IV, respectivement.

La méthode des splines est résumée dans la Chapitre I. Cette méthode constitue un sujet relativement nouveau dans le domaine des méthodes numériques. La recherche mathématique et les applications de cette technique à la résolution des équations aux dérivées partielles ont été développées seulement pendant la dernière décennie. Bien qu'elle ne soit pas aussi développée que la méthode

des différences finies et la méthode des élements finis, beaucoup de travaux de recherche sur la théorie fondamentale et la méthodologie ont démontré que cette technique, qui devient de plus en plus sophistiquée, peut atteindre une précision comparable à celle de la méthode des différences finies, tout en utilisant un plus grand maillage.

Cette technique a été appliquée dans les domaines de la mécanique des fluides, du transfert de chaleur et de l'hydraulique.

Les contributions principales de l'auteur au dévelopement de cette technique sont résumées dans le Chapitre I où est également présentée une revue du phénomène de convection naturelle autour d'un cylindre horizontal.

Le premier article (Chapitre II), comporte une étude numérique exhaustive de la convection naturelle laminaire autour d'un cylindre chaud avec trois conditions typiques à la surface du cylindre. Les solutions ont été obtenues à partir des équations de l'énergie et de Navier-Stokes, en se basant sur une formulation générale pour traiter des conditions aux limites à l'aide de splines cubiques. Cette formulation peut être facilement incorporée dans la procédure de calcul. Les résultats obtenus pour des valeurs élevées du nombre de Rayleigh indiquent l'existence de tourbillons secondaires dans la région du panache. L'apparition de ces tourbillons dépend cependant de la valeur du nombre de Biot.

L' étude de la convection naturelle laminaire transitoire autour d'un cylindre chaud soumis à diverses conditions aux limites est présentée dans le deuxième article (Chapitre III).

Quelques caractéristiques de la couche limite, obtenues par analyse dimensionnelle, sont comparées aux résultats numériques. On étudie le développement de la région du panache aussi bien que la champ local de l'écoulement et le transfert thermique à la surface du cylindre. Pour des temps courts, les solutions numériques s'approchent des résultats obtenus à partir de la théorie de la couche limite et elles sont en bon accord avec les résultats de l'analyse dimensionnelle. On fait une étude detaillée du développement de la région du panache en déterminant les trajectoires des particules. On constate le phénomène de saut et des variations périodiques du nombre de Nusselt local avant qu'il se stabilise en régime permanent. Ce phénomène est dû à l'inertie du fluide. A nombres de Rayleigh élevés (Ra $> 5 \times 10^7$), on observe l'apparition et la disparition répétées de tourbillons secondaires.

Le troisième article (Chapitre IV) est consacré à l'étude de la convection naturelle autour d'un cylindre horizontal maintenu à 0°C et immergé dans de l'eau à une température près du point de densité maximum. Le comportement transitoire de la convection naturelle près du point de densité maximum, la stabilité de l'écoulement et l'apparition des mouvements oscillatoires sont des sujets qui sont encore mal connus et font précisément l'objet de cet article. Les solutions numériques ont été obtenues en régime transitoire aussi bien qu'en régime permanent. Les résultats indiquent que le fait d'avoir de l'eau près de son point de densité maximum a une très forte influence sur le comportement de l'écoulement. Quand la température ambiante est dans la région de $4.7°C < T_{amb} < 8°C$, l'écoulement autour du cylindre consiste en un mouvement ascendant et en un mouvement descendant. Ces zones de recirculation

sont généralement séparées par l'isotherme de 4°C quand $T_{amb} < 5.7$°C. Le comportement de ce régime double dépend fortement de la température ambiante et disparaît lorsque la température ambiante est au-dessus de 8°C ou au-dessous de 4.7°C. D'ailleurs, quand la température ambiante est dans la région de 4.8°C $< T_{amb} < 5.5$°C, le régime permanent ne peut être atteint et l'on peut obtenir seulement des solutions quasi-périodiques. Les solutions multiples ont été aussi observées lorsqu'on s'approche de cette région soit d'une température $T_{amb} < 4.8$°C, ou d'une température $T_{amb} > 5.5$°C.

ABSTRACT

This thesis is devoted to numerical studies of the laminar natural convection flow around a heated horizontal cylinder under diverse surface boundary conditions using a newly developed spline fractional step technique proposed by the author in 1987.

The key contents of this thesis consists of three papers published or that have been accepted for publication in peer-reviewed journals. They are:

(i) *Numerical Computation of the Natural Convection Flow about a Horizontal Cylinder using Splines*, Numerical Heat Transfer Vol. 17, Part A, pp.191–215.(1990)

(ii) *Transient Laminar Natural Convection from Horizontal Cylinder*, Int. J. Heat and Mass Transfer, Vol. 34 ,pp.1429–1442.(1991)

(iii) *Transient Natural Convection with Density Inversion from a Horizontal Cylinder*, (to be published in *Physics of Fluids* A).

These three papers form the contents of Chapters II, II and IV respectively.

The spline technique and its developments are briefly reviewed in Chapter I. This method constitutes a relatively new subject in the field of numerical methods. The mathematical research and applications of this technique to the numerical solution of partial differential equations have only developed during the past decade. Although it is not as developed as finite difference methods and

finite element methods, some breakthroughs have been achieved. With recent developments, it may be said that the technique, as an independent numerical method, has increased in sophistication due to attention from researchers around the world. Numerical experiments have indicated that the spline approximation can achieve an accuracy comparable to that of corresponding finite-difference methods using fewer grid points. The calculation methodology has been gradually systematised and formulated resulting in successful applications in the fields of fluid mechanics, heat transfer, hydraulics and so on.

The author's principal contributions to this technique have been summarized in Chapter I of the thesis which also contains a review of natural convection phenomena around heated horizontal cylinders.

In the first paper (Chapter II), an extensive numerical study of the laminar natural convection flow from a heated horizontal cylinder with three type surface boundary conditions has been reported. Solutions have been obtained by solving complete Navier-Stokes and energy equations. A general formulation to treat mixed boundary conditions using cubic splines has been presented. This formulation is easily incorporated into the solution procedure. Some new computations at very high Rayleigh numbers, indicate the existence of attached "separation" vortices in the downstream plume region, the appearance of these vortices being dependent on the values of the Biot number.

The study of the transient natural convection from a circular, horizontal cylinder has been presented in the second paper (Chapter III). Some characteristics of the boundary layer obtained with a scale analysis have been compared

with the numerical results. The development of the plume region as well as the surface heat transfer and local flowfield have been evaluated. At small times, the present numerical solutions approach the boundary layer results and are in good agreement with the results from the scale analysis. A more detailed study of the development of the plume region, using computed particle trajectories has been reported. Overshoot and oscillatory behaviour of the local Nusselt numbers have been observed which decay as the steady state is approached. This has been associated with fluid inertia effects. At high Rayleigh numbers, the appearance of separation vortices, which are subsequently formed, shed and reformed when $Ra > 5 \times 10^7$, has been noted.

The third paper (Chapter IV) is devoted to a numerical investigation of the free convection flow about a horizontal cylinder maintained at 0°C in a water ambient close to the point of maximum density. The transient behaviour of natural convection of water near the maximum density point from a horizontal ice cylinder has not been extensively treated and the existence of an unstable aspect to the convection, or the presence of oscillatory solutions when the physical parameters lie within a certain range of values has not been widely reported in the literature. This paper is therefore devoted to the numerical simulation of the transient laminar natural convection. Complete numerical solutions covering both the transient as well as steady state have been obtained. Principal results indicate that the proximity of the ambient temperature to the point of maximum density plays an important role in the type of convection pattern that may be obtained. When the ambient temperature is within $4.7°C < T_{amb} < 8°C$, a "dual flow" appears around the cylinder with both upward and downward flow

occurring in proximity to the cylinder in two distinct recirculating zones, generally separated by the 4°C isotherm when $T_{amb} < 5.7$°C. The dual flow behaviour is significantly modified as the ambient temperature is altered, disappearing when the ambient temperature is above 8°C, or below 4.7°C. Furthermore, when the ambient temperature is within about 4.8°C $< T_{amb} < 5.5$°C, a well defined steady state is never attained. Within this same range, solutions with an initially quasi-periodic behaviour which persist for a long time have been observed. Multiple solutions have been observed when the above range of ambient temperatures is approached from either side.

Note: *A formal attestation to the fact that the candidate was the principal contributor to the work described in the following articles is annexed to the end of this thesis. It is signed by all the co-authors.*

ACKNOWLEDGEMENT

The author was as a visiting scholar from China at the Ecole Polytechnique de Montreal from 1980 to 1983. His principal contributions to the spline method used in the present projet were performed during this period with the great help and collaporation of Professor René Kahawita. A report entitled *"Numerical Solution of Second Order Partial Differential Equations using a Cubic Spline Approximation"* was submitted to an examination commitee on 25th July 1983 (see Appendix). Since he was not registered as a student at the Ecole Polytechnique it was unfortunately not possible for him to be officially awarded the Ph.D degree. Fortunately, after five years of reseach at the Univorsity of Lanzhou, Gansu, People's Republic of China, the author was able to return to the Ecole Polytechnique as a visiting fellow in October 1988.

The author wishes to express his great gratitude to his advisor and also his good friend, Prof. René Kahawita of the Civil Engineering Department, for his kindness, wise guidance, encouragement and continuous support since 1980, from the beginning of his study of the cubic spline technique to the present form of this project. He has given the author numerous valuable suggestions during the course of frequent discussions. This work would not have been possible without his active help, support and encouragement.

Thanks are also due to Dr. D. L. Nguyen of the Civil Engineering Department and Hydro-Québec, the author's co-advisor, for his continuous encourage-

ment and support in many ways.

The author wishes to thank Mr. W. Paskievici, the previous director of the Direction des études supérieures et de la recherche de Ecole Polytechnique for his attention and support.

In addition, the author would also like to acknowledge the help from his friends and members of the personnel of Ecole Polytechnique. The arduous labour of Mr. Gaston Patenaude who realized the many figures that appear in this thesis is gratefully acknowledged.

Finally, the author owes a debt of gratitude to the Québec Ministry, the Department of Civil Engineering, the Hydraulics Section and the administration of the Ecole Polytechnique de Montréal and to University of Lanzhou of the People's Republic of China and the Natural Sciences and Engineering Research Council of Canada for financial support during his studies at the Ecole Polytechnique de Montreal.

CONTENTS

CHAPTER I   INTRODUCTION

CHAPTER II

Numerical Computation of the Natural Convection

about a Horizontal Cylinder using Splines

CHAPTER III

Transient Laminar Natural Convection from

Horizontal Cylinders

CHAPTER I   INTRODUCTION

1.1   Review of Natural Convection from Horizontal Cylinders

Natural convection heat transfer has a number of important engineering applications. Natural convection about a single horizontal cylinder of uniform temperature suspended in an infinite fluid medium has been studied both experimentally and analytically for several decades. The vertical flat-plate boundary layer solutions given by Ostrach [1953], Merk and Prins [1953,1954] obtained a similarity solution valid near the stagnation point and presented an integral solution. Another integral solution was provided by Levy [1955]. Two-dimensional laminar natural convection from horizontal cylinders under steady state conditions has been extensively investigated experimentally and numerically (Schorr and Gebhart [1970], Aihara and Saito [1972], Kuehn and Goldstein [1976] , Fand *et al.*[1977] and Shee and Singh [1982]). The principal results indicate that at small Rayleigh numbers , the cylinder behaves as a line source, with the uniform surface heat flux condition approaching that of the isothermal one.

For fairly high Rayleigh numbers, the laminar flow generated by the body forces behaves as a boundary layer wrapped around the cylinder. It is not surprising therefore, that the boundary layer approximation has been frequently used to analyse these problems. This approximation assumes that curvature effects and any pressure differences across the boundary layer are negligible. The simplified

set of equations are then solved using a variety of techniques. In general, these studies concern the nature of the portions of such flows attached to the surface. The subsequent regions where the flow may separate from the surface and rise as a buoyant plume have not been considered in detail. One of the earliest works in this area was by Hermann [1954] who obtained a solution for the differential equations under the assumption of a thin (as compared with the cylinder diameter) heated laminar layer for diatomic gases and a small temperature difference. Merk and Prins [1953-1954] presented analytical results of the heat transfer around horizontal cylinders and spheres. Using a Blasius expansion method Chiang et al.[1962,1964] predicted the heat transfer coefficients for laminar , natural convection from horizontal cylinders and spheres. Lin and Chao [1974] used a Merk type of series to obtain solutions for various two-dimensional and axisymmetric geometries with the horizontal circular cylinder as a special case. Integrations incorporating curvature effects have been made by Akagi [1965], Peterka and Richardson [1969] and Gupta and Pop [1977].

Numerical solution of the boundary layer equations for natural convection around horizontal cylinders have been reported by Mucoglu and Chen [1977], Morgan [1975], Merkin [1976,1977] and Fujii *et al.*[1979]. The results thus obtained may be taken to represent the limiting case of Rayleigh number tending to infinity for laminar flow. The plume region is of course excluded, since the development of the plume formed by separation of the boundary layer from the surface invalidates the basic assumptions. Furthermore, these results do not adequately describe the flow and heat transfer at low or moderate values of Rayleigh number nor the development of the buoyant plume which, as has just been mentioned, cannot be obtained from the boundary layer approximation.

The complete Navier-Stokes and energy equations for laminar natural convection about a horizontal isothermal circular cylinder has been solved numerically by Holster and Hale [1979] usinga finite element approach and by Kuehn and Goldstein [1980] using a finite-difference technique. In the latter, the numerical solutions are in good agreement with their experimental data . Farouk and Guceri [1981] have treated the same problem for uniform as well as nonuniform temperature and heat flux distributions on the cylinder surface. The solution for the special case of an isothermal cylinder are compared with available data in literature to verify the accuracy of the approach. Recently, Qureshi and Ahmad [1987] have provided numerical solutions using a similar technique to that indicated by Kuehn and Goldstein [1980] for a horizontal cylinder with uniform heat flux at modified Rayleigh numbers. Most recently, the author with Kahawita and Nguyen 1990] has reported on an extensive numerical study of the laminar natural convection flow from a heated horizontal cylinder with three type of surface boundary conditions using a newly developed spline fractional step technique proposed by Wang [1987a] and presented a general formulation for treating mixed boundary conditions. This paper is the first paper presented in this thesis and constitutes Chapter II.

The literature on transient free convection studies is much less abundant. The great majority of studies reported earlier in the literature on the onset of convection are concerned with a quiescent fluid layer, heated from below(or cooled from above) in the presence of a gravitational field. Experimental and theoretical studies have then been carried out in an attempt to elaborate upon the onset of convection in a horizontal layer which has a time-dependent temperature profile (see for example Foster [1965,1968,1969], Nielsen *et al.*[1973] and Genceli

[1974]). Indeed, these kinds of investigations have a wide range of applications in technology, oceanography and geophysics.

The time-dependent onset of convection has also been studied by many researchers for other geometries. Transient heating comprising a step change in uniform wall temperature was examined inside short vertical and horizontal cylinders by Evans and Stefany [1965]. Cheng and Takeuchi [1976] studied this problem within a horizontal cylinder subjected to a change in wall temperature by heating or cooling, both experimentally and theoretically.

However, general unsteady natural convection around a horizontal cylinder has not been extensively treated. A perusal of the current literature on the subject indicates that very few studies have been realized in which an attempt is made to define the typical characteristics of the problem. An experimental study by Ostroumov [1956] reported on the development of the convection regime initiated by a suddenly heated fine wire. West and Lawson [1972] also reported on a similar experiment. Parsons and Mulligan [1978,1980] presented experimental data for the transient free convective heat transfer from a horizontal wire in air. Typically, an initially pure conduction situation is followed by a convective transition regime in which leading edge effects become dominant. Finally, a transient approach to a steady state occurs. An early analytical study, using the boundary layer approximation and series continuation for small time was established by Eliott [1970] and then by Katagiri [1977]. Sako et al.[1982] presented numerical solutions of transient natural convection from a horizontal cylinder at low Rayleigh numbers using a hybrid grid. Their results for the mean Nusselt numbers at steady state agree fairly well with those of Kuehn and Goldstein [1980]. An excellent laboratory experiment providing valuable quantitative data

on the onset of convection in water was reported by Genceli [1980] (He used a horizontal cylinder subjected to a constant surface heat flux). In his paper a critical Rayleigh number which defines the onset of convection was presented. Most recently, Song [1989] reported some numerical results of transient natural convection around a horizontal wire under a constant heat flux using a finite difference method. His study however was carried out only at low Rayleigh numbers . Furthermore, a physically unrealistic boundary condition imposed at the outer limit (i.e. $T = 0$ at infinity) of his computational domain would probably lead to numerical difficulties at high Rayleigh number computations.

Transient solutions of the complete Navier-Stokes and energy equations for high Rayleigh numbers have not yet been reported. A recently investigation has been performed by Wang, Kahawita and Nguyen [1991]. Good agreement with published experimental and numerical data has been obtained. An overshoot and oscillatory behaviour in the local Nusselt numbers associated with fluid inertia effects, has been observed which dies off as the steady state is approached. At high Rayleigh numbers, the appearance of separation vortices, which are subsequently formed, shed and reformed when $Ra > 5 \times 10^7$, has been noted. This article is presented in this thesis and constitutes Chapter III.

The third paper presented in this thesis is devoted to a numerical investigation of the free convection flow about a horizontal cylinder maintained at $0°C$ in a water ambient close to the point of maximum density. Many natural phenomena involve buoyancy induced flows of cold water, i.e. water that is close to its freezing point. The mechanism of such flows is considerably complicated by the fact that its density reaches a maximum value at $3.98°C$. This gives rise to a variety of interesting phenomena. To describe the nonlinear variation of density with

temperature for water in the range of 0 to 20°C , different degree polynomials have been given by Vanier and Tien [1968], by Fujii [1974] and by Gebhart and Mollendorf [1977]. An early experiment on the melting of ice was performed by Dumoré, Merck and Prins [1953]. They submerged a sphere of ice in cold water and observed for the first time that the water in the boundary layer flowed in opposite directions on either side of the isotherm corresponding to the inversion temperature (4.8°C). Since the pioneering works of Ede [1951], Dumoré *et al.* [1953] and Merk [1954] , the behaviour of natural convection in cold water has been studied by many investigators for several different geometries and boundary conditions. For instance, Schechter and Isbin [1958] have published experimental and theoretical work on thermal free convection from a heated vertical plate in cold water. Schenk and Schenkels [1968] have reported experimental results for thermal free convection from an ice sphere.

Bendell and Gebhart [1976] carried out experiments with vertical melting ice sheets in pure ambient water near its density extremum. A minimum Nusselt number was found to occur at $T_{amb} = 5.6°C$ while a net upflow and downflow were deduced from fluid temperature measurements when $T_{amb} > 5.6°C$ and $T_{amb} < 5.6°C$ respectively. The existence of a gap in the solutions for vertical boundary-layer flows was first reported by Gebhart and Mollendorf [1978] who used the boundary layer equations coupled with a numerical shooting method. They found that numerical solutions were unobtainable in the range $4.0°C < T_{amb} < 6.8°C$. Carey, Gebhart and Mollendorf [1980], after refining the numerical method used by Gebhart and Mollendorf [1978], found that the flow was bidirectional for T_{amb} between 4.75°C and 5.98°C and that convective inversion occurred at some T_{amb} between 4.75°C and 5.81°C. Solutions could not be ob-

tained within this range of temperatures in pure water. Wilson and Vyas [1979], conducted experiments on the velocity profiles near a vertical ice surface melting into fresh water for $2°C \leq T_{amb} \leq 7°C$. The results indicated an upward steady-state motion when the water temperature was below $4.7°C$ and a downward movement when the water temperature exceeded $7°C$. For intermediate temperatures, an oscillatory bidirectional flow was observed. The calculations of Wilson and Lee [1981] also indicated that three distinct flow regimes: steady upward flow for $T_{amb} \leq 4.5°C$, steady downward flow for $T_{amb} \geq 6.0°C$ and steady dual flow or bidirectional flow for $5.7°C \leq T_{amb} \leq 6°C$ were possible. However, a gap in the range of temperatures $4.5°C \leq T_{amb} \leq 5.7°C$ where the solution failed to converge still remained. El-Hennawy et al. [1982] numerically computed multiple steady states of vertical buoyancy-induced flows. El-Henawy et al. [1986] recently discussed multiple solutions of the boundary layer equations for horizontal plane flow in cold water. Multiple solutions arose, when the temperature gap was approached from either side, in conjunction with the increasingly large buoyancy force reversal across the thermal layer.

Desai and Forbes [1971], Watson [1972] and Vasseur and Robillard [1980] have investigated the heat transfer and flow patterns in a rectangular enclosure using finite difference methods. Similarly, the effect of density inversion on natural convection within a horizontal cylindrical annulus has been studied experimentally by Seki et al.[1975] and numerically by Nguyen et al.[1982] and Vasseur et al. [1983]. Gilpin [1975] and Cheng et al. [1976,1978] studied the effect of cooling in a horizontal cylinder of water through the maximum density point of $4°C$. Saitoh [1976,1980] investigated both theoretically and experimentally the heat transfer characteristics in natural convection about a horizontal

ice cylinder immersed in water at an ambient temperature near the maximum density point. At about $T_{amb} = 6°C$, a minimum Nusselt number was obtained, an instability in the flow was observed, and it was found that two different computational solutions were obtained at $T_{amb} = 6°C$ when the spatial mesh length was varied (Saitoh [1976]). These unstable aspects of the solutions appeared to correspond to his experimental observations. Ho and Chen [1986] have reported the results of a numerical simulation of the melting of ice around a horizontal cylinder. They have provided results on the shape of the melt cavity formed and its dependence on the temperature of the cylinder. In contrast to the steady flow situation, the transient behaviour of natural convection of water near the maximum density point from a horizontal ice cylinder has not been extensively treated. The existence of an unstable aspect to the convection, or the presence of oscillatory solutions when the physical parameters lie within a certain range of values has not been widely reported. The parallel problem for the case of a vertical plane has been investigated by Gebhart *et al.* [1978] as well as many other researchers as mentioned earlier. On the other hand, studies that provide an insight into the physical mechanism of the above instability is more or less non-existent in the literature.

The third article which froms Chapter III in this thesis is devoted to a numerical investigation of the free convection flow about a horizontal cylinder maintained at 0°C in a water ambient close to the point of maximum density. The two dimensional time dependent Navier-Stokes and energy equations have been solved. Complete numerical solutions covering both the transient as well as steady state have been obtained. A time dependent "characteristic based" boundary condition has been incorporated into the numerical procedure by discretizing

it in implicit mixed boundary condition form. As discussed later, this boundary condition avoids temperature oscillations caused by numerical reflection observed when the leading surface of the plume traverses the artificial outer boundary. A detailed discussion of this effect has been reported by Abarbanel *et al.* [1991] and the use of artificial boundaries to limit the computational domain is discussed in some detail in the review article by Givoli [1991].

Principal results indicate that the proximity of the ambient temperature to the point of maximum density plays an important role in the type of convection pattern that may be obtained. When the ambient temperature is within $4.7°C < T_{amb} < 8°C$, a "dual flow" appears around the cylinder with both upward and downward flow occurring in proximity to the cylinder in two distinct recirculating zones, generally separated by the 4°C isotherm when $T_{amb} < 5.7°C$. The dual flow behaviour is significantly modified as the ambient temperature is altered, disappearing when the ambient temperature is above 8°C, or below 4.7°C. Furthermore, when the ambient temperature is within about $4.8°C < T_{amb} < 5.5°C$, a well defined steady state is never attained. Within this same range, solutions with an initially quasi-periodic behaviour which persist for a long time have been observed. Multiple solutions have been observed when the above range of ambient temperature is approached from either side. The results of the computations have been compared with published experimental and numerical data with satisfactory agreement being obtained. The transient surface vorticity distribution as well as steady state values for certain ambient temperatures have been presented.

1.2 Review of Spline Method

The cubic spline technique constitutes a relatively new subject in the field of numerical methods. The mathematical research and applications of this technique to the numerical solution of partial differential equations have only developed during the past decade. Although it is not as developed as finite difference methods and finite element methods, some breakthroughs have been achieved. With recent developments, it may be said that the technique, as an independent numerical method, has increased in sophistication due to increased attention from researchers around the world. The calculation methodology has been gradually systematised and reformulated resulting in successful applications that have been reported in the literature in the fields of fluid mechanics, thermodynamics (particularly in natural convection flow), hydraulics and so on. The attractive intrinsic properties and advantages of this technique for certain types of problems as well as some application limitations have now become clear.

The main advantages of using a cubic spline collocation procedure are that:

1) The govering matrix system obtained is always tridiagonal thus permitting the use of the Thomas algorithm in the inversion procedure.

2) The matrix system obtained may be reduced to a scalar set of equations in terms of the function itself, its first derivative or its second derivative at the grid points while maintaining a tridiagonal formulation.

3) The requirement of a uniform mesh is not necessary. However, for a uniform mesh, the spline approximation is fourth order accurate for the first derivatives while being third order for a nonuniform grid. The second derivative is always approximated to second order.

4) Since the values of the first or second derivatives may be evaluated directly, boundary conditions containing derivatives may be directly incorporated into the solution procedure thus avoiding the difficulty that exists with some conventional finite-difference schemes where 1st order approximations to surface derivatives must be constructed even in higher order schemes to preserve stability.

The term "spline" was first used by Schoenberg [1946] . Before 1967, the basic mathematical theory of the spline function had been established (for example, see Holladay [1957], Walsh et al. [1962] and deBoor and Lunch [1966]). Nearly all the early work has been included in the book by Ahlberg *et al.*[1967] entitled "The theory of splines and their applications". The most important applications reported are in numerical differentiation and integration, as well as in curve fitting. The use of cubic splines to solve partial differential equations was initiated by Parramicheal and Whiteman [1973] who solved a one dimensional (two-point boundary value) heat conduction equation.

Rubin *et al.*[1975,1976,1977] systematically studied the cubic spline collocation procedure for the numerical solution of a partial differential equation (PDE), discussed the truncation errors of the procedure and its stability and presented a general formulation resulting in a 3x3 matrix system for treating PDE. In order to solve the two-dimensional problem, they proposed a Spline-Alternating-Direction-Implicit (SADI) procedure . In a similar way, Jain and Tariq [1981] presented a spline function which depends on a parameter for uniform mesh spacing.

The author's earlier research works and principal contributions to this technique were performed during 1980-1983 as a visiting scholar from China with

the collaboration of Professor R. Kahawita at the Ecole Polytechnique de Montreal and as a research associate supported by Professor S. Lin at Concordia University (1983 February – June). Based on Rubin et al's work, a procedure to transfer the 3x3 matrices referred to earlier into a scalar tridiagonal system was developed (Wang and Kahawita [1983a,1983b]). The advantage of this formulation is that solutions may be obtained exclusively in terms of the function values themselves, their first derivatives or their second derivatives. Furthermore, a tridiagonal system has to be evaluated instead of a 3x3 matrix. According to the particular requirements of the problem and its imposed boundary conditions, any one of the three forms of equations may be chosen for the solution procedure. This considerably simplifies the computational procedure. Subsequently, a spline explicit method that introduced a weighting parameter into the coefficient of the second derivative term was developed Wang and Kahawita [1983c,1984]. The successful applications of above spline formulations in the field of fluid mechanics, hydraulic and themodynamics have been reported (Wang and Kahawita [1983d,1983e, 1984,1987], Lin, Wang and Kahawita [1983, 1984] and Wang, Lin and Kahawita [1985]).

The author has recently proposed a spline method with a parameter using fractional steps (SMFS) in each coordinate direction (Wang [1987a,1987b], Wang and Kahawita [1988]). This technique retains the advantages of the SADI procedure, but requires only a single tridiagonal matrix system to be evaluated in each computational step without the disadvantages related to the calculus of the first and second derivatives. This technique together with the previously developed tridiagonal solution technique for the system containing either the function values at the grid points, the first derivatives, or the second derivatives only, simplifies

writing the code and reduces CPU time. An application of the SMFS in the estuary hydraulic/thermal model indicated that the CPU time may be reduced by a factor about fifth when compared with the SADI method (Wang [1987a-b], Wang and Kahawita [1990a-b]).

Finally, we have seen with pleasure that the spline method and its applications in heat transfer and fluid flow have developed rapidly in the last few years by many investigators (see for example, Lauriat *et al.*[1985], Shaw *et al.*[1987a,1987b], Hung *et al.*[1989] and Chen [1987]). All results obtained thus far, indicate that the method appears to be efficient. Numerical experiments have indicated that the spline approximation can achieve an accuracy comparable to that of corresponding finite-difference methods using fewer grid points resulting in a significant reduction in computer core memory requirements (Lauriat *et al.*[1985] and Shaw *et al.*[1987]). Consequently, many problems involving heat transfer and fluid flow may now be solved on a personal computer.

CHAPTER II

NUMERICAL COMPUTATION OF THE NATURAL

CONVECTION ABOUT A HORIZONTAL

CYLINDER USING SPLINES

INTRODUCTION

Two-dimensional laminar natural convection from horizontal cylinders under steady state conditions has been extensively investigated analytically, numerically and experimentally. However, for fairly high Rayleigh numbers , for example, when $Ra \geq 10^7$, the numecical results obtained by solving the Navier-Stokes and energy equations have not been reported in the literature. It seems that in this case a efficient and flexible numerical method is needed. Since for $Ra \geq 10^5$ the laminar flow generated by the body forces behaves as a boundary layer around the cylinder, the boundary layer approximation has been frequently used to analyse these problems. The results thus obtained may be taken to represent the limiting case of Rayleigh number (Ra) tending to infinity for laminar flow. Of course, the plume region is excluded, since the development of the plume formed by separation of the boundary layer from the surface invalidates the basic assumptions. Furthermore, these results do not adequately describe the flow and heat transfer at low or moderate values of Rayleigh number neither do they describe the development of the buoyant plume.

The numerical study presented in this Chapter is devoted to the laminar natural convection flow from a heated horizontal cylinder under diverse surface boundary conditions at high Rayleigh numbers. The spline approximation scheme and numerical procedure have been reported in detail. A general formulation to treat mixed boundary conditions using the spline approximation has been

introduced. The usual assumption that the change of inflow to outflow at the outer boundary is near $\theta = 150°$, has not been adopted here, since numerical tests have indicated that the position of this demarcation line between inflow and outflow varies with Rayleigh number. Numerical solutions have been obtained by solving the Navier-Stokes and energy equations in stream function and vorticity form with $11 \times 21(r \times \theta)$, 21×23 or 17x31 grid points on an IBM PC AT for values of Ra^* up to 2.5×10^8 (uniform heat flux) or $Ra = 2 \times 10^7$ (constant surface temperature) for a $Pr = 0.7$.

The results for the isothermal boundary condition as well as for the uniform heat flux are in good agreement with published experimental data and with other solutions presently available in the literature. Some new computations at very high Rayleigh numbers, indicate the existence of attached recirculation vortices in the downstream plume region, the appearance of these vortices being dependant on the values of the Biot number. All results were computed on a personal computer using unequally spaced grids that provided good results with a minimum number of computational points. The numerical scheme presented here appears to be sufficiently versatile to permit computation of a large range of problems.

The principal numerical results have been published in the following paper:
Numerical Heat Transfer, *Vol. 17, Part A, No.2, pp.191–215.(1990)*

NUMERICAL COMPUTATION OF THE NATURAL CONVECTION FLOW ABOUT A HORIZONTAL CYLINDER USING SPLINES

P. Wang and R. Kahawita

Department of Civil Engineering, Ecole Polytechnique de Montreal, Montreal, Quebec H3C 3A7, Canada

T. H. Nguyen

Department of Mechanical Engineering, Ecole Polytechnique de Montreal, Montreal, Quebec H3C 3A7, Canada

The present work is devoted to the numerical study of laminar natural convection flow from a heated horizontal cylinder under diverse surface boundary conditions using the spline fractional step method. A general formulation to treat mixed boundary conditions using the spline approximation has been presented. Numerical solutions have been obtained by solving the Navier-Stokes and energy equations. The results for the isothermal boundary condition as well as for the uniform heat flux are in good agreement with published experimental data and with other solutions presently available in the literature. Some new computations at very high Rayleigh numbers indicate the existence of attached separation vortices in the downstream plume region, the appearance of these vortices being dependent on the values of the Biot number. All results were computed on a personal computer using unequally spaced grids that provided good results with a minimum number of computational points. The numerical scheme presented here appears to be sufficiently versatile to permit computation of a large range of problems.

INTRODUCTION

Two-dimensional laminar natural convection from horizontal cylinders under steady-state conditions has been extensively investigated analytically, numerically, and experimentally [1–6]. The principal results indicate that at small Rayleigh numbers (Ra < 0.1), the cylinder behaves as a line source, with the uniform surface heat flux approaching that of the isothermal condition [5]. For fairly high Rayleigh numbers ($10^5 \leq$ Ra $\leq 10^8$), the laminar flow generated by the body forces behaves as a boundary layer around the cylinder. It is not surprising therefore that the boundary layer approximation has been frequently used to analyze these problems. This approximation assumes that curvature effects and any pressure differences across the boundary layer are negligible. The simplified set of equations is then solved using various techniques [7–10]. The results thus obtained may be taken to represent the limiting case of Rayleigh number (Ra) tending to infinity for laminar flow. The plume region is of course excluded, since the development of the plume formed by separation of the boundary layer from the surface invalidates the basic assumptions. Furthermore, these results do not adequately describe the flow and heat transfer at low or moderate values of Rayleigh number nor the development of the buoyant plume, which, as has been just mentioned, cannot be obtained from the boundary layer approximation [3].

192   P. WANG ET AL.

NOMENCLATURE

Bi	Biot number, $h'D/k'$	t'	time
D	cylinder diameter	T	dimensionless temperature
g	gravitational acceleration	T'	temperature
h	local heat transfer coefficient	T'_w	temperature of cylinder surface
h'	local heat transfer coefficient inside cylinder	T'_∞	temperature of ambient fluid
$\bar{h}$	average heat transfer coefficient around cylinder	T'_0	temperature inside cylinder
		u	dimensionless radial velocity ($= UD/\alpha$)
k	thermal conductivity of fluid	U	radial velocity, positive outward
k'	thermal conductivity of fluid inside cylinder	U^*	modified dimensionless radial velocity ($= UD/\alpha\text{Ra}^{0.25}$)
L	radial distance between cylinder surface and outer boundary of solution domain	v	dimensionless angular velocity ($= VD/\alpha$)
		V	angular velocity, positive counterclockwise
Nu	local Nusselt number ($= hD/k$)	V^*	modified dimensionless angular velocity ($= VD/\alpha\text{Ra}^{0.5}$)
$\overline{\text{Nu}}$	average Nusselt number ($= \bar{h}D/k$)	Y	radial distance from cylinder surface
Pr	Prandtl number ($= \mu/\alpha$)	Y^*	$Y\text{Ra}^{0.25}/D$
q''	surface heat flux	α	thermal diffusivity
R	radial coordinate	β	coefficient of thermal expansion
R_0	cylinder radius	θ	angular coordinate; zero is downward vertical, positive counterclockwise on right half of cylinder
R_f	radius of (fictitious) outer boundary		
r	dimensionless radial coordinate ($= R/D$)		
Ra	Rayleigh number [$= g\beta D^3(T'_w - T'_\infty)/\mu\alpha$]	μ	kinematic viscosity
		Ψ	dimensionless stream function
Ra*	modified Rayleigh number ($= g\beta q''D^4/k\alpha\mu$)	Ω	dimensionless vorticity
Ra**	Rayleigh number for mixed boundary condition [$= g\beta D^3(T'_w - T'_0)/\mu\alpha$]	**Subscripts**	
t	dimensionless time ($= t'\alpha/D^2$)	i, j	nodal positions in radial and angular directions, respectively

---

Kuehn and Goldstein [3] numerically solved the complete Navier-Stokes and energy equations for laminar natural convection about a horizontal isothermal circular cylinder for $1 \le \text{Ra} \le 10^7$ using a finite-difference technique. The numerical solution was in good agreement with their experimental data for Ra $= 10^5$. Farouk and Guceri [4] attacked the same problem for uniform as well as nonuniform temperature and heat flux distributions on the cylinder surface. Recently, Qureshi and Ahmad [5] have provided numerical solutions using a technique similar to that indicated in [3] for a horizontal cylinder with uniform heat flux at modified Rayleigh numbers (Ra* $=$ Ra $\times$ Nu) between 10^{-2} and 10^7. They have compared their computations with their own experimental results for Ra* $= 2.07 \times 10^6$ and Ra* $= 6.3 \times 10^6$.

The present study is devoted to a numerical investigation of the laminar natural convection flow from a heated horizontal cylinder under diverse surface boundary conditions using the spline fractional step method [11]. Since the pioneering work of Rubin et al. [12–14], the spline integration technique and its applications in heat transfer and fluid flow have developed rapidly [15–20]. Numerical experiments have indicated that the spline approximation can achieve an accuracy comparable to that of corresponding finite-difference methods using fewer grid points (see, for example [18, 21]), resulting in a significant reduction in computer core memory requirements. Consequently, many

FLOW ABOUT A HORIZONTAL CYLINDER

problems involving heat transfer and fluid flow may now be solved on a personal computer.

A spline method using fractional steps in each coordinate direction has recently been proposed by Wang [11]. This technique, together with the previously developed tridiagonal solution technique for the system [15, 16] containing either the function values at the grid points, the first derivatives, or the second derivatives only, simplifies writing the code and reduces CPU time. As anticipated, fewer grid points are required to solve the present problem. Numerical solutions have been obtained by solving the Navier-Stokes and energy equations with 11×21 (r by θ), 21×23, or 17×31 grid points on an IMB-PC/AT for values of Ra* up to 2.5×10^8 (uniform heat flux) or Ra $= 2 \times 10^7$ (constant surface temperature) for Pr $= 0.7$.

GOVERNING EQUATIONS

The natural convection flow from a horizontal cylinder is governed by the continuity equation, the two-dimensional Navier-Stokes equation, and an energy equation. In cylindrical polar coordinates, the nondimensional equations in stream function and vorticity form (using the Boussinesq approximation for the body forces) may be written

$$\Delta^2 \Psi = -\Omega \tag{1}$$

$$\frac{\partial \Omega}{\partial t} + u \frac{\partial \Omega}{\partial r} + \frac{v}{r} \frac{\partial \Omega}{\partial \theta} = \text{Pr} \, \Delta^2 \Omega + \text{Pr} \, \text{Ra} \left(\sin \theta \, \frac{\partial T}{\partial r} + \cos \theta \, \frac{1}{r} \frac{\partial T}{\partial \theta} \right) \tag{2}$$

$$\frac{\partial T}{\partial t} + u \frac{\partial T}{\partial r} + v \frac{\partial T}{\partial \theta} = \Delta^2 T \tag{3}$$

with

$$\Delta^2 = \frac{\partial^2}{\partial r^2} + \frac{1}{r} \frac{\partial}{\partial r} + \frac{1}{r^2} \frac{\partial^2}{\partial \theta^2} \tag{4}$$

and

$$u = \frac{1}{r} \frac{\partial \Psi}{\partial \theta} \qquad v = - \frac{\partial \Psi}{\partial r} \tag{5}$$

Since the flow is symmetric about a vertical plane passing through the axis of the cylinder, only the half-plane need be considered. The boundary conditions then become

$$u = v = \Psi = 0 \qquad \Omega = - \frac{\partial^2 \Psi}{\partial r^2}$$

and (i)

$$\frac{\partial T}{\partial r} = -1 \tag{6a}$$

or (ii)

$$T = 1 \tag{6b}$$

or (iii)

$$\frac{\partial T}{\partial r} = \text{Bi} \, (T - 1) \tag{6c}$$

on the cylinder surface and

$$\psi = v = \Omega = \frac{\partial T}{\partial \theta} = 0 \tag{7}$$

on the lines of symmetry. Condition (iii) is of course relevant to the case of a tube carrying a hot fluid.

Placing a circular line far away from the cylinder to represent the outer boundary, the boundary conditions are

At the inflow region ($u < 0$):

$$v = \frac{\partial^2 \Psi}{\partial r^2} = T = 0 \qquad \Omega = -\frac{1}{r^2} \frac{\partial^2 \Psi}{\partial \theta^2} \tag{8}$$

On the outflow region ($u > 0$):

$$v = \frac{\partial^2 \Psi}{\partial r^2} = 0 \qquad \Omega = -\frac{1}{r^2} \frac{\partial^2 \Psi}{\partial \theta^2} \tag{9}$$

The fluid is thus assumed to approach or leave the cylinder in the radial direction, i.e., the streamlines are normal to the outer (artificially imposed) boundary. The temperature of the fluid entrained into the flow field is at the ambient value, but at the outflow region the temperature distsribution is not known a priori. The commonly used boundary condition for outflow is to assume that the temperature gradient normal to the pseudo-boundary is zero, thus implying that the heat transfer is dominated by convective movement rather than by conduction [3]. This obviously requires that the outflow velocities be sufficiently large, a condition that is probably satisfied within the scope of the present study, which is restricted to steady-state convection. For the transient flow from rest to a steady state, however, the validity of this boundary condition may have to be examined in further detail. Some flow features and the influence of the outer boundary condition on transient natural convection will be presented in a forthcoming report.

NUMERICAL PROCEDURE

In this study, a spline method of fractional steps (SMFS) [11] is used to generate an algorithm resulting in a tridiagonal system containing either function values or first derivatives at the grid points. The fundamental formulations of the technique have been

reported elsewhere [15, 16]. Boundary conditions that specify heat flux or other temperature gradient conditions may be easily incorporated directly into the solution procedure. This avoids the difficulty that exists with some conventional finite-difference schemes where first-order approximations to surface derivatives must be constructed even in higher order schemes to preserve stability.

The assumption that the change of inflow to outflow at the outer boundary is near $\theta = 150°$ has not been adopted here, since numerical tests indicated that the position of this demarcation line between inflow and outflow varied with Rayleigh number. An increase in the Rayleigh number caused the line to shift toward the vertical, i.e., toward $\theta = 180°$. For example, this change is observed to be near $\theta = 160°$ for Ra $= 10^5$ (surface temperature constant) at $L = 0.7$. However, for Ra $= 10^7$ and $L = 0.5$ its position was between $\theta = 168°$ and $171°$. Thus in the computer program, the only boundary condition imposed at the outer circular limit depends on the direction of the radial velocity, with the appropriate temperature boundary condition being automatically incorporated into the calculation procedure.

The computational procedure followed is first to solve the energy equation, which provides the temperature field necessary for the solution of the vorticity equation. Solution of Poisson's equation for the stream function then completes the procedure. The SMFS schemes representing the governing equations (1)–(3) are of the following forms.

Energy Equation

The first step is taken in the radial direction, the spline approximation being

$$T_{i,j}^{n+1*} = T_{i,j}^n - \Delta t \left(u_{i,j}^n - \frac{1}{r_i} \right)(T_r)_{i,j}^{n+1*} + \Delta t(T_{rr})_{i,j}^{n+1*} \qquad i = 0, M \qquad (10)$$

or in the more general form of [15, 16]

$$T_{i,j}^{n+1*} = F_{i,j} + R_{i,j}(T_r)_{i,j}^{n+1*} + Q_{i,j}(T_{rr})_{i,j}^{n+1*} \qquad (11)$$

where $(T_r)_{i,j}$ and $(T_{rr})_{i,j}$ represent the spline approximated values of $\partial T/\partial r$ and $\partial^2 T/\partial r^2$ at the grid points (i, j), and $F_{i,j}$, $R_{i,j}$, and $Q_{i,j}$ are known from the previous time step.

The boundary conditions at the cylinder surface are

Case i: $$(T_r)_{0,j} = -1$$

Case ii: $$T_{0,j} = 1$$

Case iii: $$(T_r)_{0,j} = \text{Bi}\,(T_{0,j} - 1)$$

and at the outer boundary

$$\begin{aligned} T_{M,j} &= 0 && \text{if } u \leq 0 \\ (T_r)_{M,j} &= 0 && \text{if } u > 0 \end{aligned} \qquad (12)$$

Equation (11) has been transformed [13] into a single tridiagonal system containing the function values only,

$$a_{i,j}T_{i-1,j}^{n+1*} + b_{i,j}T_{i,j}^{n+1*} + c_{i,j}T_{i+1,j}^{n+1*} = d_{i,j} \qquad i = 1, M-1 \qquad (13)$$

or another single tridiagonal system for the first derivatives,

$$A_{i,j}(T_r)_{i-1,j}^{n+1*} + B_{i,j}(T_r)_{i,j}^{n+1*} + C_{i,j}(T_r)_{i+1,j}^{n+1*} = D_{i,j} \qquad (14)$$

If the surface temperature condition is specified, Eq. (13) may be directly evaluated. Then system (14) is in the preferred form for treating case i, which is discussed in detail in a following section. Then, from $(T_r)_{i,j}^{n+1*}$, $T_{i,j}^{n+1*}$ may be found from the recursive relation [11].

At the second step, the values of T are updated from the intermediate values T^{n+1*} by substituting into T^{n+1} as in standard fractional step methods. The spline discretized form is

$$T_{i,j}^{n+1} = T_{i,j}^{n+1*} - \Delta t \left(v_{i,j}^n - \frac{1}{r_i} \right)(T_\theta)_{i,j}^{n+1} + \frac{\Delta t}{r^2}(T_{\theta\theta})_{i,j}^{n+1}$$

the single tridiagonal system containing the first derivatives is

$$A_{i,j}'(T_\theta)_{i,j-1}^{n+1} + B_{i,j}'(T_\theta)_{i,j}^{n+1} + C_{i,j}'(T_\theta)_{i,j+1}^{n+1} = D_{i,j}' \qquad j = 1, N-1 \qquad (15)$$

The procedure for evaluating the values of $(T_\theta)_{i,j}^{n+1}$ and $T_{i,j}^{n+1}$ is the same as in the first step.

It is important to note that the values with superscript $n + 1*$ are the intermediate values only, while the values with superscript $n + 1$ are the final values at the $n + 1$ time level.

Vorticity Equation

The first step in the radial direction is written

$$\Omega_{i,j}^{n+1*} = \Omega_{i,j}^n - \Delta t \left(u_{i,j}^n - \frac{\mathrm{Pr}}{r_i} \right)(\Omega_r)_{i,j}^{n+1*} + \Delta t\, \mathrm{Pr}\, (\Omega_{rr})_{i,j}^{n+1*}$$

$$+ 0.5\, \Delta t\, \mathrm{Pr}\, \mathrm{Ra} \left[\sin\theta_j (T_r)_{i,j}^{n+1} + \frac{\cos\theta_j}{r_i}(T_\theta)_{i,j}^{n+1} \right]$$

$$= F_{i,j} + R_{i,j}(\Omega_r)_{i,j}^{n+1*} + Q_{i,j}(\Omega_{rr})_{i,j}^{n+1*} \qquad (16)$$

Eq. (16) may be rewritten

$$a_{i,j}\Omega_{i-1,j}^{n+1*} + b_{i,j}\Omega_{i,j}^{n+1*} + c_{i,j}\Omega_{i+1,j}^{n+1*} = d_{i,j} \qquad i = 1, M-1 \qquad (17)$$

with the following boundary conditions:

$$\Omega_{0,j}^{n+1^*} = -(\Psi_{rr})_{0,j}^n = -\left[2(\Psi_r)_{i,j} - \frac{6\Psi_{i,j}^n}{h_1} \right] \Big/ h_1$$

and

$$\Omega_{M,j}^{n+1^*} = -\frac{(\Psi_{\theta\theta})_{M,j}^n}{R_f^2}$$

where $(\Psi_{\theta\theta})$ may be evaluated from the stream function equation. Thus Ω may be calculated directly.

In the second step, we have

$$\Omega_{i,j}^{n+1} = F_{i,j} + R_{i,j}(\Omega_\theta)_{i,j}^{n+1} + Q_{i,j}(\Omega_{\theta\theta})_{i,j}^{n+1} \qquad j = 1, N-1 \tag{18}$$

Equation (18) may be rewritten in the form of Eq. (14) with the boundary conditions $\Omega_{i,0}^{n+1} = 0$ and $\Omega_{i,N}^{n+1} = 0$.

It is interesting to note that in the computational procedure Ω_r, Ω_{rr}, Ω_θ, and $\Omega_{\theta\theta}$ are not presented explicitly, although they are contained in Eqs. (16) and (18). This is an advantage of the SMFS scheme over the spline-alternating-direction-implicit (SADI) method.

Stream Function Equation

The stream function is evaluated in a false transient form using the SADI method. No difficulties arise, since the boundary conditions are appropriately specified. To obtain steady-state solutions, repeated iterations until convergence are necessary.

TREATMENT OF MIXED BOUNDARY CONDITIONS

If the case of a temperature source within the cylinder, for example, a fluid with constant temperature T_0' passing inside the cylinder is considered and if h' and k' represent thermal conductivity and heat transfer coefficients, respectively, the implied surface boundary conditions in dimensionless form are

$$\frac{\partial T}{\partial r} = \text{Bi} (T - 1) \tag{19}$$

The spline discretized form is then

$$(T_r)_{0,j} = \text{Bi} (T_{0,j} - 1) \tag{20}$$

Using cubic spline relations and Eq. (11), Eq. (20) has been transformed into the following form (where the index j has been omitted) [22]:

$$b_0 T_0 + c_0 T_1 = d_0 \tag{21}$$

where $b_0 = 1 - [(R_1 + 4Q_1/h_1)(3/h_1 + h_1/2Q_1) - 6Q_1/h^2)]/(\text{Bi} \times K)$

$\qquad c_0 = -(1 - 3R_1 - 6Q_1/h_1^2)/(\text{Bi} \times K)$

$\qquad d_0 = 1 + [F_1 + (h_1 R_1/2 + 2Q_1)F_0/Q_0]/(\text{Bi} \times K)$

with $\quad K = (R_1 + 4Q_1/h_1)(R_0 h_1/2Q_0 - 2) + 2Q_1/h_1$

Equation (17) may also be rewritten in the form containing first derivatives:

$$B_0(T_r)_0 + C_0(T_r)_1 = D_0 \qquad\qquad (22)$$

where $B_0 = 1 - \text{Bi} [(Q_0 - 4R_0/h_1)z_1 - 2r_1 z_0/h_1]/(y_0 z_1 - y_1 z_0)$

$\qquad C_0 = \text{Bi} [2R_0 z_1/h_1 + (Q_1 + 4R_1/h_1)z_0]/(y_0 z_1 - y_1 z_0)$

$\qquad D_0 = -\text{Bi} + \text{Bi} [(F_0 z_1 - F_1 z_0)/(y_0 z_1 - y_1 z_0)]$

with $\quad y_0 = 1 + 6Q_0/h_1^2$

$\qquad y_1 = -6Q_1/h_1^2$

$\qquad z_0 = 1 - y_0$

$\qquad z_1 = 1 - y_1$

The above forms are of the same accuracy as the system described by Eq. (13) or Eq. (14).

NUMERICAL RESULTS AND DISCUSSION

The flow and temperature fields and heat transfer results were obtained for isothermal and uniform heat flux boundary conditions for $\text{Pr} = 0.7$. The nonlinear coupled partial differential equations were solved by considering a grid 11×21 ($r \times \theta$), 21×23, or 17×31 on a nonuniform mesh with $r_{i+1}/r_i = 1.3$ and $\theta_{j+1}/\theta_j = 0.87$, or $r_{i+1}/r_i = 1.09$ and $\theta_{j+1}/\theta_j = 0.9$, or $r_{i+1}/r_i = 1.15$ and $\theta_{j+1}/\theta_j = 0.93$, respectively. Near the cylinder surface and in the plume region, the grid spacing chosen was very fine, as shown in Fig. 1. The position of the outer boundary was moved inward as the Rayleigh number increased, but the total number of nodal points remained fixed. Numerical tests indicated that when $L > 12.5/\text{Ra}^{0.25}$ (for constant surface temperature), the position of the outer circular boundary for the moderately large Rayleigh numbers was sufficiently distant. This is because R_f far exceeds the boundary layer thickness and the plume region is fully developed. Numerical tests for $\text{Ra} = 10^5$ on grids of 11×21 and 21×23 were performed. The results for local and average Nusselt numbers at the constant temperature cylinder surface for different R_f are reported in Table 1, and the temperature distribution at $\theta = 180°$, the plume centerline, is presented in Fig. 2. In Table 1 it is noted that the local as well as average Nusselt numbers are virtually indistinguishable from one another, while a slight difference in the temperature is barely perceptible at the outer boundary. This indicates that although the spacing has been changed by a factor of about 1.5, the influence on the results is negligible.

The criterion for the steady-state solution is that the maximum relative change in flow and temperature fields satisfy

$$\frac{|\Phi_{i,j}^{n+1} - \Phi_{i,j}^n|_{\max}}{|\Phi_{i,j}^n|_{\max}} < \epsilon = 2 \times 10^{-5}$$

where Φ represents the stream function and temperature.

FLOW ABOUT A HORIZONTAL CYLINDER
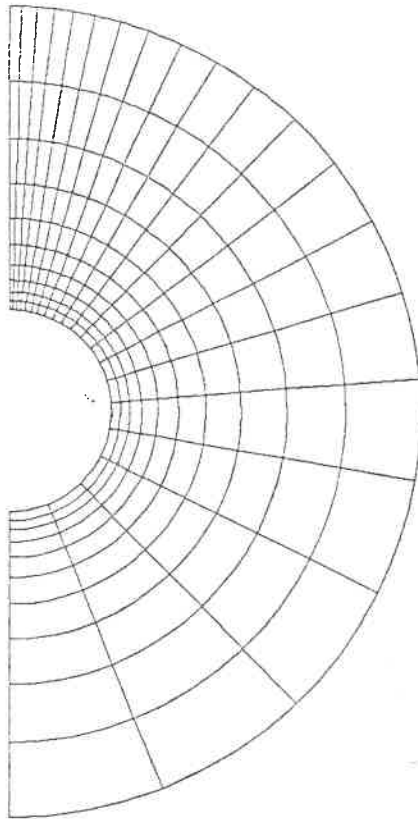
Fig. 1 Coordinate system.

As a further check on the accuracy of the results reported here, an energy balance has been enjoyed by comparing the heat transfer between each section. Mathematically,

$$\int_0^\pi -\frac{\partial T}{\partial r} R_0 \, d\theta = \int_0^\pi \left(uT - \frac{\partial T}{\partial r} \right) r \, d\theta \qquad (R_0 < r < R_f) \tag{23}$$

For a large number of these computations, the energy balance was satisfied to within an error of 2%.

Table 1 Influence of Outer Boundary and Mesh Size on Local and Average Heat Transfer Coefficients at Ra = 10^5, T_w = 1 [Nu = $-(\partial T/\partial r)_w$]

		Nu for different values of θ							
L	Mesh size	0°	46°	82°	120°	150°	176°	180°	$\overline{Nu}$
0.7	11 × 21	9.98	9.55	9.04	8.07	5.80	2.10	1.94	7.967
1.0	11 × 21	9.97	9.55	9.04	8.08	5.81	2.11	1.94	7.972
1.5	21 × 23	9.98	9.55	9.04	8.07	5.80	2.10	1.94	7.961

P. WANG ET AL.
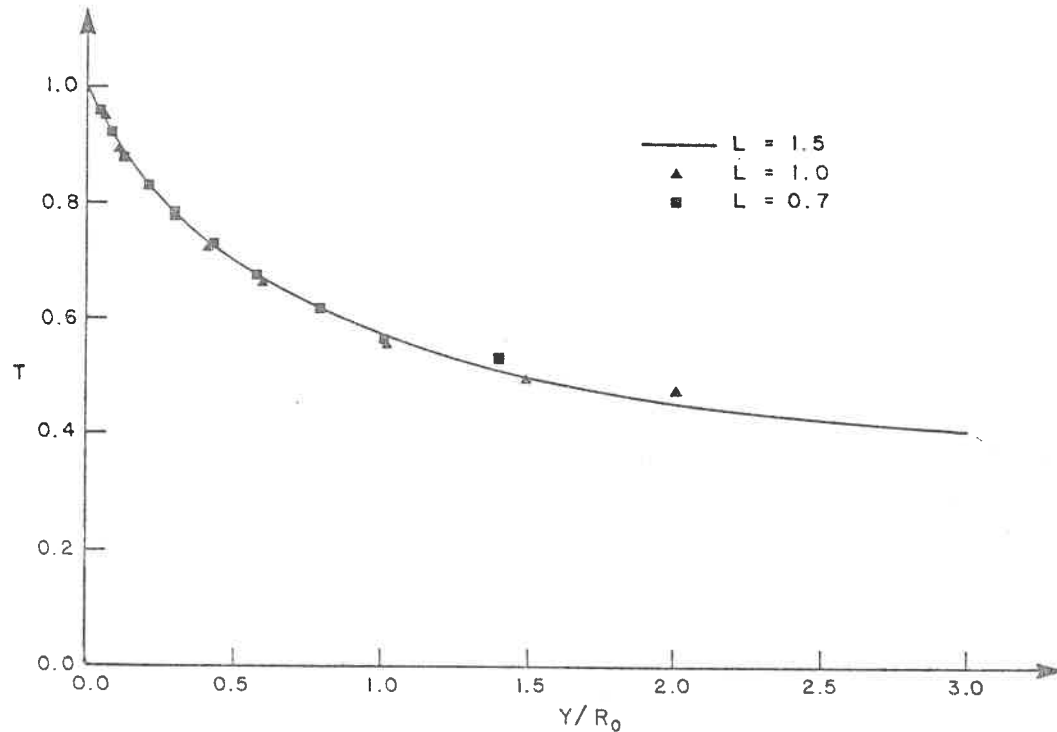
Fig. 2 Influence of L, the distance between surface and outer boundary, on temperature distribution at $\theta = 180°$.

Case i: Uniform Heat Flux

Figure 3 shows the streamlines and isotherms for $Ra^* = 10^7$ and 10^8. The local Nusselt number ($Nu = hD/k = 1/T_w$) distribution is shown in Fig. 4 and Table 2 with a comparison of the results from [5]. For $Ra^* = 2.07 \times 10^6$ and 6.3×10^6, the present results are in good agreement with the experiments of Qureshi and Ahmad [5] as shown in Table 2. (These authors, unfortunately, made no direct comparison between their experimental and numerical results except in the plume region, where according to them, the test cylinder did not approach the ideal boundary condition.) For $Ra^* = 10^5$, 10^6, and 10^7, the present results are similar to those of [5], the difference in general being less than 2%. In the plume, the present Nusselt number results are slightly larger than those reported in [5], and lower in other regions. For $Ra^* > 10^7$ the present results closely approach the results obtained from a boundary layer type solution. Based on the boundary layer analysis of Wilks [8], Churchill [9] suggested a correlation between the Nusselt and Rayleigh numbers for the uniform heat flux condition, which for the present case is [5]

$$Nu = 0.527(Ra^*)^{0.2}$$

The comparison between the present numerical solutions and this correlation is shown in Fig. 5. With increasing Rayleigh number, the results closely approach each other. It appears therefore that the boundary layer solutions are of acceptable accuracy for values of Ra^* greater than about 10^6.
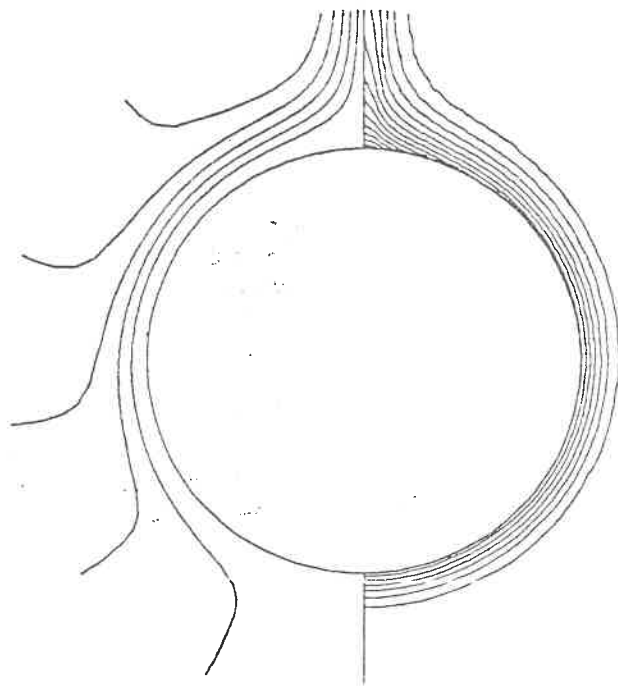
(a)
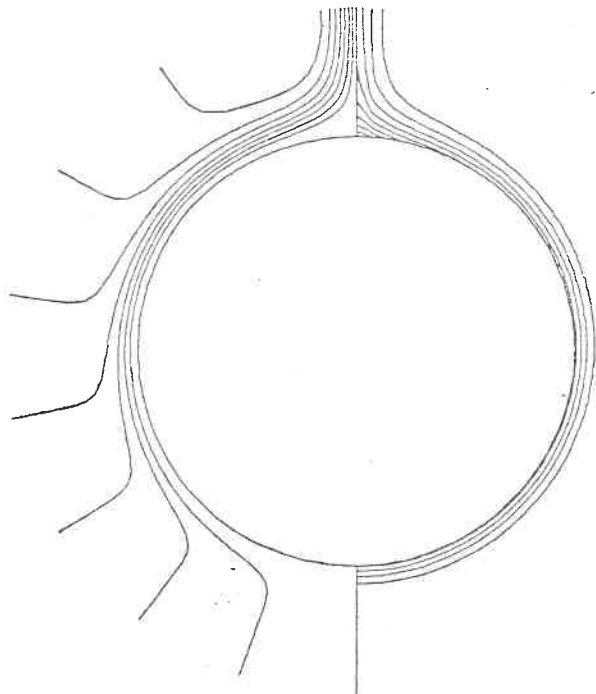
(b)

Fig. 3 Isotherms (left) and streamlines (right) for Ra*, Pr = 0.7: (a) Ra* = 10^7 ($\Delta\Psi$ = 5, T_{max} = 0.14, and ΔT = 0.02); (b) Ra* = 10^8 ($\Delta\Psi$ = 10, T_{max} = 0.08, and ΔT = 0.01).

P. WANG ET AL.
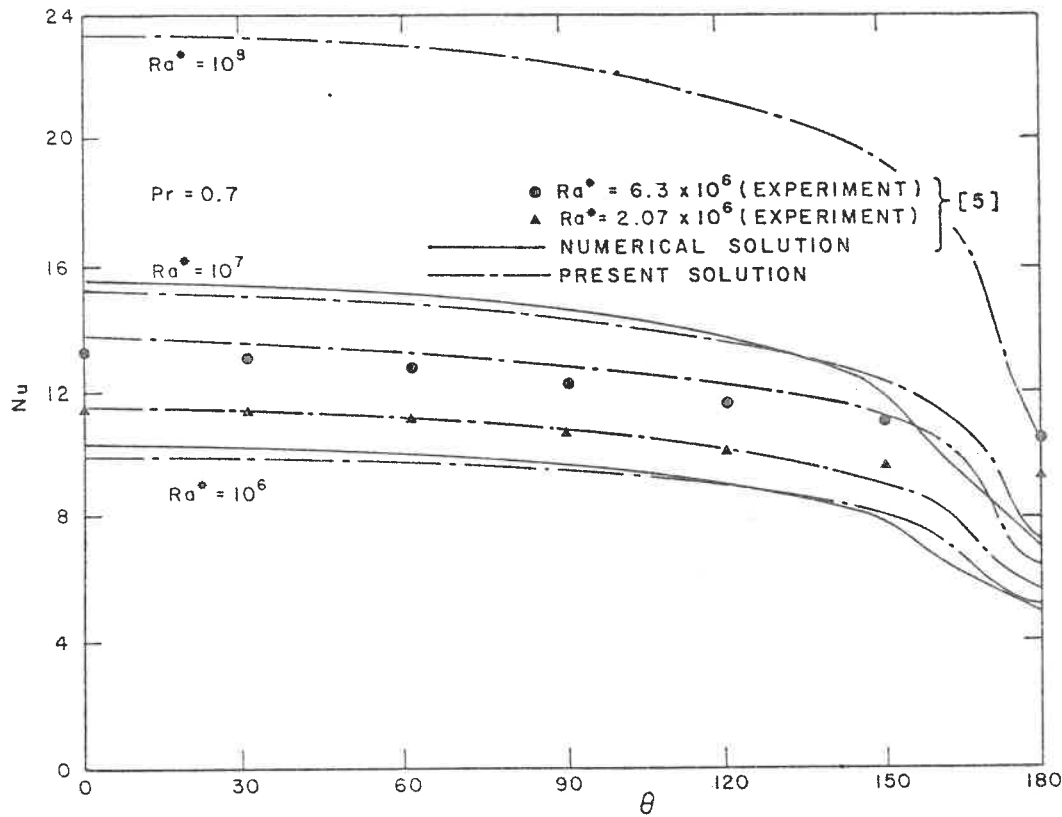
Fig. 4 Comparison between computed local Nusselt number and experimental data of [5].

Case ii: Isothermal Cylinder Surface

Solutions using the spline technique have been obtained for values of Rayleigh number up to 2×10^7 at a Prandtl number of 0.7. In fact, when $Ra = 10^7$, the induced convection velocities become very intense with the same order of magnitude as those obtained in case i with $Ra^* = 2.5 \times 10^8$ (in fact, $Ra^* = Ra \times Nu$). Figures 6(a) and 6(b) show the streamlines and isotherms for $Ra = 10^5$ and 2×10^7, respectively. The radial and tangential velocity distributions at $Ra = 2 \times 10^7$ are shown in Figs. 7 and 8,

Table 2 Comparison Between Present Computed Local and Average Heat Transfer Coefficients and Those of Ref. [5] ($Nu = 1/T_w$)

Ra*	Mesh size	Nu for different values of θ							$\overline{Nu}$
		0°	30°	60°	90°	120°	150°	180°	
10^6	11×21	9.87	9.83	9.60	9.24	8.94	7.91	5.02	8.88
	Ref. [5]	10.23	10.16	9.95	9.59	9.04	7.84	4.85	9.02
10^7	11×21	15.04	15.00	14.72	14.08	13.58	12.28	7.14	13.57
	21×23	15.02	14.92	14.67	14.04	13.59	12.30	7.23	13.56
	Ref. [5]	15.50	15.39	15.08	14.57	13.77	12.07	6.88	13.70
10^8	17×31	23.12	22.84	22.57	21.92	20.85	19.63	10.87	21.00
2.5×10^8	17×31	28.05	27.34	26.98	26.18	25.01	23.17	12.26	25.08

FLOW ABOUT A HORIZONTAL CYLINDER
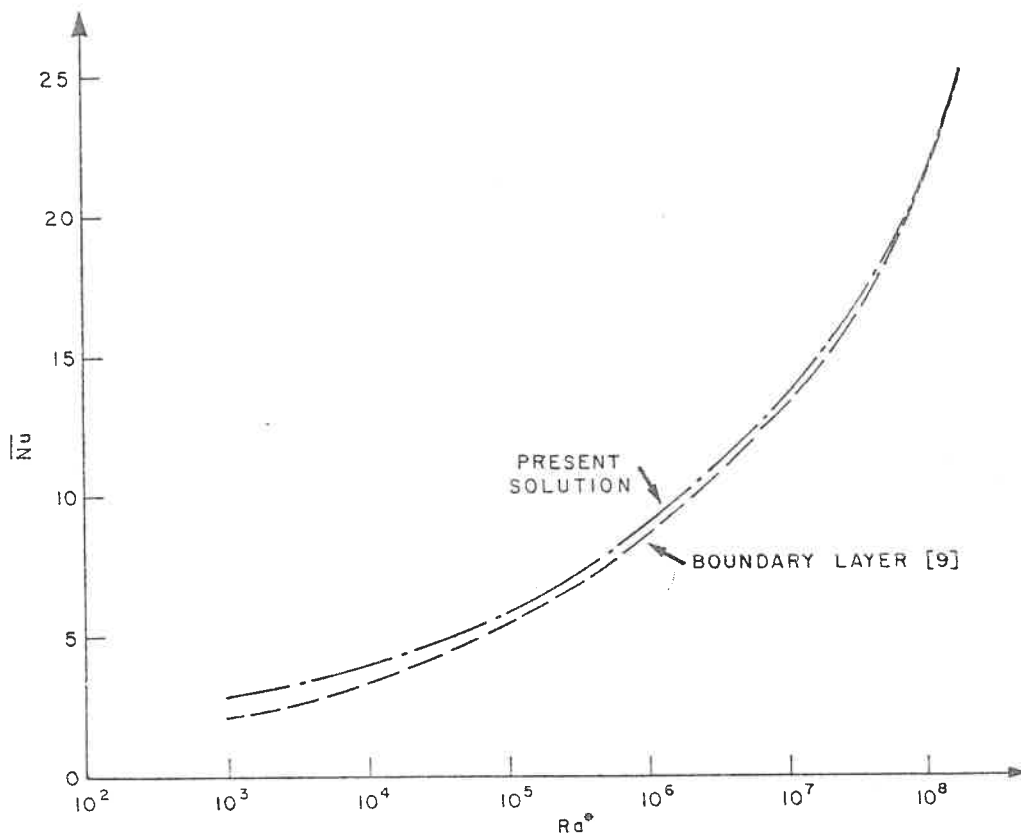
Fig. 5 Comparison between present numerical solution and boundary layer solution of [9].

while that for temperature is presented in Fig. 9. For Ra $=$ 10^5, the present results are in good agreement with Kuehn and Goldstein's [3] experiments. Figure 10 shows the comparison between the present results and the experimental results, as well as numerically computed temperatures at $\theta = 90°$ and $180°$ for Ra $=$ 10^5 from [3]. In both cases, the present solution provides improved agreement with the measured data. The spatial variation of the surface heat transfer coefficient is presented in Fig. 11. Again, satisfactory agreement with the measured data is evident. Comparison between the computed tangential velocity profiles for Ra $=$ 10^5 and $\theta = 90°$ with the experimental measurements and numerical results from [3] is given in Fig. 12. The present results coincide with the numerical solutions reported in [3] for $Y^* < 3$ and agree very well with Aihara and Saito's [6] measured data for $Y^* < 1$ and $Y^* > 4$. With increasing Rayleigh number, the convection increases in strength until at a Rayleigh number of about 2×10^7, the maximum tangential velocity has increased to about 13 times its value at Ra $=$ 10^5, while the boundary layer thickness has diminished to about 3% of the cylinder radius (cf. Figs. 6(b) and 10). The comparison between local heat transfer coefficients with those in [3] for $10^2 \leq$ Ra $\leq 10^7$ is shown in Table 3. The difference between the two numerical solutions for average Nusselt numbers is less than 2%, but as in case i, the present results are larger than those of [3] in the plume region, while being lower in other regions. This difference may be due to the different numerical methods used and also to the somewhat arbitrary definition employed in [3] as to the position at which the
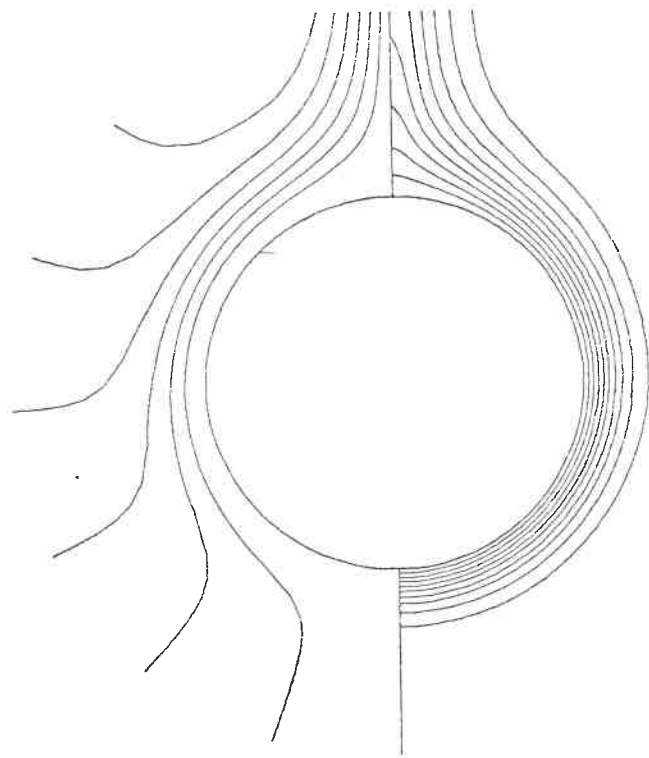
(a)
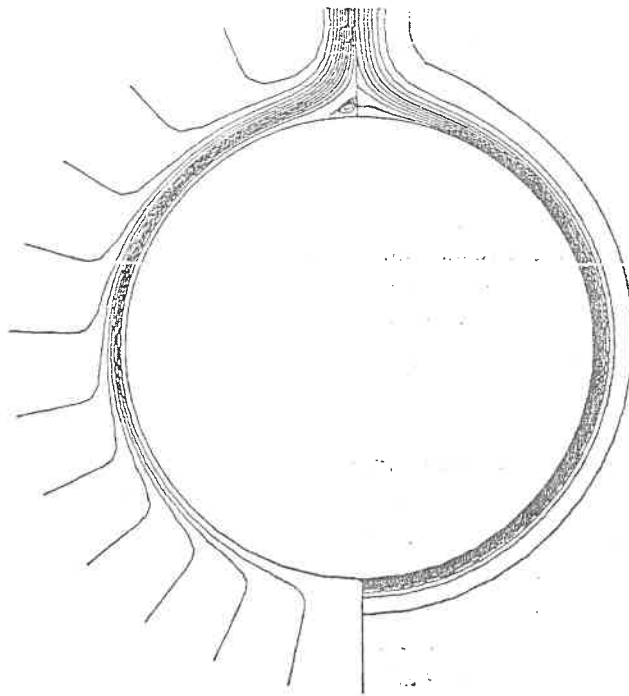
(b)

Fig. 6   Isotherms and streamlines for Ra, Pr — 0.7: (a) Ra —
10^5 ($\Delta\Psi$ — 5, ΔT — 0.1); (b) Ra — 2×10^7 ($\Delta\Psi$ — 10, while
$\Delta\Psi$ — −0.2 for separation vortices, ΔT — 0.1).

FLOW ABOUT A HORIZONTAL CYLINDER
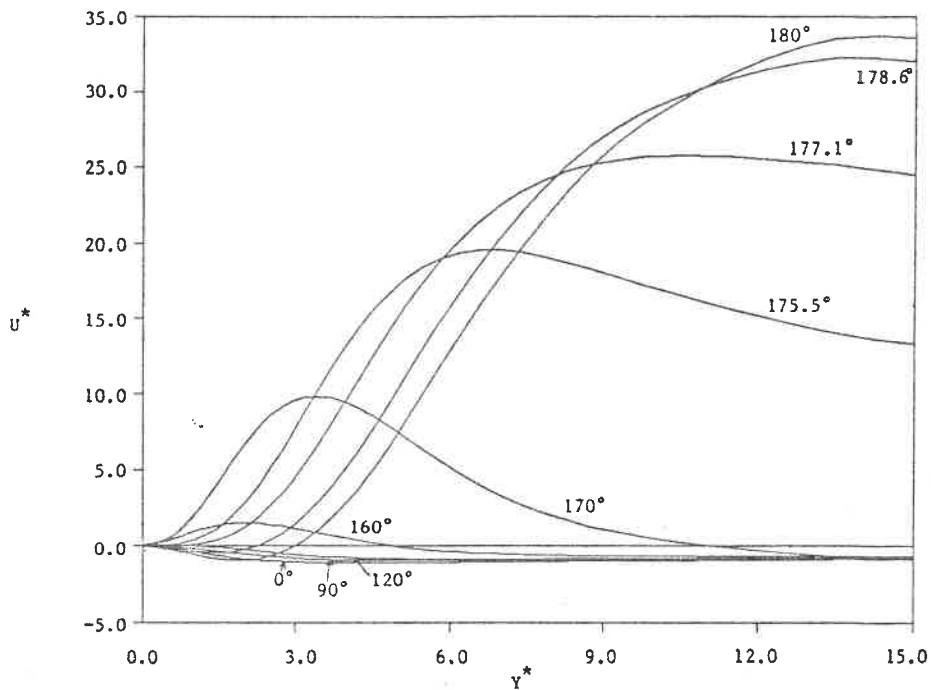
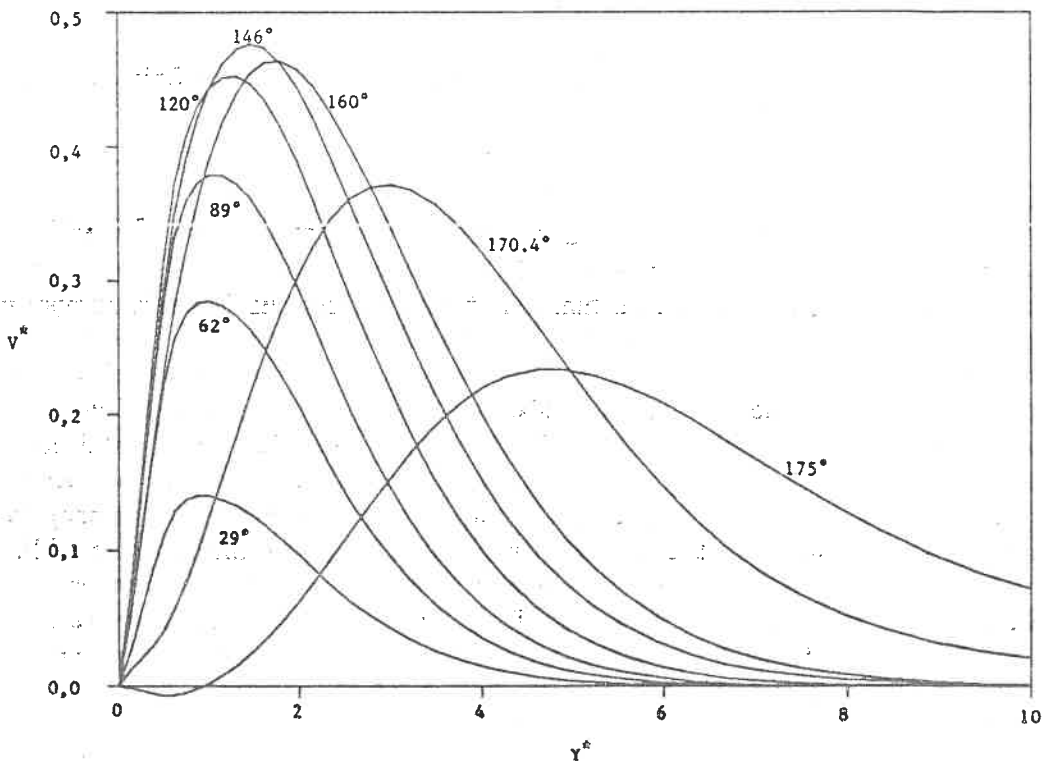**Fig. 7** Radial velocity distribution for Ra $= 2 \times 10^7$.

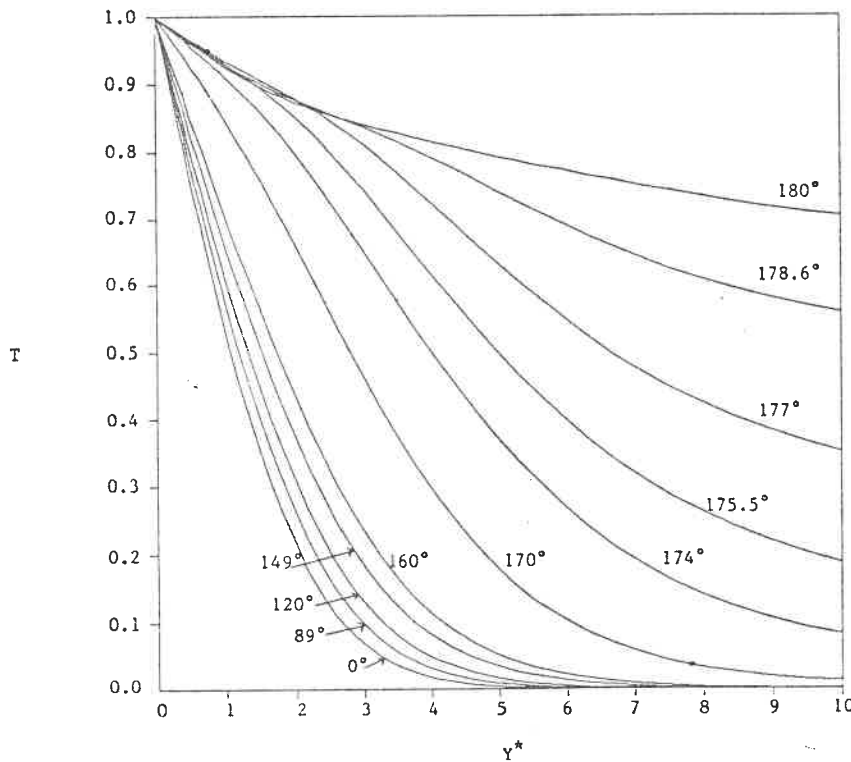**Fig. 8** Tangential velocity distribution for Ra $= 2 \times 10^7$.

P. WANG ET AL.

Fig. 9 Temperature distribution for Ra $= 2 \times 10^7$.

change from inflow to outflow occurs. It may be noted here that similar finite-difference schemes were used in [3] and [5].

Case iii: Mixed Boundary Conditions

Figure 13 shows the streamlines and isotherms for Ra** $= 2 \times 10^7$ at Bi $= 1$, 10, and 50, while those for Ra** $= 4 \times 10^8$ are shown in Fig. 14. The average heat transfer coefficients are shown as a function of Biot number and Rayleigh number in Fig. 15. When Bi < 1, the variation of heat transfer coefficient Nu $= -(T_r)_0$ with increasing Rayleigh number is not large; however, at larger Biot numbers, this variation becomes significant, and the convection also increases in strength. The present calculated tangential velocity profiles at $\theta = 139.22°$ (near v_{max}) for Ra** $= 10^7$ at different Biot numbers are shown in Fig. 16. It is clearly seen that an increased Biot number results in stronger convection with an accompanying reduction in both the velocity and thermal boundary layer thickness, as shown in Fig. 13; for the limiting case of Biot number tending to infinity, the problem reduces to the case of the isothermal surface. The numerical results then indicate that for Bi > 500, the surface temperature variation becomes less than 5% and the mixed and isothermal boundary conditions become equivalent. Furthermore, when Ra** $> 10^5$, the heat transfer coefficient increases rapidly with increasing Rayleigh number, the convective activity becomes much stronger, and the boundary layer region becomes very thin. In fact, the present numerical tests indicate that when Ra** $\geq 2 \times 10^7$ and Bi > 500, separation vortices in the plume region close
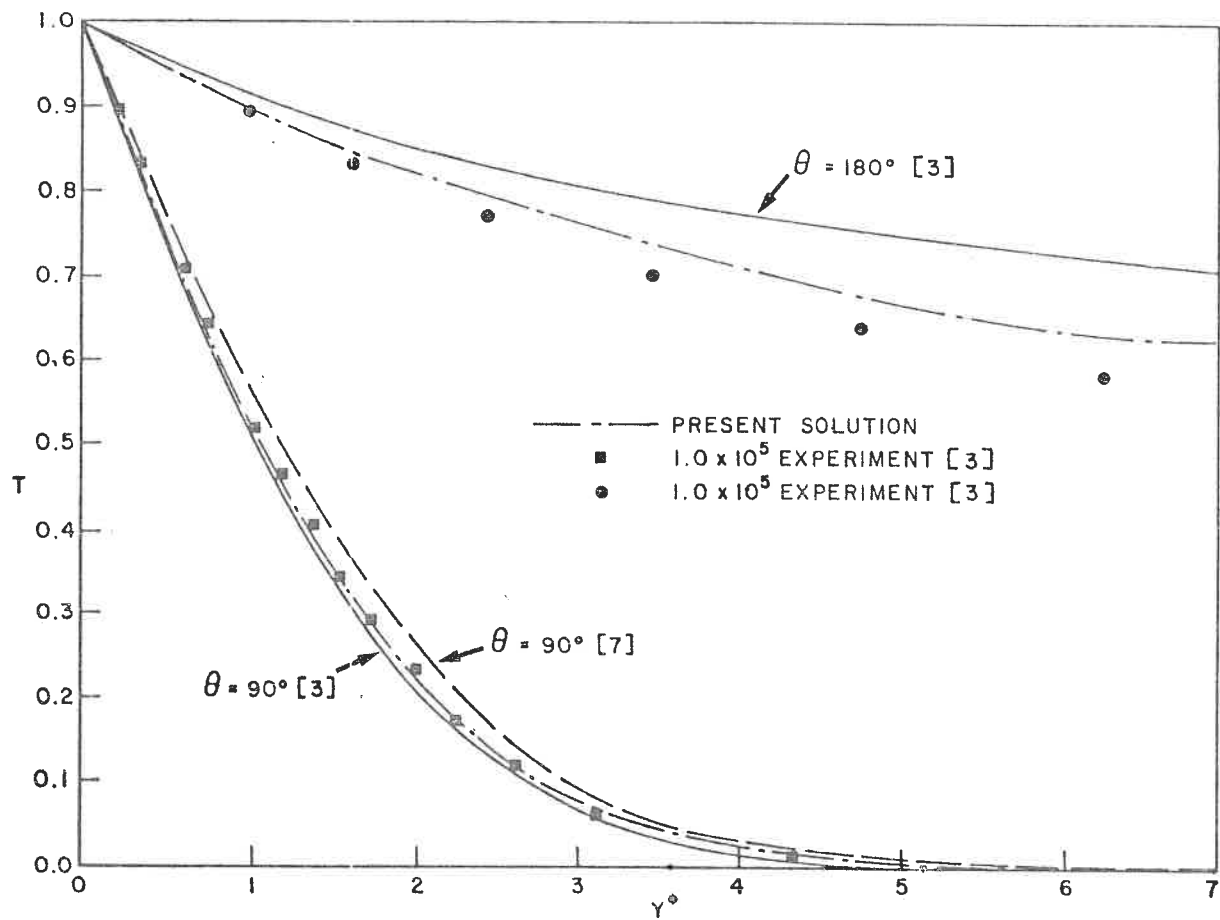
Fig. 10 Comparison between numerically computed and experimentally measured temperature profiles ($\theta = 90°$ and $180°$, Ra $= 10^5$).
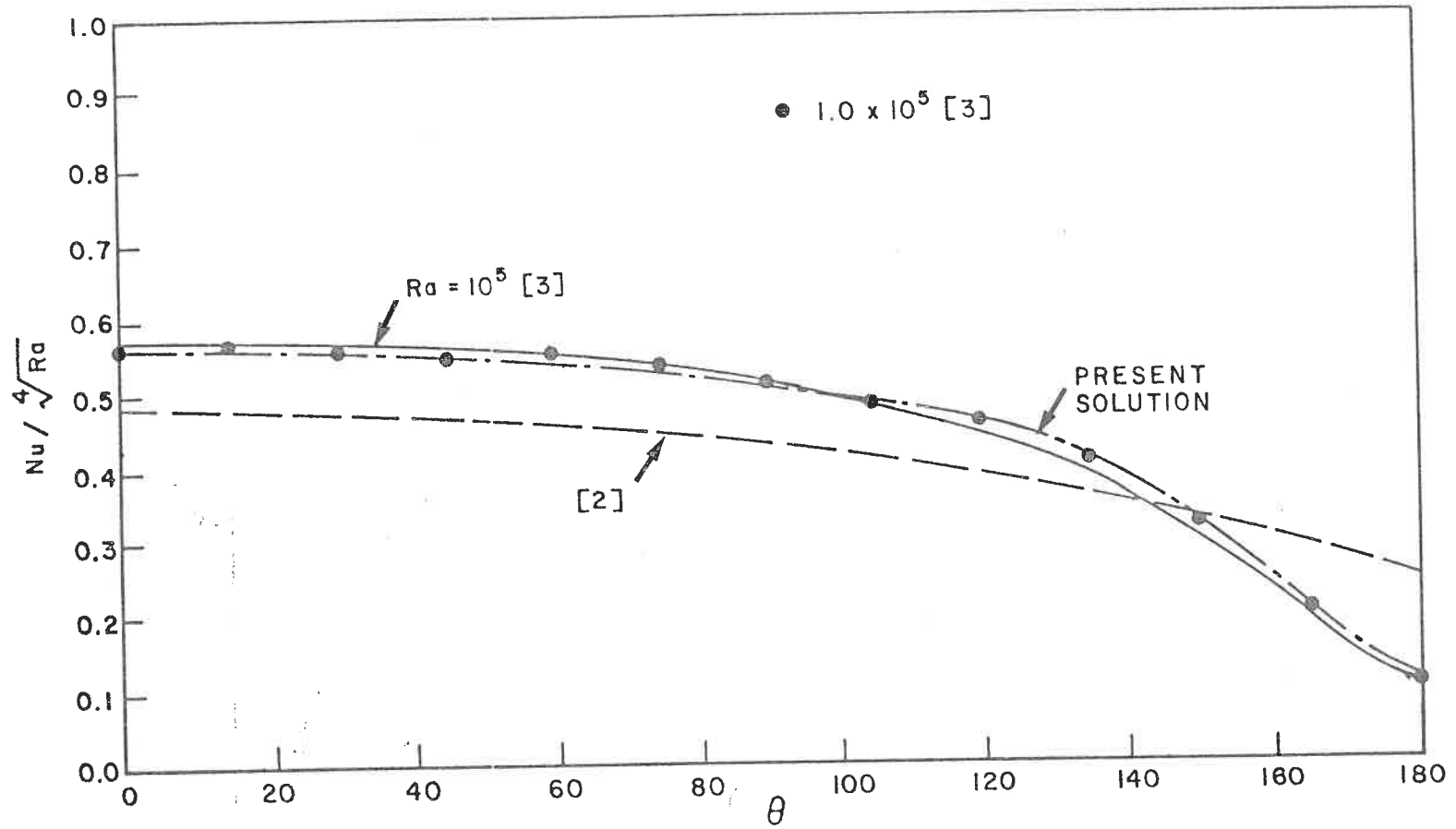
Fig. 11 Comparison between numerical and experimental local heat transfer coefficients at Ra $= 10^5$.
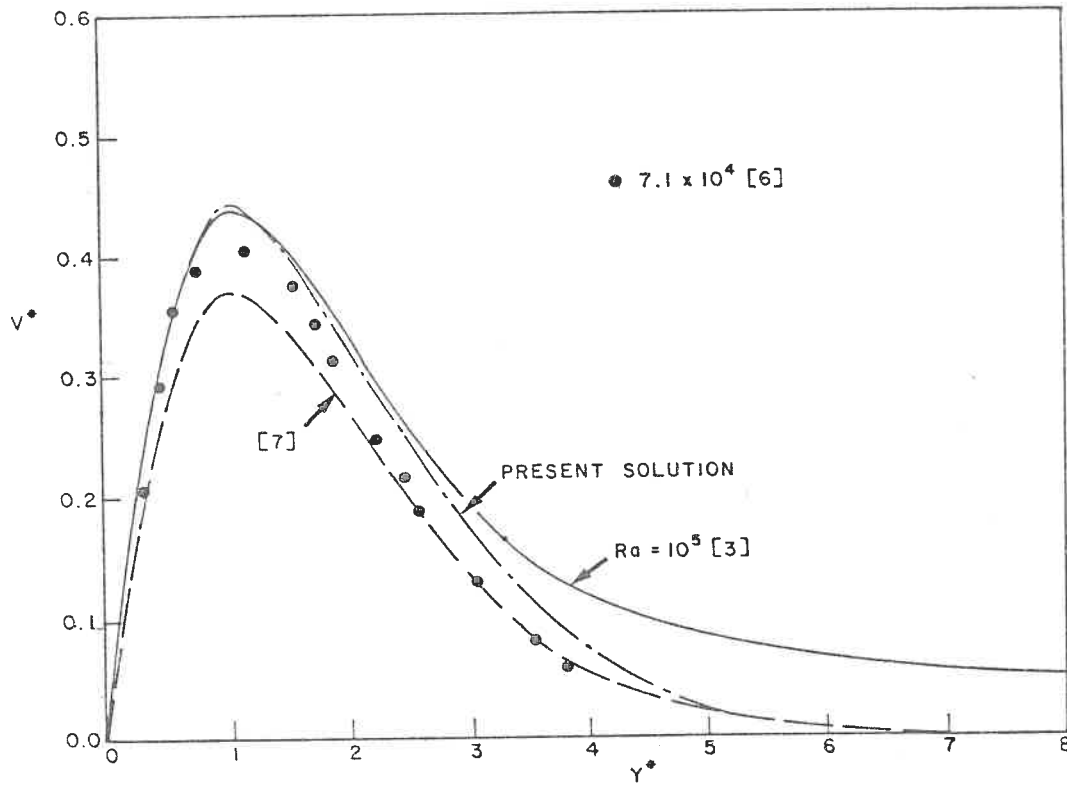
FLOW ABOUT A HORIZONTAL CYLINDER

Fig. 12 Comparison between experimental and numerically determined tangential velocity at $\theta = 90°$ and $Ra = 10^5$.

Table 3 Comparison Between Present Computed Local and Average Heat Transfer Coefficients and those of Ref. [13] $[T_w = 1, \text{Nu} = -(\partial T/\partial r)_w]$

| Ra		Nu for different values of θ							$\overline{\text{Nu}}$
		0°	30°	60°	90°	120°	150°	180°	
10^3	present	3.86	3.82	3.70	3.45	2.93	1.98	1.20	3.06
	Ref. [3]	3.89	2.85	3.72	3.45	2.93	2.01	1.22	3.09
10^4	present	6.03	5.98	5.80	5.56	4.87	3.32	1.50	4.86
	Ref. [3]	6.24	6.19	6.01	5.64	4.82	3.14	1.46	4.94
10^5	present	9.80	9.69	9.48	8.90	8.00	5.80	1.94	7.97
	Ref. [3]	10.15	10.03	9.65	9.02	7.91	5.29	1.72	8.00
10^6	present	16.48	16.29	15.95	14.85	13.35	10.58	2.52	13.46
	Ref. [3]	16.99	16.78	16.18	15.19	13.60	9.38	2.12	13.52
10^7	present	28.27	27.98	26.95	25.40	23.00	19.68	4.20	23.29
	Ref. [3]	29.41	29.02	27.95	26.20	23.46	16.48	2.51	23.32
2×10^7	present	33.46	33.07	31.92	30.07	27.18	23.38	5.42	27.58
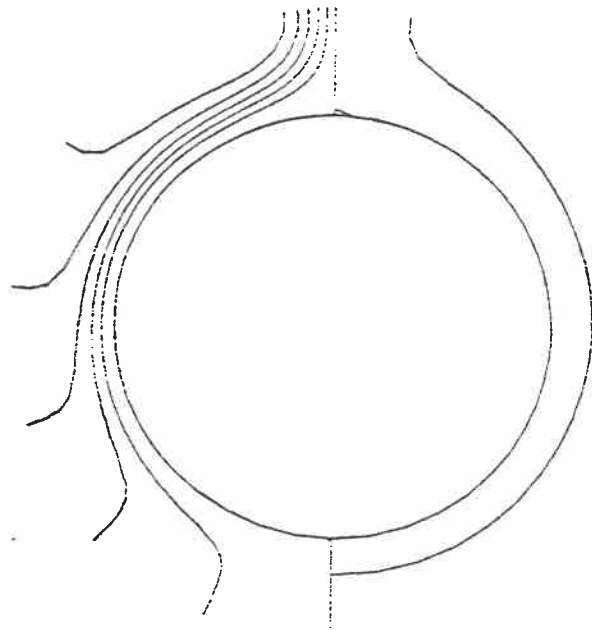
(a)
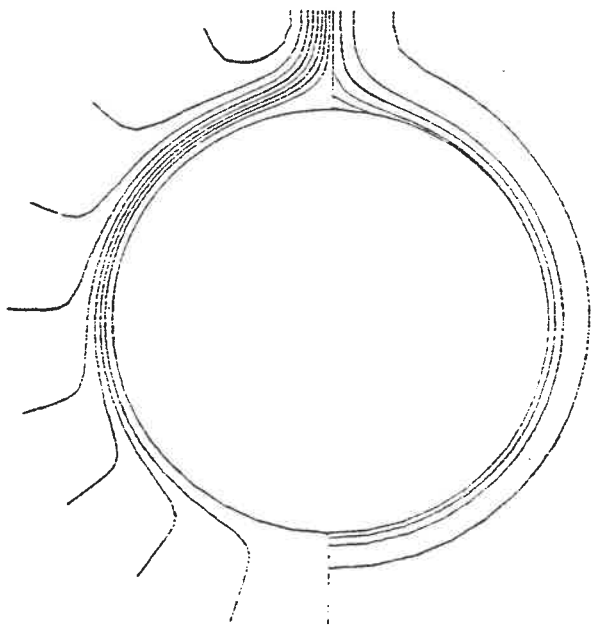
(b)

Fig. 13 Isotherms and streamlines for Ra** = 2 × 10⁷, Pr = 0.7: (a) Bi = 1 (Δ¥ = 10, ΔT = 0.1); (b) Bi = 10 (Δ¥ = 10, ΔT = 0.1).
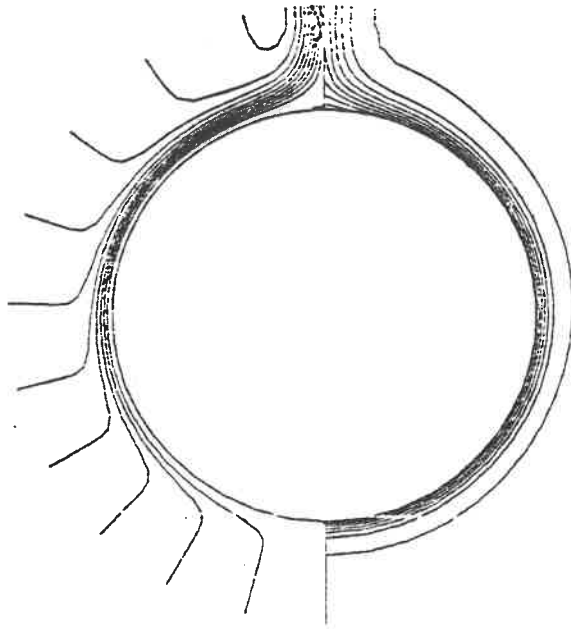
(c)

Fig. 13 Isotherms and streamlines for $Ra^{**} = 2 \times 10^7$, $Pr = 0.7$ (*Continued*): (c) $Bi = 50$ ($\Delta\Psi = 10$, $\Delta T = 0.1$).
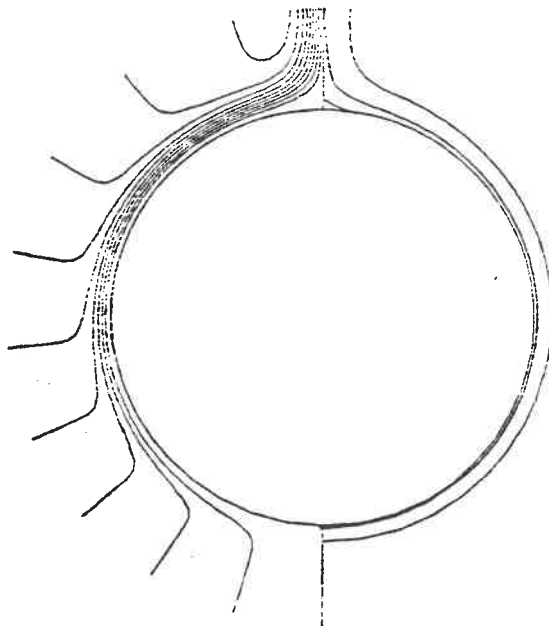

Fig. 14 Isotherms and streamlines for $Ra^{**} = 4 \times 10^8$, $Pr = 0.7$ ($\Delta\Psi = 10$, $T_{max} = 0.072$, and $\Delta T = 0.02$).
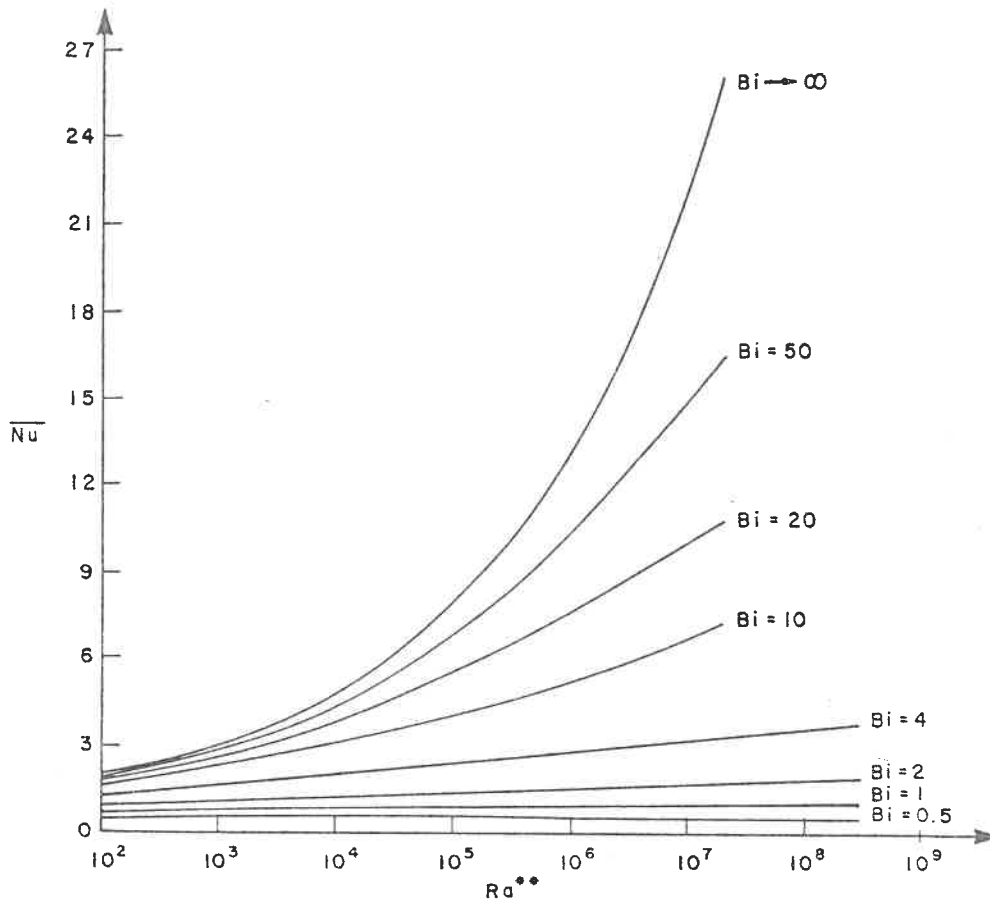
Fig. 15 Influence of Biot number on average heat transfer coefficient for $10^2 \leq Ra^{**} \leq 10^8$.

to the cylinder surface appear as shown in Fig. 6(b). The corresponding variation of temperature distribution is shown in Fig. 9. However, it is interesting to note that for Bi = 1, the numerical solution was continued up to $Ra^{**} = 4 \times 10^9$ without any formation of separation vortices as shown in Fig. 14. The boundary layer thickness and the tangential velocity are of about the same order as for the case of $Ra = 2 \times 10^7$, but the surface temperature is very small.

In order to further investigate the origin of these vortices, computations were first repeated with a refined grid in order to ascertain whether their cause may be purely numerical. Even under these conditions, the vortices were persistent, leading to the conclusion that they originate from the physics of the flow. The higher Biot numbers result in higher surface temperatures, therefore causing a Benard-type instability with local convection cells that resemble separation vortices. Detailed computations in the region between $\theta = 170°$ and $180°$ (the vertical plane of symmetry) indicated that the average radial temperature along the line $\theta = 170°$ was larger than that along $\theta = 180°$. It seems reasonable to speculate that therefore a sort of "minicavity" with one sidewall hotter than the other is formed, leading to the circulation. An examination of the local Nusselt numbers in the vicinity of the separation region indicates that they plunge steeply when vortices are present, while when the vortices are absent, there is still a drop in the

FLOW ABOUT A HORIZONTAL CYLINDER

Nusselt numbers, although it is much less marked. The vortices therefore act to transport heat from the hotter to the cooler regions, thus reducing the surface heat transfer. This phenomenon will be further discussed in a subsequent report.

For this case, the present authors have not been able to locate published numerical or experimental results for purposes of comparison. A more interesting case with practical applications, where the natural convection flow outside the cylinder is combined with a forced convection flow inside the cylinder, merits attention. In such a case, the specified boundary conditions on the external and internal surface heat transfer form a coupled system.

CONCLUSIONS

This paper has reported on the results of a numerical investigation into the natural convection flow around a heated horizontal cylinder at various Rayleigh numbers using multistep spline integration techniques. A general formulation to treat mixed boundary conditions using cubic splines has been presented. This formulation is easily incorporated into the solution procedure. All results were computed on a personal computer using unequally spaced grids that provided good results with a minimum number of computational points. Some new computations at very high Rayleigh numbers indicate the existence of attached "separation" vortices in the downstream plume region, the appearance of these vortices being dependent on the values of the Biot number. The numerical scheme presented here appears to be versatile, so that a large range of computations may be made. Solutions for the transient phase of natural convection will be presented in a later report.
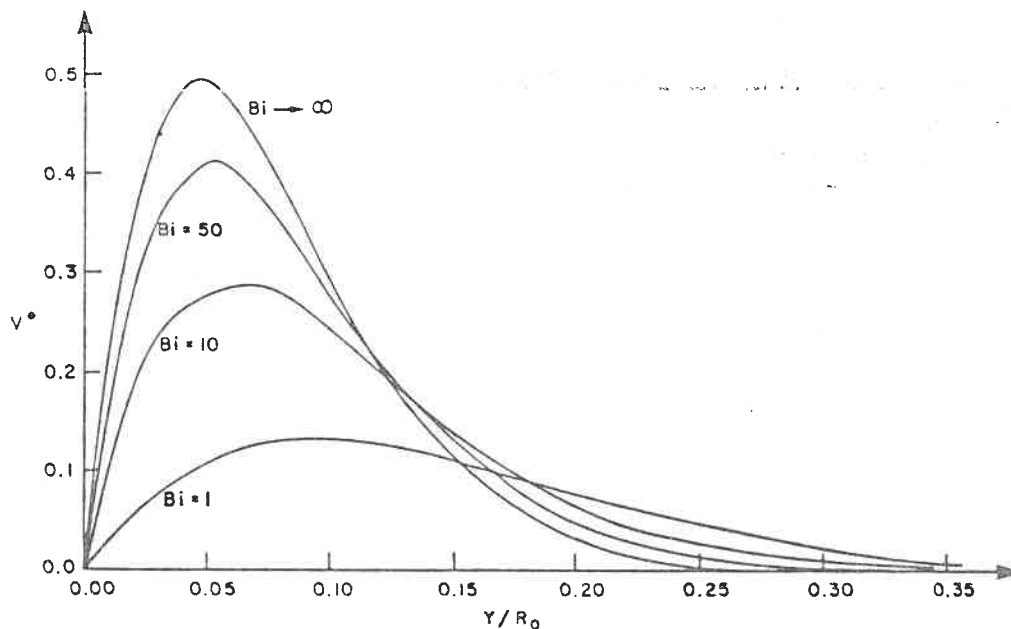

Fig. 16 Tangential velocity profiles at $\theta = 139.22°$ and $Ra^{**} = 10^7$ for various Bi.

P. WANG ET AL.

REFERENCES

1. V. T. Morgan, The Overall Convective Heat Transfer from Smooth Circular Cylinders, *Adv. Heat Transfer*, vol. 11, pp. 199–264, 1975.
2. J. H. Merkin, Free Convection Boundary Layers on Cylinders of Elliptic Cross Section, *J. Heat Transfer*, vol. 99, pp. 453–457, 1977.
3. T. H. Kuehn and R. J. Goldstein, Numerical Solution to the Navier-Stokes Equations for Laminar Natural Convection about a Horizontal Isothermal Circular Cylinder, *Int. J. Heat Mass Transfer*, vol. 23, pp. 971–979, 1980.
4. B. Farouk and S. I. Guceri, Natural Convection from a Horizontal Cylinder—Laminar Regime, *J. Heat Transfer*, vol. 103, pp. 522–527, 1981.
5. Z. H. Qureshi and R. Ahmad, Natural Convection from a Uniform Heat Flux Horizontal Cylinder at Moderate Rayleigh Numbers, *Numer. Heat Transfer*, vol. 11, pp. 199–212, 1987.
6. T. Aihara and E. Saito, Measurement of Free Convection Velocity Field around the Periphery of a Horizontal Torus, *J. Heat Transfer*, vol. 94, pp. 95–98, 1972.
7. T. Chiang and J. Kaye, On Laminar Free Convection from a Horizontal Cylinder, Proc. 4th Natl. Congr. Appl. Mech., pp. 1213–1219, 1962.
8. G. Wilks, External Natural Convection about Two-Dimensional Bodies with Constant Heat Flux, *Int. J. Heat Mass Transfer*, vol. 15, pp. 351–354, 1972.
9. S. W. Churchill, Laminar Free Convection from a Horizontal Cylinder with a Uniform Heat Flux Density, *Lett. Heat Mass Transfer*, vol. 1, pp. 109–112, 1974.
10. S. W. Churchill and H. S. Chu, Correlating Equations for Laminar and Turbulent Free Convection from a Horizontal Cylinder, *Int. J. Heat Mass Transfer*, vol. 18, pp. 1049–1053, 1975.
11. P. Wang, Spline Method of Fractional Steps in Numerical Model of Unsteady Natural Convection Flow at High Rayleigh Number, *Numer. Heat Transfer*, vol. 11, no. 1, pp. 95–118, 1987.
12. S. G. Rubin and R. A. Graves, Viscous Flow Solutions with a Cubic Spline Approximation, *Comput. Fluids*, vol. 3, pp. 1–36, 1975.
13. S. G. Rubin and P. K. Khosla, Higher Order Numerical Solutions using Cubic Splines, *AIAA J.*, vol. 14, pp. 851–859, 1976.
14. S. G. Rubin and P. K. Khosla, Polynomial Interpolation Methods for Viscous Flow Calculations, *J. Comput. Phys.*, vol. 24, pp. 217–244, 1977.
15. P. Wang and R. Kahawita, Numerical Integration of Partial Differential Equations using Cubic Splines, *Int. J. Comput. Math.*, vol. 13, pp. 271–286, 1983.
16. P. Wang and R. Kahawita, A Two-Dimensional Numerical Model of Estuarine Circulation using Cubic Splines, *Can. J. Civ. Eng.*, vol. 10, pp. 116–124, 1983.
17. P. Wang, S. Lin, and R. Kahawita, The Cubic Spline Integration Technique for Solving Fusion Welding Problems, *ASME Trans. J. Heat Transfer*, vol. 107, pp. 485–489, 1985.
18. G. Lauriat and I. Altimir, A New Formulation of the SADI Method for the Prediction of Natural Convection Flows in Cavities, *Comput. Fluids*, vol. 13, pp. 141–155, 1985.
19. P. Wang and R. Kahawita, The Numerical Solution of the Unsteady Natural Convection Flow in a Square Cavity at High Rayleigh Number using the SADI Method, *Appl. Math. Mech.*, vol. 8, no. 3, pp. 219–228, 1987.
20. P. Wang, The Method of Fractional Steps for Solving Navier-Stokes Equations using Parametric Splines (in Chinese), *Acta Aerodyn. Sinica*, vol. 5, no. 3, pp. 218–225, 1987.
21. H. J. Show, C. K. Chen, and J. W. Cleaver, Cubic Spline Numerical Solution for Two-Dimensional Natural Convection in a Partially Divided Enclosure, *Numer. Heat Transfer*, vol. 12, pp. 439–455, 1987.

FLOW ABOUT A HORIZONTAL CYLINDER

22. P. Wang, Variable Time Step Methods using Cubic Splines for the One-Dimensional Stefan Problem with Mixed Boundary Conditions (in Chinese), in *1984 Proceedings of National Conference on Heat and Mass Transfer,* pp. 38–43, Science Press, Beijing, Peoples' Republic of China, 1986.

Requests for reprints should be sent to R. Kahawita.

CHAPTER III

TRANSIENT LAMINAR NATURAL CONVECTION

FROM HORIZONTAL CYLINDERS

INTRODUCTION

In this Chapter, the unsteady laminar natural convection flow from a heated horizontal cylinder under diverse surface boundary conditions has been investigated numerically. Although the laminar natural convection from horizontal cylinders has been extensively investigated analytically, numerically and experimentally as mentioned in Chapter II, most prior work has concentrated on steady state situations with either a specified surface temperature or a uniform surface heat flux. Studies on transient free convection have been much less abundant. The great majority of studies reported in the literature were concerned with geometries such as vertical cylinders or plates. Unsteady natural convection from horizontal cylinders has not been extensively treated.

To this author's knowledge, transient solutions of the complete Navier-Stokes and energy equations for high Rayleigh numbers have not yet been reported. It appears that the primary difficulty to be overcome by the numerical procedure is the manner in which the outer (artificially imposed) boundary conditions, particularly the thermal condition at the outflow boundary of the plume is to be specified.

In the present investigation, a scale analysis to theoretically predict the types of flow and heat transfer patterns that can develop near the cylinder surface has been introduced. Some characteristics of the boundary layer obtained with this

scale analysis have been compared with the numerical results. The development of the plume region as well as the surface heat transfer and local flowfield have been evaluated. At small times, the present numerical solutions approach the boundary layer results and are in good agreement with the results from the scale analysis. Some advantages of spline techniqueare that a variable grid spacing may be used, the method is of high accuracy, requires fewer grid points for a given problem and can therefore be used on a personal computer since core storage requivement are economised. In addition, due to the various formulations possible, i.e. using the variable, its first derivative or its second derivative as the "operational variable", higher order boundary conditions may be easily incorporated into the numerical scheme.

All results have been obtained using a personal computer. Computational results have been obtained for a range of Rayleigh numbers between 0.1 to 2×10^7. Good agreement with published experimental and numerical data has been obtained. Overshoot and oscillatory behaviour of the local Nusselt numbers have been observed which decay as the steady state is approached. This has been associated with fluid inertia effects. At high Rayleigh numbers, the appearance of separation vortices, which are subsequently formed, shed and reformed when $Ra > 5 \times 10^7$, has been noted. A more detailed study of the development of the plume region, using computed particle trajectories has been reported.

The principal results of this investigation have been published in the following paper:

Int. J. Heat Mass Transfer, *Vol. 34, No.6, pp.1429-1442.(1991)*

Transient laminar natural convection from horizontal cylinders

P. WANG,† R. KAHAWITA† and D. L. NGUYEN†‡

† Department of Civil Engineering, Ecole Polytechnique de Montréal, Montréal, Québec, H3C 3A7, Canada
‡ VP Recherche, Hydro-Québec, Varennes, Québec, J3X 1S1, Canada

Abstract—The unsteady laminar natural convection flow from a heated horizontal cylinder under diverse surface boundary conditions is investigated numerically using the spline fractional step method. Some characteristics of the boundary layer obtained with a scale analysis are compared with the numerical results. The development of the plume region as well as the surface heat transfer and local flow field are evaluated. At small times, the present numerical solutions approach the boundary layer results and are in good agreement with the results from the scale analysis. A more detailed study of the development of the plume region, using computed particle trajectories is reported. All results are obtained using a personal computer. Qualitative comparisons between the present results and flow visualization experiments partially verify the numerical results.

INTRODUCTION

TWO-DIMENSIONAL laminar natural convection from horizontal cylinders has been extensively investigated analytically, numerically and experimentally. Most prior work has concentrated on steady-state situations with either a specified surface temperature or a uniform surface heat flux. Thus Kuehn and Goldstein [1] numerically solved the complete Navier–Stokes and energy equations for laminar natural convection from a horizontal isothermal cylinder using a finite-difference technique. Farouk and Guceri [2] attacked the same problem for uniform as well as non-uniform surface temperature and heat flux distributions on the cylinder. Qureshi and Ahmad [3] provided numerical solutions for a horizontal cylinder with uniform heat flux using a technique similar to that indicated in ref. [1]. The authors [4] recently reported on an extensive numerical study of the laminar natural convection flow from a heated horizontal cylinder using a newly developed spline fractional step technique [5].

The literature on transient free convection studies is much less abundant. The great majority of studies reported in the literature are concerned with geometries such as vertical cylinders or plates. Typically, an initially pure conduction situation is followed by a convective transition regime in which leading edge effects become dominant. Finally, a transient approach to a steady state occurs. Unsteady natural convection from a horizontal cylinder has not been extensively treated. A perusal of the current literature on the subject indicates that very few studies have been realized in which an attempt is made to define the typical characteristics of the problem. An experimental study by Ostroumov [6] reported on the development of the convection regime initiated by a suddenly heated fine wire. Vest and Lawson [7] also

reported on a similar experiment. Parsons and Mulligan [8] presented experimental data for the transient free convective heat transfer from a horizontal wire in air. An early analytical study, using the boundary layer approximation and series continuation for small time was established by Elliott [9]. He considered large Grashof numbers and derived solutions for the stream function and the temperature field. Values of the skin friction and heat transfer coefficient obtained for small time were then extrapolated to infinite time to predict their final steady-state values. These results are of course, invalid in the plume region where the boundary layer assumption breaks down. Based on ref. [9], Gupta and Pop [10] performed a perturbation analysis of the boundary layer equations for the unsteady free convection past a circular cylinder in order to estimate the influence of curvature effects on the surface heat transfer as well as on the skin friction. Their results indicated that the curvature leads to an increase in both skin friction and heat transfer rate from the surface of the cylinder. In a study similar to that of ref. [8], Katagiri and Pop [11] reported numerical solutions to the unsteady free convection for an isothermal horizontal cylinder the temperature of which is suddenly increased to a large Grashof number. Sako *et al.* [12] presented numerical solutions to the transient natural convection from a horizontal cylinder at low Rayleigh numbers using a hybrid grid. Their results for the mean Nusselt numbers at steady state agree fairly well with those of Kuehn and Goldstein [1]. Genceli [13] presented experimental data for the onset of convection in water around a horizontal cylinder subjected to a constant surface heat flux. A critical Rayleigh number which defines the onset of convection was reported. Most recently, Song [14] published some numerical results of transient natural convection around a horizontal wire under a constant

NOMENCLATURE

D	cylinder diameter	V	angular velocity, positive counterclockwise
g	gravitational acceleration		
h	local heat transfer coefficient	V^*	modified dimensionless angular velocity, $VD/(\alpha\, Ra^{0.5})$
k	fluid thermal conductivity		
L	dimensionless radial distance between cylinder surface and outer boundary of solution domain	Y	radial distance from cylinder surface
		Y^*	$(Y\, Ra^{0.25})/D$.
Nu	Nusselt number, hD/k		
p'	pressure	Greek symbols	
Pr	Prandtl number, μ/α	α	thermal diffusivity
q''	surface heat flux	β	coefficient of thermal expansion
r	dimensionless radial coordinate, r'/D	δ_T	thickness of the thermal boundary layer
r'	radial coordinate	δ_v	thickness of the viscous layer
Ra	Rayleigh number, $g\beta D^3(T'_w - T'_\infty)/\mu\alpha$	θ	angular coordinate; zero is downward vertical, positive counter-clockwise on right half of cylinder
Ra^*	modified Rayleigh number, $g\beta q'' D^4/k\alpha\mu$		
t	dimensionless time, $t'\alpha/D^2$ (* signifies steady state almost attained)	μ	kinematic viscosity
		τ	time scale for the form of the thermal boundary layer
t'	time		
T	dimensionless temperature	τ_d	delay time
T'	temperature	Ψ	dimensionless stream function
T'_w	temperature of cylinder surface	Ω	dimensionless vorticity.
T'_∞	temperature of ambient fluid		
u	dimensionless radial velocity, UD/α	Superscript	
		$^-$	average value.
U	radial velocity, positive outwards		
U^*	modified dimensionless radial velocity, $UD/(\alpha\, Ra^{0.25})$	Subscripts	
		i, j	nodal positions in the radial and angular directions, respectively.
v	dimensionless angular velocity, VD/α		

heat flux using a finite difference method. His study however, was carried out only at low Rayleigh numbers ($0.12 < Ra^* < 20$). Furthermore, a physically unrealistic boundary condition imposed at the outer limit (i.e. $T = 0$ at $r = \infty$) of his computational domain would probably lead to numerical difficulties at high Rayleigh number computations.

To the authors' knowledge, transient solutions of the complete Navier–Stokes and energy equations for high Rayleigh numbers have not yet been reported. It appears that the primary difficulty to be overcome by the numerical procedure is the manner in which the outer (artificially imposed) boundary conditions, particularly the thermal condition at the outflow boundary of the plume is to be specified. A commonly used condition for the steady-state problem is to assume that the temperature gradient normal to the pseudo boundary is zero, thus implying that the heat transfer is dominated by convective movement rather than by conduction [1]. This obviously requires that the outflow velocities are sufficiently large, a condition that is probably satisfied within the scope of the steady-state case, since the plume region is fully developed. For the transient case however, before the full development of the plume, the validity of this assumption is not at all obvious.

Consequently, the present investigation is devoted to the numerical simulation of the transient laminar natural convection flow about a finite horizontal cylinder for a complete range of Rayleigh numbers using the spline method presented in ref. [4]. The advantages of this technique are that a variable grid spacing may be used, thus obviating the need for hybrid grids with their attendant interpolations; it is of high accuracy; requires fewer grid points for a given problem and can therefore be used on a personal computer. In addition, due to the various formulations possible, i.e. using the variable, its first derivative or its second derivative as the 'operational variable', higher order boundary conditions can be easily incorporated into the numerical scheme [15]. Computational results have been obtained for a range of Rayleigh numbers between 0.1 and 2×10^7.

GOVERNING EQUATIONS

The natural convection flow from a horizontal cylinder is governed by the continuity equation, the two-dimensional Navier–Stokes equation and the energy equation. In cylindrical polar coordinates, they take the following form:

continuity

$$\frac{\partial u'}{\partial r'} + \frac{u'}{r'} + \frac{1}{r'}\frac{\partial v'}{\partial \theta} = 0 \tag{1}$$

momentum, in the radial (r) direction

$$\frac{\partial u'}{\partial t'} + u'\frac{\partial u'}{\partial r'} + \frac{v'}{r'}\frac{\partial v'}{\partial \theta} - \frac{v'^2}{r'} = \frac{1}{\rho}\frac{\partial p'}{\partial r'}$$

$$-g\cos\theta[1 - \beta(T' - T'_\infty)]$$

$$+\mu\left(\frac{\partial^2 u'}{\partial r'^2} + \frac{1}{r'}\frac{\partial u'}{\partial r'} + \frac{u'}{r'^2} + \frac{1}{r'^2}\frac{\partial^2 u'}{\partial \theta^2} - \frac{2}{r'^2}\frac{\partial v'}{\partial \theta}\right) \tag{2}$$

momentum, in the circumferential (θ) direction

$$\frac{\partial v'}{\partial t'} + u'\frac{\partial v'}{\partial r'} + \frac{v'}{r'}\frac{\partial v'}{\partial \theta} + \frac{u'v'}{r'} = \frac{1}{\rho r'}\frac{\partial p'}{\partial \theta}$$

$$+g\sin\theta[1 - \beta(T' - T'_\infty)]$$

$$+\mu\left(\frac{\partial^2 v'}{\partial r'^2} + \frac{1}{r'}\frac{\partial v'}{\partial r'} + \frac{v'}{r'^2} + \frac{1}{r'^2}\frac{\partial^2 v'}{\partial \theta^2} + \frac{2}{r'^2}\frac{\partial u'}{\partial \theta}\right) \tag{3}$$

energy

$$\frac{\partial T'}{\partial t'} + u'\frac{\partial T'}{\partial r'} + \frac{v'}{r'}\frac{\partial T'}{\partial \theta}$$

$$= \alpha\left(\frac{\partial^2 T'}{\partial r'^2} + \frac{1}{r'}\frac{\partial T'}{\partial r'} + \frac{1}{r'^2}\frac{\partial^2 T'}{\partial \theta^2}\right). \tag{4}$$

The non-dimensional equations in stream function and vorticity form (using the Boussinesq approximation for the body forces) may be written as

$$\nabla^2\Psi = -\Omega \tag{5}$$

$$\frac{\partial\Omega}{\partial t} + u\frac{\partial\Omega}{\partial r} + \frac{v}{r}\frac{\partial\Omega}{\partial \theta} = Pr\,\nabla^2\Omega$$

$$+ Pr\,Ra\left(\sin\theta\frac{\partial T}{\partial r} + \cos\theta\frac{1}{r}\frac{\partial T}{\partial \theta}\right) \tag{6}$$

$$\frac{\partial T}{\partial t} + u\frac{\partial T}{\partial r} + \frac{v}{r}\frac{\partial T}{\partial \theta} = \nabla^2 T \tag{7}$$

with

$$\nabla^2 = \frac{\partial^2}{\partial r^2} + \frac{1}{r}\frac{\partial}{\partial r} + \frac{1}{r^2}\frac{\partial^2}{\partial \theta^2} \tag{8}$$

and

$$u = \frac{1}{r}\frac{\partial\Psi}{\partial \theta}, \quad v = -\frac{\partial\Psi}{\partial r}. \tag{9}$$

Boundary conditions

Since the flow is symmetric about a vertical plane passing through the axis of the cylinder, only the half-plane need be considered. The boundary conditions then become

$$u = v = \Psi = 0$$

$$\Omega = -\frac{\partial^2\Psi}{\partial r^2}$$

and

$$T = 1$$

or

$$\frac{\partial T}{\partial r} = -1$$

on the cylinder surface and

$$\Psi = v = \Omega = \frac{\partial T}{\partial \theta} = 0 \tag{10}$$

on the lines of symmetry.

At the inflow region ($u < 0$)

$$v = \frac{\partial\Psi}{\partial r} = 0 = T, \quad \Omega = -\frac{1}{r^2}\frac{\partial^2\Psi}{\partial\theta^2} \tag{11}$$

on the outflow region ($u > 0$)

$$v = \frac{\partial\Psi}{\partial r} = 0, \quad \Omega = -\frac{1}{r^2}\frac{\partial^2\Psi}{\partial\theta^2}. \tag{12}$$

For the temperature boundary condition, attempts were made to develop a modified relation that may better express the intrinsic feature of the transient flow, without success. In the present study therefore, the commonly used boundary condition for outflow, i.e. a zero temperature gradient normal to the pseudo boundary has been adopted

$$\frac{\partial T}{\partial r} = 0. \tag{13}$$

Fortunately, numerical tests indicated [4] that during the transient state at higher Rayleigh numbers when the outflow boundary is far enough away from the cylinder surface, its influence on both the heat transfer and fluid flow near the surface of the cylinder is negligible, and the convection effects always dominate over conduction so that the latter can be usually neglected. A detailed discussion of this point will be presented in a forthcoming report.

NUMERICAL CONSIDERATIONS

The spline fractional step method (SFSM) [5] was used to generate an algorithm resulting in a tridiagonal system containing either function values or first derivatives at the grid points. The essential feature of this method is that at each computational step, the problem is treated as a one-dimensional case in implicit form so that only one tridiagonal matrix system needs to be evaluated. The SFSM schemes representing the governing equations (5)–(7) and the boundary condition imposed at the outer circular limit have been reported in detail in ref. [4] and will therefore not be elucidated further.

RESULTS AND DISCUSSION

Scale analysis

Before solving equations (5)–(7) numerically, it is useful to rely on pure scaling arguments to theoretically predict the types of flow and heat transfer patterns that can develop near the cylinder surface. The scale analysis follows that due to Patterson and Imberger [16] for the natural convection flow in a rectangular cavity.

Immediately after the start of heating ($t' = 0$), the fluid bordering the cylinder surface is motionless, so that the energy equation (4) expresses a balance between thermal inertia and conduction normal to the cylinder surface. Taking $\Delta T'$, t' and $\delta_{T'}$ as the scales of changes on T', t' and the radial coordinate r' in equation (4) and assuming $\partial^2 T'/\partial r'^2 \gg \partial^2 T'/\partial \theta^2$ and $r' \gg \delta_{T'}$, the following relation may be obtained from equation (4):

$$\frac{\Delta T'}{t'} \sim \alpha \frac{\Delta T'}{\delta_{T'}^2}. \tag{14}$$

So

$$\delta_{T'} \sim (\alpha t')^{0.5}. \tag{15}$$

The heated layer $\delta_{T'}$ will naturally tend to rise along the cylinder wall. As in ref. [17] the velocity scale of this tangential motion may be obtained from the two momentum equations (2) and (3) by eliminating the pressure and retaining the dominant terms. For $Pr > 1$ (marginally valid for $Pr \simeq 1$ [17]), from the balance between buoyancy force and viscous force, the initial tangential velocity scale is

$$v' \sim \frac{g\beta'\Delta T' \sin\theta}{\mu} t'. \tag{16}$$

Comparing with the vertical velocity scale for the rectangular cavity [16], it may be seen that the difference arises just in the term $\sin\theta$ inside the coefficient, since the dependence of tangential velocity will obviously depend on position θ.

The buoyancy forces act to accelerate the fluid only over the thickness $\delta_{T'}$; heat is being convected into this layer by the tangential velocity equation (16), and the layer will continue to grow until the heat conducted in from the boundary balances that convected away. For the present case, the convection term is of the order of $(\bar{v}'\Delta T'/R\pi)$ and the conduction term is of the order of $(\alpha\Delta T'/\delta_{T'}^2)$, thus

$$\frac{\bar{v}'\Delta T'}{R\pi} \sim \frac{\alpha\Delta T'}{\delta_{T'}^2} \tag{17}$$

or

$$\bar{v}'\Delta T'\delta_{T'} \sim \frac{\alpha\Delta T'}{\delta_{T'}} R\pi.$$

This relation, in fact, expresses the above balance. Here $\bar{v}'$ represents the average tangential velocity

$$\bar{v}' = \frac{1}{\pi}\int_0^\pi v' \, d\theta \sim \frac{2}{\pi} \frac{g\beta\Delta T'\alpha}{\mu} t'.$$

From equation (16) we obtain

$$t' \sim \frac{\pi D^2}{2\alpha} Ra^{-0.5}$$

and

$$\delta_{T'} \sim \left(\frac{\pi}{2}\right)^{0.5} D \, Ra^{-0.25}$$

or in dimensionless form

$$\tau \sim \frac{\pi}{2} Ra^{-0.5} \tag{18}$$

and

$$\delta_T \sim \left(\frac{\pi}{2}\right)^{0.5} Ra^{-0.25}. \tag{19}$$

Here, τ represents the time scale of the thermal boundary layer formed. It is interesting to note that this time scale differs by a factor of $\pi/2$ over that ($\tau \sim Ra^{-0.5}$) for a rectangular cavity with height D and horizontal length D. This is because the fluid particles move along the cylinder surface in the boundary layer.

For the case of the constant heat flux surface boundary condition, taking into account the relation $Ra^* = Ra \, Nu$ and the correlation $Nu = 0.800(Ra^*)^{0.175}$ [3], the following relation may be obtained from equation (18):

$$\tau \sim 1.4(Ra^*)^{-0.413}. \tag{18'}$$

The viscous layer is governed by an inertial-viscous balance. From equation (3), the thickness of the viscous layer is about the order of $(\mu^{0.5}t^{0.5})$, i.e.

$$\delta_v \sim \mu^{0.5}t^{0.5} \tag{20}$$

thus

$$\delta_v \sim Pr^{0.5} \, \delta_T \tag{21}$$

which is the same relation as for a rectangular cavity [16].

Numerical solution

Numerical results have been obtained for various boundary conditions. In this paper, due to space limitations, the transient flow and temperature fields and heat transfer results will be discussed principally for the isothermal surface boundary condition although some computations for the constant heat flux case have also been presented.

The time dependent non-linear coupled partial differential equations were solved by considering an $(r-\theta)$ grid 11×21, 21×23, or 17×31 on a non-uniform mesh with $r_{i+1}/r_i = 1.30$ and $\theta_{j+1}/\theta_j = 0.87$ or $r_{i+1}/r_i = 1.10$ and $\theta_{j+1}/\theta_j = 0.91$ or $r_{i+1}/r_i = 1.15$ and $\theta_{j+1}/\theta_j = 0.93$, respectively. Near the cylinder surface and in the plume region, a very fine grid spacing was

chosen. (The angular coordinate θ is measured from the lower symmetry line, positive counterclockwise on the right half of the cylinder.) The change from inflow to outflow is computed automatically as in ref. [4] with no special assumption being required. The time step used in the present calculation was, in general, $\Delta t = 10/Ra$ for the vorticity and energy equations while the stream function equation was solved in false transient form.

Small time solution. At time $t = 0$, the temperature at the surface is increased suddenly from T_∞ to T_w and maintained at this value. Heat is transferred initially by pure conduction to the surrounding medium and for all Rayleigh numbers, this initial conductive phase is characterized by concentric circles for the isotherms in the axial plane, until a certain critical time is reached. Figures 1 and 2 show a typical sequence of the different stages of development at $Ra = 10$ (low Rayleigh number) and 10^7 (high Rayleigh number). Patterns similar to Fig. 1 have been

observed in experiments using a heated wire [7]. For comparison with the experimental data of Genceli [13], a corresponding numerical solution compatible with a cylinder diameter of 25 mm was obtained with $Ra^* = 745\,000$ and $\alpha = 1.43 \times 10^{-7}$ for water at an ambient temperature of 20°C. The isotherm patterns are presented in Fig. 3 for different times. They are in very good agreement with Genceli's photographs using interferometry. According to equation (18′), for the present case $t_c' \sim 22$ and $R_c \sim 20$ (his definition). Comparing the present results with the experiments of ref. [13], the present results have been computed at times slightly advanced with respect to the experiments, as shown in Fig. 3.

A comparison between the present results and the experimental temperature profiles [13] at the top of the cylinder is presented in Fig. 4. The agreement is very good for specific values of critical delay time as well as for the development stage. However, beyond this critical period, a transient region is subsequently
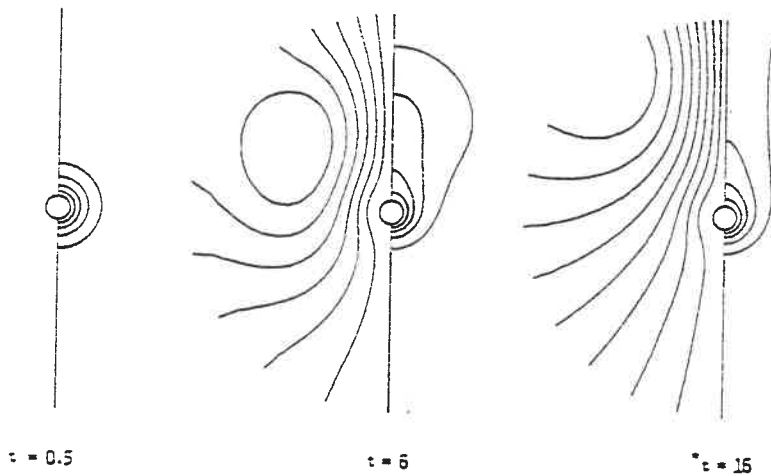
FIG. 1. Isotherms (right) and streamlines (left) at different stages of development for $Ra = 10$ and $Pr = 0.7$ ($\Delta\Psi = 1$ and $\Delta T = 0.1$).

$t = 0.5$ $t = 6$ $t = 15$

$t = 0.0002$ $t = 0.0002$ $t = 0.002$
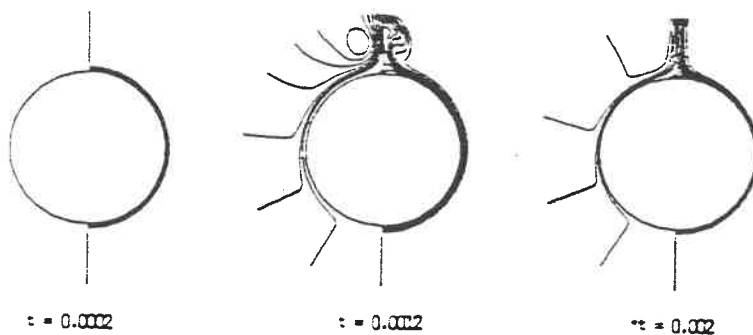
FIG. 2. Isotherms (right) and streamlines (left) at different stages of development for $Ra = 10^7$ and $Pr = 0.7$ ($\Delta\Psi = 20$ and $\Delta T = 0.1$).
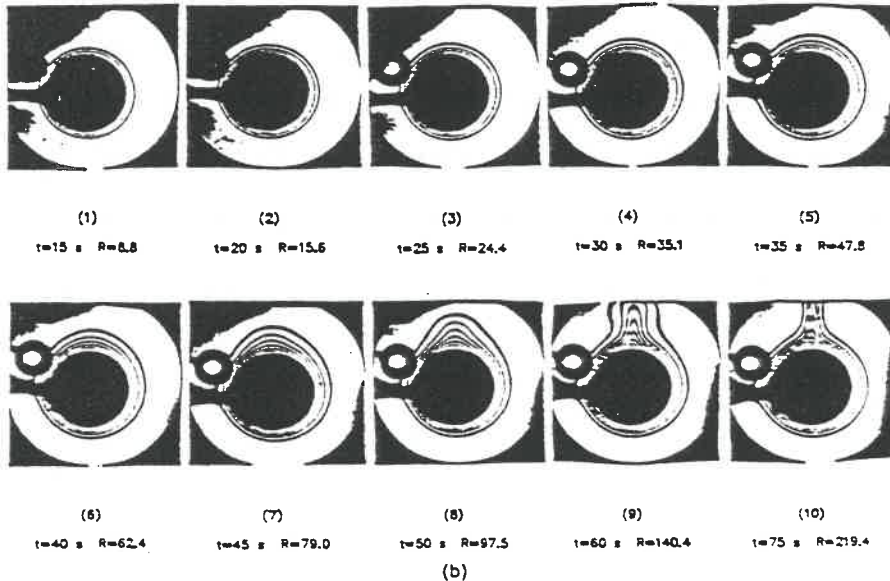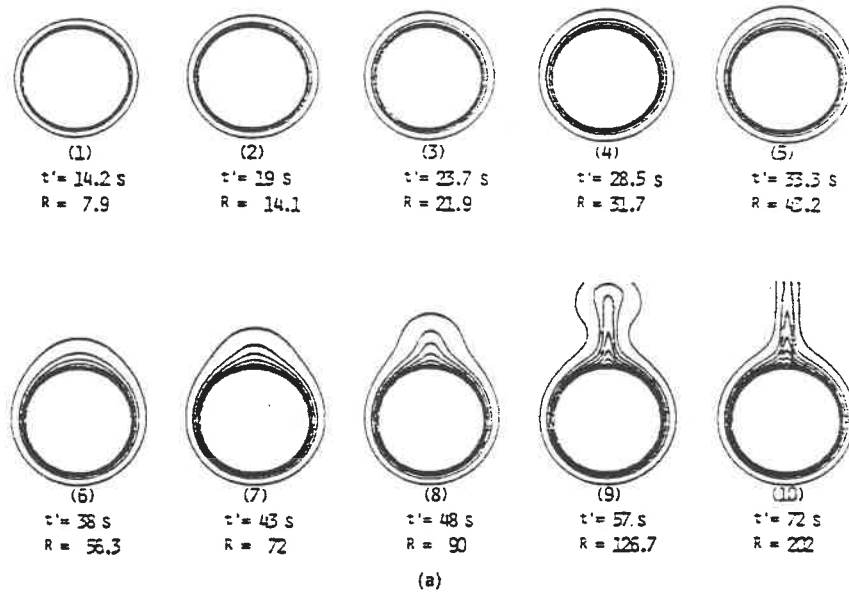
FIG. 3. (a) Isotherms at different stages of development for $Ra^* = 745\,000$ and $Pr = 7.01$ ($\Delta T = 0.2$).
(b) Corresponding experiment from ref. [13].

formed with convective effects where particles start rising towards the top of the cylinder. This phenomenon has also been observed in the experiments of Parsons and Mulligan [8] and this period of time called the 'delay time' is denoted by τ_d. Numerical tests indicate that the value of τ_d is slightly greater than the τ obtained from a scale analysis. Further-

more, when $t \simeq \tau$, the thermal boundary layer thickness at first reaches its equilibrium (steady state) value (except for the plume region); then overshoots to a slightly greater thickness (attained at $t = \tau_d$) and finally backs down to its steady-state position. This phenomenon becomes more accentuated at low Rayleigh numbers. For example, the variation of tem-
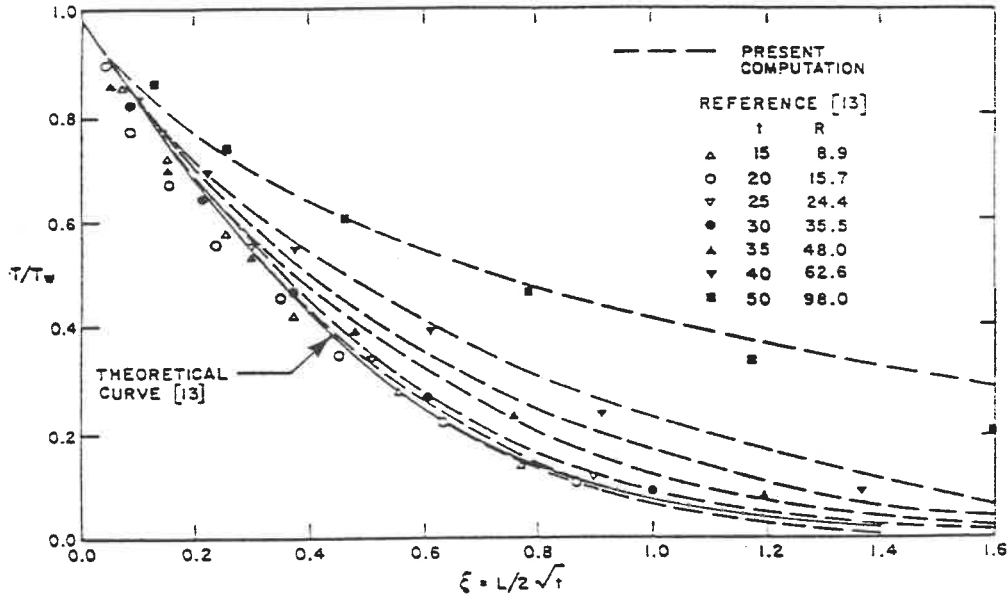
FIG. 4. Comparison between numerically computed and experimentally measured temperature profiles [13] at the top of the cylinder.

perature profiles at different times for $\theta = 90°$ and $Ra = 10$ is exhibited in Fig. 5(a). It is clearly seen that the temperature profile at a dimensionless time of $t = 0.9$ first approaches its steady-state thickness, then subsequently overshoots to its maximum value at about $t = 3.5$ while the corresponding average Nusselt number on the cylinder surface attains its minimum value (Fig. 5(b)), and then finally becomes thinner

at the steady state. (This behaviour has also been observed by Parsons and Mulligan [8] at low Rayleigh numbers who call it the 'overshoot' of the steady state.)

Figure 6 indicates the comparison between the boundary layer solutions of ref. [12] and the present results for the tangential velocity profiles at $\theta = 90°$ for $Ra = 10^6$. (The parameter t^* has been defined in ref. [12] as $2(2Pr\,Ra)^{0.25}t^{0.5}$.) The radial temperature
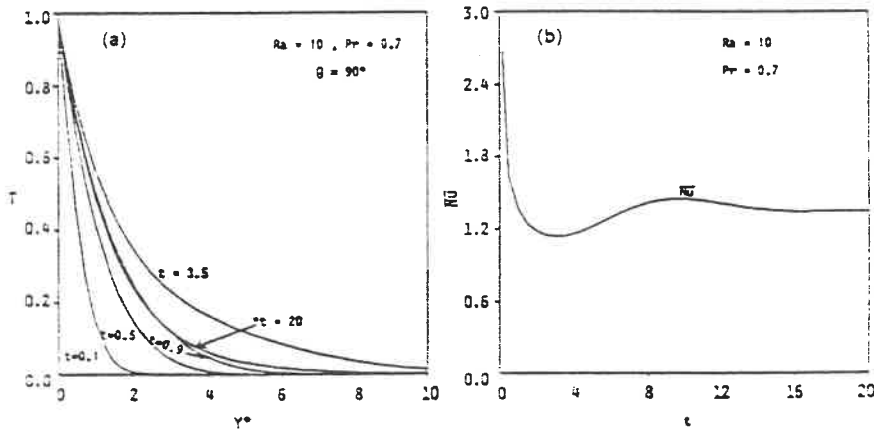
FIG. 5. For $Ra = 10$ and $Pr = 0.7$ at $\theta = 90°$: (a) radial temperature distribution at various times; (b) time histories of Nusselt numbers.
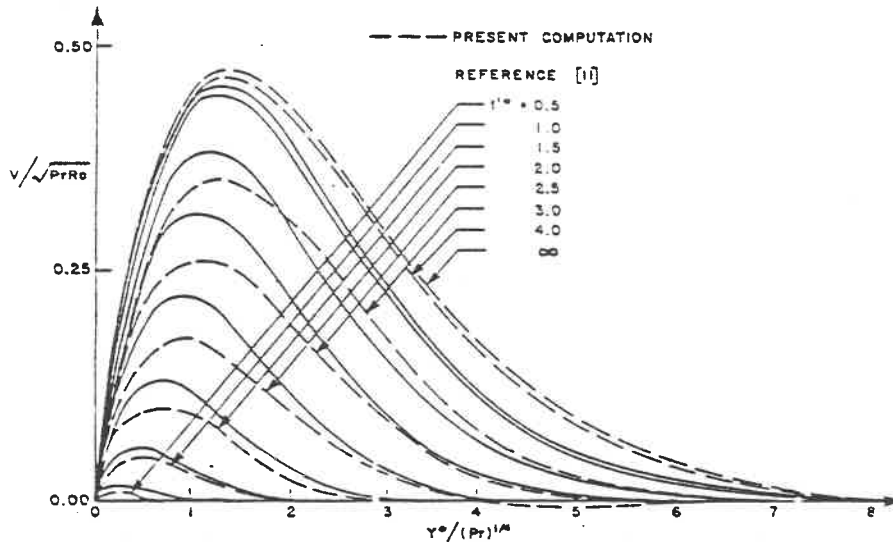
Fig. 6. Computed tangential velocity profiles compared with boundary layer results for $Ra = 10^6$, $Pr = 0.7$ and $\theta = 90°$ at various times.

profiles at $\theta = 0°$ are found to be virtually indistinguishable from those in ref. [12] and have not been reproduced here. However, the marked difference between the velocity profiles at small times is hardly surprising, since it is well known that the boundary layer assumptions break down when the viscous boundary layer is weak or nonexistent.

It is interesting to note that for $Ra = 10^6$ the thermal boundary layer was formed when $t \sim 0.0018$. This value coincides with that of τ from the scale analysis (in fact, $\tau \sim \pi/2 Ra^{-0.5} \sim 0.0016$). For $Ra = 10^5$ and 10^7, the time taken to form the thermal boundary layer is about $t \sim 0.005$ and 0.00056, respectively; which compares favourably with the corresponding values from a scale analysis of $\tau \sim 0.0049$ and 0.0005. These results demonstrate that equation (18) obtained from the scale analysis, is a reliable guide in predicting the duration of the transient time of the pure conduction stage for higher Rayleigh numbers.

The overshoot phenomenon. Figures 7(a) and (b) are the profiles of temperature and tangential velocity for different times at $\theta = 132°$ and $Ra = 10^5$. The 'overshoot' behaviour is more evident and it is easy to see that the fluid particles rotate while rising. The negative V^* at large values of Y^* in Fig. 7(b) implies just such a recirculation.

It is important to note that for higher Rayleigh numbers the 'overshoot' phenomenon is strong in the region $120° < \theta < 170°$. Particularly for $Ra = 10^7$, the maximum 'overshoot' occurs near $\theta = 160°$. At this stage, the diffusion of heat from the surface dominates over any convective effects so that the buoyancy forces act to accelerate only the fluid within the narrow thermal region δ_T. Once convection starts however, fresh

fluid is entrained into the heated region so that its temperature is reduced with an accompanying reduction in body forces. The overshoot behaviour is therefore most likely caused by fluid inertia effects. In order to further ascertain the details of the initiation of the convection regime, numerical experiments using particle trajectories were performed. The results (to be discussed later) indicate that as soon as the temperature of the cylinder surface is raised from T_∞ to T_w, particles adjoining the cylinder surface at $\theta = 90°$ commence moving and follow a path approximately tangential to the surface of the cylinder until they approach the top ($\theta = 180°$) where they separate and form a weak recirculating vortex region as shown in Figs. 1 and 2. It must be emphasized that during this whole transient process, the velocities involved are extremely low. Interestingly, the expected movement of fluid particles near the top of the cylinder occurs at $t > \tau$, that is, the development of the plume region lags behind the formation of the thermal boundary layer. This means that the onset of motion results from the natural convection along the approximately vertical portions of the cylinder surface near $\theta = 90°$ and not from a Bénard type convective instability in the statically unstable conduction temperature profile near $\theta = 180°$.

The development of the plume region. The development of the plume region is presented in further detail for $Ra = 10^6$ in Fig. 8. With the progress of time, convective effects become increasingly dominant. When $t > \tau$, i.e. after the boundary layer has formed, the tangential velocity continues to increase. This increase in convection causes development of the plume region. The upward flow along
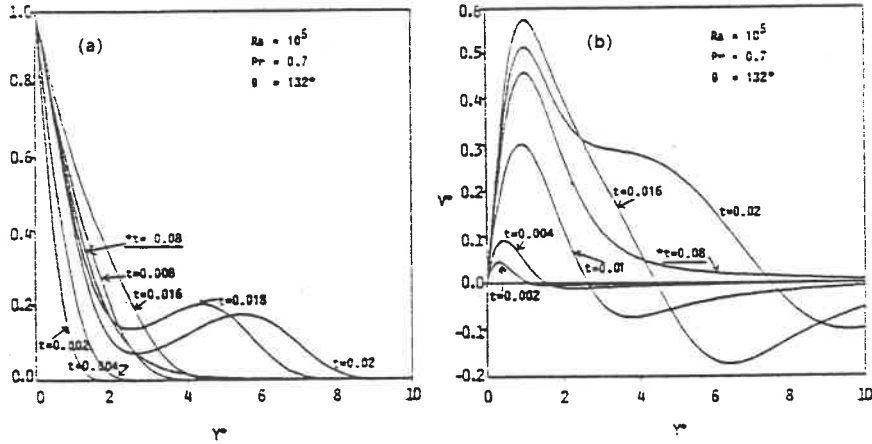
FIG. 7. Numerical results for $Ra = 10^5$, $Pr = 0.7$ and $\theta = 132°$: (a) radial temperature distribution at various times; (b) tangential velocity profiles at various times.
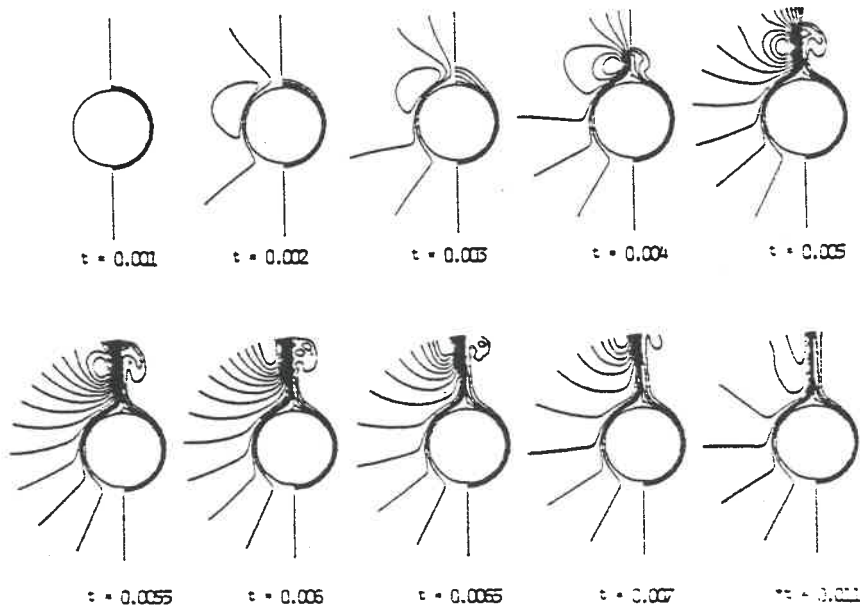

FIG. 8. Transient isotherms and streamlines for $Ra = 10^6$ and $Pr = 0.7$ ($\Delta\Psi = 10$ and $\Delta T = 0.2$).

the surface of the cylinder transports heated fluid to the top of the cylinder and gradually forms a distinct temperature front between the heated fluid and the unheated ambient as shown in Figs. 2 and 8. At the transient stage, the fluid at the top of the cylinder detaches itself and rises while rotating at the same time because of viscous effects. At a higher Rayleigh number, the rotation is quite evident and the leading edge of the heated fluid forms a 'mushroom' pattern which gradually degrades into the final (steady) state form of a convection plume. At very high Rayleigh number (about $Ra = 5 \times 10^7$), small separation vortices, symmetrically disposed near the top surface of the cylinder are formed, grow moderately, are shed
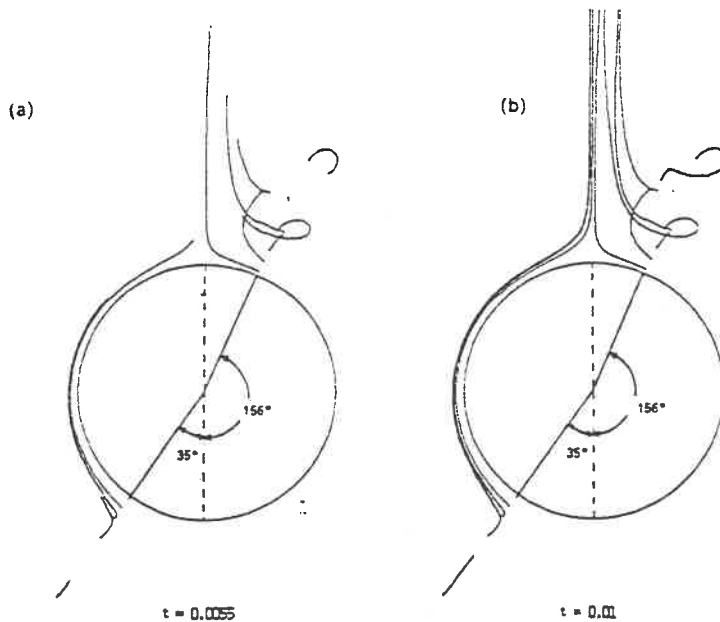
FIG. 9. Particle trajectories at different times for $Ra = 10^6$: (a) $t = 0.006$; (b) $t = 0.01$.

into the plume and then reformed again with this sequence repeating itself. (At the present time, it is unclear whether this rather interesting behaviour is due to deficiencies in the model (the use of a symmetric half-plane for example) or whether it is a physically realistic phenomenon.)

The particle trajectories presented in Fig. 9 provide other means with which to analyse the development of the fluid patterns for $Ra = 10^6$. For low Rayleigh numbers ($Ra < 10$), particles rise with almost no rotation anywhere. However, at higher Rayleigh numbers, particles which initially are within the region of $90° < \theta < 270°$ (except inside the boundary layer and at the vertical line) rise while rotating simultaneously. For example, trajectories of particles initially placed along a radial line at $\theta \simeq 156°$ are presented in Fig. 9. It is interesting to note that particles close to the cylinder surface have fairly stable paths after they are entrained into the boundary layer as shown in the left half of the figure (at the line $\theta \simeq 325°$ or $\theta \simeq 35°$). These trajectories are in basic qualitative agreement with experimental observations [6].

Local and average Nusselt numbers. The time variation of local surface Nusselt numbers for $Ra = 10^4$, 10^5 and 10^6 is shown in Figs. 10 and 11(a) and (b). For $Ra = 10^4$, comparison between the present results and those of Sako *et al.* [12] are presented. The agreement is quite good.

In general, at the initial stage, the local Nusselt numbers are uniformly distributed since heat transmission is by conduction. With time, convection begins to set in so that for $Ra = 10^6$ at $t = 0.0012$, the

maximum difference between the Nusselt numbers is about 20% indicating that convective effects are becoming significant. Finally at steady state, there is about a 84% difference between the value of Nu at the top and at the bottom of the cylinder. The 'overshoot' behaviour although present, is less marked than that at low Rayleigh number.

The time variation of the mean Nusselt numbers at the cylinder surface for different Rayleigh numbers is presented in Fig. 12. For lower Rayleigh numbers they are in good agreement with the results presented in ref. [12], however, due to space limitations they have not been reproduced here. Since the cylinder surface temperature increases suddenly from T_∞ to T_w, the starting heat transfer coefficients are initially large, then decrease quickly as the thickness of the thermal region grows until it reaches its minimum value and then increases again until it gradually attains its steady state. The lower the Rayleigh number, the more pronounced is the 'overshoot'. For example, values range from about 17% of steady state at $Ra = 1$ to about 2% for $Ra = 10^7$. After the 'overshoot' and before attaining a steady state, the values of Nu at the higher Rayleigh numbers suffer very small oscillations that are almost impossible to detect in the figures. It is possible that this effect is caused by fluid inertia effects that lag behind the body forces driving them, so that the steady state of even the velocity field is attained in an oscillatory manner and not in smooth monotonic fashion.

For lower Rayleigh numbers, a boundary layer cannot be formed and convection is relatively weak, so
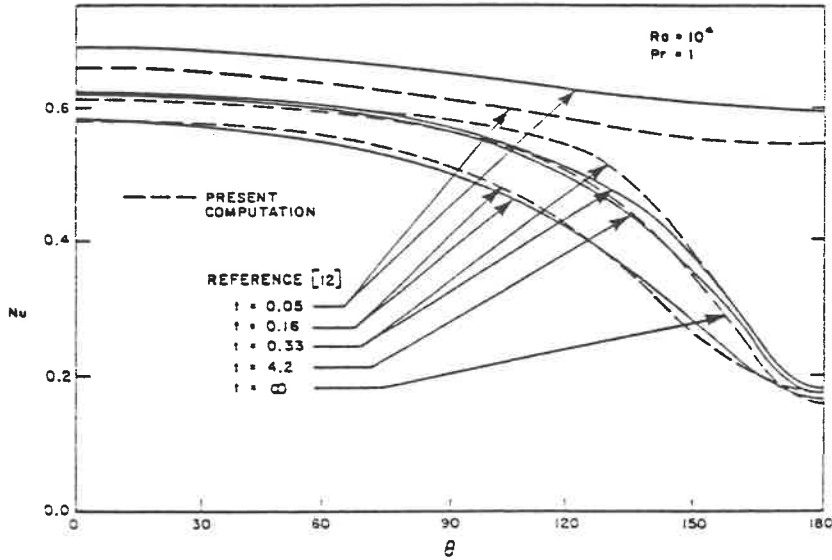
FIG. 10. Comparison between the present solution and those of ref. [12] for local heat transfer coefficients at $Ra = 10^4$ at different times.
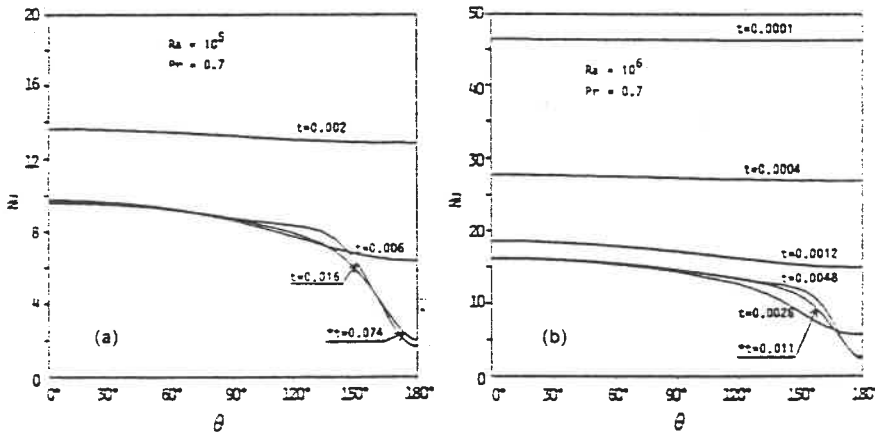

FIG. 11. Distribution of local Nusselt numbers at various times for $Pr = 0.7$ and: (a) $Ra = 10^5$; (b) $Ra = 10^6$.

that conduction effects are dominant except far away from the cylinder surface. However, at higher Rayleigh number, the effect of conduction is in general, limited to the boundary layer; outside this layer convection effects are always dominant.

The influence of Prandtl number Pr on Nu is shown in Fig. 12(a) for $Ra = 10^5$. The higher the Prandtl number, the higher the value of the Nusselt numbers.

Variation of surface vorticity. Figures 13(a) and (b) show the time variation of the vorticity distribution on the cylinder surface for $Ra = 10^6$ and 10^7, respec-

tively. For higher Rayleigh numbers, the 'overshoot' phenomenon is strong in the range of $120° < \theta < 170°$ instead of in the range of $90° < \theta < 150°$ [11] observed at lower Rayleigh numbers. It is evident that an increase in Ra causes not only an increase in the value of the vorticity but also causes the range of the 'overshoot' to shift towards the vertical. It is interesting to note that at the initial stage, the surface vorticity increases everywhere, however after a certain time ($t > \tau$) the values of vorticity decrease quickly in the range of $170° < \theta < 180°$ for $Ra \geqslant 10^5$, this decrease becoming more pronounced the higher the
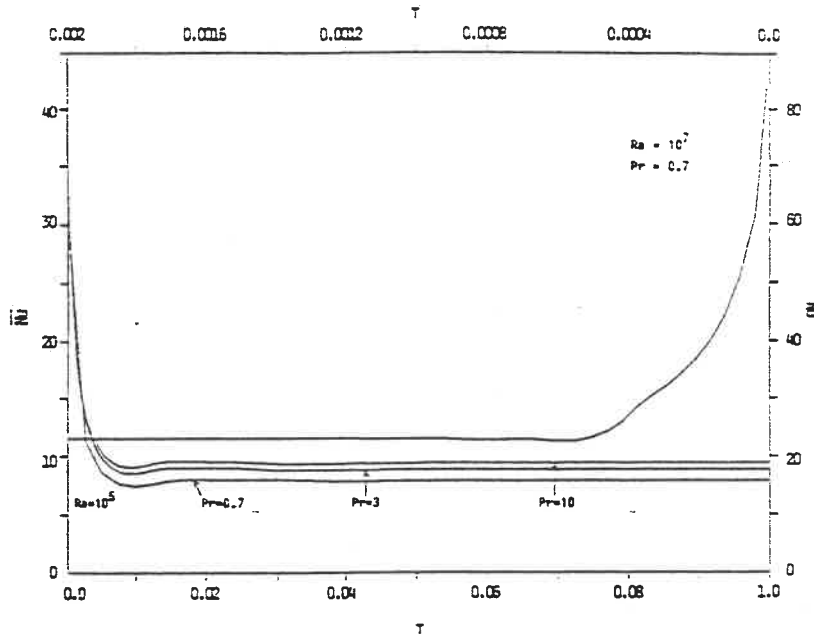
FIG. 12. Time histories of $\overline{Nu}$ for various Rayleigh numbers: (a) $Ra = 10^5$ and $Pr = 0.7$, 3 and 10; (b) $Ra = 10^7$ and $Pr = 0.7$.
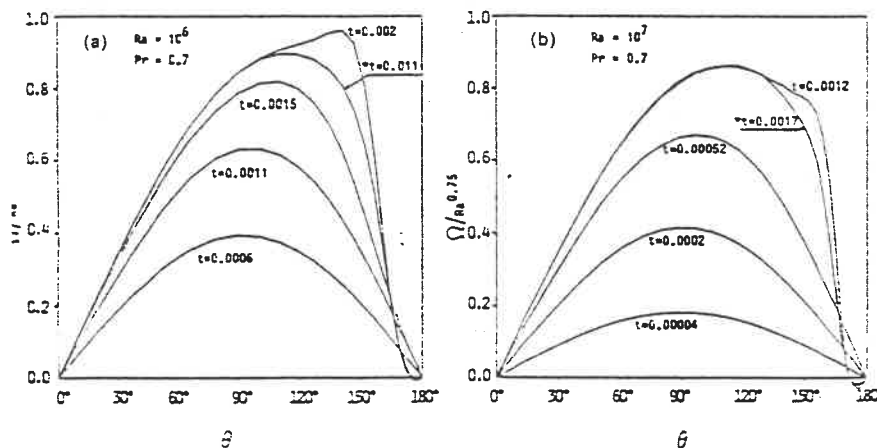

FIG. 13. Surface vorticity distribution at various times for $Pr = 0.7$ and: (a) $Ra = 10^6$: (b) $Ra = 10^7$.

Rayleigh number. When $Ra \geqslant 10^6$ a counter-rotating vortex is formed near the top of the cylinder. This appears to be due to the following causes: on the one hand in the region near the top of the cylinder the heat transfer is relatively low so that the buoyancy force and therefore the rise velocity associated with it becomes quite weak; on the other hand when $Ra \geqslant 10^6$ the convection becomes very strong and results in a local heated region close to the surface near $\theta = 170°$ so that a horizontal inverse temperature

gradient (which may be a direct cause of the counter-rotating vortex) is formed. When $Ra > 5 \times 10^7$ the final steady counter-rotating vortex cannot be obtained, however the phenomenon where it forms, is then shed and reforms has been observed. It has also been noted that at high Rayleigh numbers, under constant heat flux or small Biot number surface boundary conditions, the counter-rotating vortex may be formed in the transient stage, but finally disappears, since the heat transfer coefficients near the top

of the cylinder are relatively large compared with the isothermal case.

Instability. A rather interesting numerical feature has been observed during the development of the plume region. For high Rayleigh numbers, for example $Ra \geqslant 10^6$, the plume flow behaves in a laminar fashion below a certain characteristic distance measured vertically from the top of the cylinder. However, beyond this distance, the temperature distribution exhibits some oscillations, indicated in Fig. 8 ($t = 0.006$), that can eventually cause instability in the numerical procedure. In particular, for Rayleigh numbers exceeding 10^7 at large values of the dimensionless distance L (for example, $L > 1$), difficulties were encountered in attempts to obtain a convergent numerical solution. This is possibly a prelude to the development of the transition from laminar flow to turbulence.

CONCLUSIONS

The transient natural convection from a circular, horizontal cylinder has been studied numerically using spline integration techniques. Good agreement with published experimental and numerical data has been obtained. Overshoot and oscillatory behaviour of the local Nusselt numbers have been observed which decay as the steady state is approached. This has been associated with fluid inertia effects. At high Rayleigh numbers, the appearance of separation vortices, which are subsequently formed, shed and reformed when $Ra > 5 \times 10^7$, has been noted.

REFERENCES

1. T. H. Kuehn and R. J. Goldstein, Numerical solution to the Navier–Stokes equations for laminar natural convection about a horizontal isothermal circular cylinder, *Int. J. Heat Mass Transfer* 23, 971–979 (1980).
2. B. Farouk and S. I. Guceri, Natural convection from a horizontal cylinder—laminar regime. *J. Heat Transfer* 103, 522–527 (1981).
3. Z. H. Qureshi and R. Ahmad, Natural convection from a uniform heat flux horizontal cylinder at moderate Rayleigh numbers, *Numer. Heat Transfer* 11, 199–212 (1987).
4. P. Wang, R. Kahawita and T. H. Nguyen, Numerical computation of the natural convection flow about a horizontal cylinder using splines, *Numer. Heat Transfer* 17, Part A, 191–215 (1990).
5. P. Wang, Spline method of fractional steps in numerical model of unsteady natural convection flow at high Rayleigh number, *Numer. Heat Transfer* 11, 95–118 (1987).
6. G. A. Ostroumov, Unsteady heat convection near a horizontal cylinder. *Sov. Tech. Phys.* 1, 2627–2641 (1956).
7. C. M. Vest and M. L. Lawson, Onset of convection near a suddenly heated horizontal wire. *Int. J. Heat Mass Transfer* 15, 1281–1283 (1972).
8. J. R. Parsons, Jr. and J. C. Mulligan, Transient free convection from a suddenly heated horizontal wire. *J. Heat Transfer* 100, 423–428 (1978).
9. L. Elliott, Free convection on a two-dimensional or axisymmetric body, *Q. J. Mech. Math.* 23, 153–162 (1970).
10. A. S. Gupta and I. Pop, Effects of curvature on unsteady free convection past a circular cylinder, *Physics Fluids* 20, 162–163 (1977).
11. M. Katagiri and I. Pop, Transient free convection from an isothermal horizontal circular cylinder, *Wärme- und Stoffübertr.* 12, 73–81 (1979).
12. M. Sako, T. Chiba, J. M. S. Garza and A. Yanagida, Numerical solution of transient natural convective heat transfer from a horizontal cylinder, *Jap. Heat Transfer* 24–44 (1982).
13. O. F. Genceli, The onset of manifest convection from suddenly heated horizontal cylinders, *Wärme- und Stoffübertr.* 13, 163–169 (1980).
14. Y. W. Song, Numerical solution of transient natural convection around a horizontal wire, *J. Heat Transfer* 111, 574–576 (1989).
15. P. Wang and R. Kahawita, Numerical integration of partial differential equations using cubic splines, *Int. J. Comput. Math.* 13, 271–286 (1983).
16. J. Patterson and J. Imberger, Unsteady natural convection in a rectangular cavity, *J. Fluid Mech.* 100, 65–86 (1980).
17. A. Bejan, *Convection Heat Transfer*. Wiley, New York (1984).

CONVECTION NATURELLE LAMINAIRE VARIABLE AUTOUR DE CYLINDRES HORIZONTAUX

Résumé—La convection naturelle laminaire variable autour d'un cylindre chaud horizontal avec diverses conditions aux limites est étudiée numériquement en utilisant une méthode spline à échelons fractionnels. Quelques caractéristiques de la couche limite, obtenues avec une analyse d'échelle, sont comparées aux résultats numériques. On évalue le développement de la région de panache aussi bien que le champ local d'écoulement et le transfert thermique en surface. Pour les temps petits, les solutions numériques approchent les résultats de la couche limite et elles sont en bon accord avec les résultats de l'analyse d'échelle. On fait une étude détaillée du développement de la région de panache en utilisant des trajectoires calculées de particules. Tous les résultats ont été obtenus en utilisant un calculateur personnel. Des comparaisons qualitatives entre les résultats de calcul et les visualisations d'écoulement vérifient partiellement les résultats numériques.

ZEITLICH VERÄNDERLICHE LAMINARE NATÜRLICHE KONVEKTION AN EINEM WAAGERECHTEN ZYLINDER

Zusammenfassung—Die instationäre laminare natürliche Konvektion an einem beheizten waagerechten Zylinder wird numerisch mit Hilfe des Spline-Schrittverfahrens für verschiedene Randbedingungen an der Oberfläche untersucht. Einige Eigenschaften der Grenzschicht, die mit Hilfe einer Abschätzung der Größenordnung ermittelt worden sind, werden mit numerischen Ergebnissen verglichen. Die Entwicklung der Auftriebsfahne wie auch der Wärmeübergang an der Oberfläche und das örtliche Strömungsfeld werden berechnet. Für kleine Zeiten nähern sich die numerischen Ergebnisse denjenigen der Grenzschichtlösung. Sie summen in diesem Fall gut mit den Ergebnissen aus der Größenordnungsabschätzung überein. Das Gebiet der Auftriebsfahne wird unter Verwendung berechneter Partikelbahnkurven eingehender untersucht. Sämtliche Ergebnisse beruhen auf Berechnungen mit einem Personal-Computer. Ein qualitativer Vergleich zwischen den vorliegenden Ergebnissen und experimentellen Strömungsbeobachtungen bestätigt teilweise die numerischen Ergebnisse.

ПЕРЕХОДНЫЙ РЕЖИМ ЛАМИНАРНОЙ ЕСТЕСТВЕННОЙ КОНВЕКЦИИ ВОЗЛЕ ГОРИЗОНТАЛЬНЫХ ЦИЛИНДРОВ

Аннотация—С использованием сплайнового метода дробных шагов численно исследуется нестационарное ламинарное естественноконвективное течение от нагретого горизонтального цилиндра при различных граничных условиях на поверхности. Некоторые характеристики пограничного слоя, полученные при анализе размерностей, сравниваются с численными результатами. Оцениваются развитие области восходящего потока, а также поверхностный теплоперенос и локальные характеристики поля течения. При малых интервалах времени найденные численные решения приближаются к результатам, полученным в приближении пограничного слоя, и хорошо согласуются с результатами анализа размерностей. Более детально описывается развитие области восходящего потока на основе рассчитанных траекторий частиц. Все результаты получены на персональном компьютере. Качественные сравнения полученных данных и экспериментов по визуализации течения частично подтверждают достоверность численных результатов.

CHAPTER IV

TRANSIENT NATURAL CONVECTION WITH DENSITY

INVERSION FROM A HORIZONTAL CYLINDER

INTRODUCTION

Many natural phenomena involve buoyancy induced flows of cold water, i.e. water that is close to its freezing point. The mechanism of such flows is considerably complicated by the fact that its density reaches a maximum value at $3.98°C$. This gives rise to a variety of interesting phenomena. The behaviour of steady state natural convection in cold water has been studied by many investigators for several different geometries and boundary conditions.

In contrast to the steady flow situation, the transient behaviour of natural convection of water near the maximum density point from a horizontal ice cylinder has not been extensively treated. The existence of an unstable aspect to the convection, or the presence of oscillatory solutions when the physical parameters lie within a certain range of values has been observed but not widely reported. The parallel problem for the case of a vertical plane has been reported in the literature. On the other hand, studies that provide an insight into the physical mechanism of the above instability is more or less non-existent.

The investigation presented in this Chapter, is therefore devoted to the numerical simulation of the transient laminar natural convection flow about a horizontal cylinder at $0°C$. Numerical tests exploring the region where a gap in the solutions exists, as well as some preliminary physical intepretations based on the numerical results have been attempted.

Good agreement with published experimental and numerical data has been obtained. The appearance of a dual flow region has been documented and studied. The minimum Nusselt number at about 5.3°C has been verified numerically.

A more detailed investigation into the behaviour of the solutions in the range of $4.8°C < T_{amb} < 5.5°C$ was undertaken in order to obtain more information on the solution behaviour in this critical region. Quasi-periodic solutions as well as solutions displaying sudden catastrophic instability after a long period of quiescent behaviour were encountered. Additional computations using high precision and a non-reflecting boundary condition resulted in stable solutions, indicating that the instability was probably of numerical origin. In the range of $5.56°C \leq T_{amb} \leq 5.63°C$ and close to $T_{amb} = 4.75°C$, multiple solutions were found. The study has served to underline the importance of using correctly posed infinite boundary conditions as well as high precision in the computations when treating natural convection flows with reversing buoyancy.

Most of the present results have been obtained using an IBM Model 70 $PS/2$ computer operating at a clock speed of 20 Mhz. However, some extended computations were made on an IBM RISC 6000 and a mainframe using double (64 bit) precision. These solutions have been fully discussed.

The results of this investigation are reported in the following paper (to be published in **Physics of Fluids A**):

"Transient Natural Convection with Density Inversion from a Horizontal Cylinder".

TRANSIENT NATURAL CONVECTION WITH DENSITY INVERSION FROM A HORIZONTAL CYLINDER

ABSTRACT

This paper is devoted to a numerical investigation of the free convection flow about a horizontal cylinder maintained at 0°C in a water ambient close to the point of maximum density. Complete numerical solutions covering both the transient as well as steady state have been obtained. Principal results indicate that the proximity of the ambient temperature to the point of maximum density plays an important role in the type of convection pattern that may be obtained. When the ambient temperature is within $4.7°C < T_{amb} < 8°C$, a "dual flow" appears around the cylinder with both upward and downward flow occurring in proximity to the cylinder in two distinct recirculating zones, generally separated by the 4°C isotherm when $T_{amb} < 5.7°C$. The dual flow behaviour is significantly modified as the ambient temperature is altered, disappearing when the ambient temperature is above 8°C, or below 4.7°C. Furthermore, when the ambient temperature is within about $4.8°C < T_{amb} < 5.5°C$, a well defined steady state is never attained. Within this same range, solutions with an initially quasi-periodic behaviour which persist for a long time have been observed. Multiple solutions have been observed when the above range of ambient temperature is approached from either side.

The results of the computations have been compared with published experimental and numerical data with satisfactory agreement being obtained.

INTRODUCTION

Many natural phenomena involve buoyancy induced flows of cold water, i.e. water that is close to its freezing point. The mechanism of such flows is considerably complicated by the fact that its density reaches a maximum value at $3.98°C$. This gives rise to a variety of interesting phenomena. An early experiment on the melting of ice was performed by Dumoré, Merck and Prins[2] in 1953. They submerged a sphere of ice in cold water and observed for the first time that the water in the boundary layer flowed in opposite directions on either side of the isotherm corresponding to the inversion temperature ($4°C$). Merk[3] supplied the first analysis of such motions using the boundary layer equations; he calculated the local heat transfer at low temperatures around a melting sphere. The reversal in convective behaviour was predicted and the minimum heat transfer was found to occur at $T_{amb} = 5.3°C$. Since the pioneering works of Ede[1], Dumoré *et al.*[2] and Merk[3], the behaviour of natural convection in cold water has been studied by many investigators for several different geometries and boundary conditions. For instance, Schechter and Isbin[4] published experimental and theoretical work on thermal free convection from a heated vertical plate in cold water. Schenk and Schenkels[5] reported experimental results for thermal free convection from an ice sphere. Bendell and Gebhart[6] carried out experiments with vertical melting ice sheets in pure ambient water near its density extremum. A minimum Nusselt number was found to occur at $T_{amb} = 5.6°C$ while a net upflow and downflow were deduced from fluid temperature measurements when $T_{amb} > 5.6°C$ and

$T_{amb} < 5.6°C$ respectively.

The rather surprising discovery of a gap in the solutions for vertical boundary layer flows was first reported by Gebhart and Mollendorf[7] who used the boundary layer equations coupled with a numerical shooting method. They found that numerical solutions were unobtainable in the range $4.0°C < T_{amb} < 6.8°C$. Carey, Gebhart and Mollendorf[8], after refining the numerical method used by Gebhart and Mollendorf[7], found that the flow was bidirectional for T_{amb} between 4.75°C and 5.98°C and that convective inversion occurred at some T_{amb} between 4.75°C and 5.81°C. Solutions could not be obtained within this range of temperatures in pure water. Wilson and Vyas[9], conducted experiments on the velocity profiles near a vertical ice surface melting into fresh water for $2°C \leq T_{amb} \leq 7°C$. The results indicated an upward steady-state motion when the water temperature was below 4.7°C and a downward movement when the water temperature exceeded 7°C. For intermediate temperatures, an oscillatory bidirectional flow was observed. The calculations of Wilson and Lee[10] also indicated that three distinct flow regimes: steady upward flow for $T_{amb} \leq 4.5°C$, steady downward flow for $T_{amb} \geq 6.0°C$ and steady dual flow or bidirectional flow for $5.7°C \leq T_{amb} \leq 6°C$ were possible. However, a gap in the range of temperatures $4.5°C \leq T_{amb} \leq 5.7°C$ where the solution failed to converge still remained. Gebhart and Mollendorf[11] numerically computed multiple steady states of vertical buoyancy-induced flows. El-Henawy et al.[12] recently discussed multiple solutions of the boundary layer equations for horizontal plane flow in cold water. Multiple solutions arise, when the temperature gap is approached from either side, in conjunction with the increasingly large buoyancy force reversal across the thermal layer.

Desai and Forbes[13], Watson[14] and Vasseur and Robillard[15] have numerically

investigated the heat transfer and flow patterns in a rectangular enclosure using finite difference methods. Similarly, the effect of density inversion on natural convection within a horizontal cylindrical annulus has been studied experimentally by Seki *et al.*[16] and numerically by Nguyen *et al.*[17] and Vasseur *et al.*[18]. Gilpin[19] studied the effect of cooling in a horizontal cylinder of water through the maximum density point of 4°C. Saitoh[20] and Saitoh *et al.*[21] investigated both theoretically and experimentally the heat transfer characteristics in natural convection about a horizontal ice cylinder immersed in water at an ambient temperature near the maximum density point. At about $T_{amb} = 6°C$, a minimum Nusselt number was obtained, an instability in the flow was observed, and it was found that two different computer solutions appeared at $T_{amb} = 6°C$ when the spatial mesh length was varied[20]. These unstable aspects of the solutions appeared to correspond to his experimental observations. Ho and Chen[22] have reported the results of a numerical simulation of the melting of ice around a horizontal cylinder. They have provided results on the shape of the melt cavity formed and its dependence on the temperature of the cylinder.

In contrast to the steady flow situation, the transient behaviour of natural convection of water near the maximum density point from a horizontal ice cylinder has not been extensively treated. The existence of an unstable aspect to the convection, or the presence of oscillatory solutions when the physical parameters lie within a certain range of values has not been widely reported. The parallel problem for the case of a vertical plane has been investigated by Gebhart *et al.*[7] as well as many other researchers as mentioned earlier. On the other hand, studies that provide an insight into the physical mechanism of the above instability is more or less non-existent in the literature. The present investigation is therefore

devoted to the numerical simulation of the transient laminar natural convection flow about a horizontal cylinder at 0°C using a cubic spline integration technique [23-25]. Numerical tests exploring the region where a gap in the solutions exists, as well as some preliminary physical intepretations based on the numerical results have been attempted. The spline technique used retains the advantages of the SADI (Spline Alternating Direction Implicit) procedure, but requires only a single tridiagonal matrix system to be evaluated at each computational step, without the disadvantages related to the calculus of the first and second derivatives. Recently, the authors[26,27] have reported the results of an extensive numerical study of the laminar natural convection flow about a heated horizontal cylinder under diverse boundary conditions using this new technique, with the computations being performed on a personal computer. Most of the present results have been obtained using an IBM Model 70 $PS/2$ computer operating at a clock speed of 20 Mhz. However, some extended computations were made on an IBM RISC 6000 and a mainframe using double (64 bit) precision. These will be discussed later.

GOVERNING EQUATIONS

The non-dimensional equations in stream function and vorticity form (using the Boussinesq approximation for the body forces) may be written using polar coordinates as:

$$\nabla^2 \Psi = -\Omega \tag{1}$$

$$\frac{\partial \Omega}{\partial t} + u \frac{\partial \Omega}{\partial r} + \frac{v}{r} \frac{\partial \Omega}{\partial \theta} = \mathrm{Pr} \, \nabla^2 \Omega + A \left(\sin \theta \frac{\partial \Delta \bar{\rho}}{\partial r} + \cos \theta \frac{1}{r} \frac{\partial \Delta \bar{\rho}}{\partial \theta} \right) \tag{2}$$

$$\frac{\partial T}{\partial t} + u \frac{\partial T}{\partial r} + \frac{v}{r} \frac{\partial T}{\partial \theta} = \nabla^2 T \tag{3}$$

with

$$\nabla^2 = \frac{\partial^2}{\partial r^2} + \frac{1}{r} \frac{\partial}{\partial r} + \frac{1}{r^2} \frac{\partial^2}{\partial \theta^2}$$

$$\Delta \bar{\rho} = (\bar{\rho} - \rho(T))/\bar{\rho}$$

and

$$u = \frac{1}{r} \frac{\partial \Psi}{\partial \theta} , \qquad v = -\frac{\partial \Psi}{\partial r} \tag{4}$$

where r, θ and t refer to the radial, angular and time coordinates respectively. (θ is measured counterclockwise from the bottom). Here T, Ψ and Ω denote the dimensionless temperature, stream function and vorticity respectively while u and v are dimensionless radial and angular velocity. $A = gD^3/\alpha^2$ is a size parameter, D is the cylinder diameter, g the gravitational acceleration and α the thermal diffusivity. Pr is the Prandtl number while $\bar{\rho}$ refers to the average value of water density.

To describe the nonlinear variation of density with temperature for water in the range of 0 to 20°C, different density correlations have been given by Vanier

and Tien[28], by Fujii[29] and by Gebhart and Mollendorf[30]. Following Fujii[29], in the temperature range of 0°C to around 20°C, the density-temperature relationship of water may be approximated by the following equation :

$$\rho_0/\rho = 1 + \beta_1 T + \beta_2 T^2 + \beta_3 T^3 + \beta_4 T^4 \tag{5}$$

where

$$\rho_0 = 0.9998396(\text{g/cm}^3)$$

$$\beta_1 = -0.678964520 \times 10^{-4}(°\text{C})^{-1}$$

$$\beta_2 = 0.907294338 \times 10^{-5}(°\text{C})^{-2}$$

$$\beta_3 = -0.964568125 \times 10^{-7}(°\text{C})^{-3}$$

$$\beta_4 = 0.873702983 \times 10^{-9}(°\text{C})^{-4}$$

Equation (5) is concident with Landolt-Börnstein's experimental results[31] up to the last decimal place. The other popular density relation for pure and saline water in the range of 0 to 20°C developed by Gebhart and Mollendorf[30] contains only a single temperature term. This simplicity is very useful in the analysis of thermally driven flows. The present work however, employs equation (5) in order to facilitate comparison with the results of other researchers.

Boundary Conditions

Since the flow is symmetric about a vertical plane passing through the axis of the cylinder, only the half-plane need be considered. The boundary conditions then become:

$$u = v = \Psi = 0,$$

$$\Omega = -\frac{\partial^2 \Psi}{\partial r^2},$$

and

$$T = 0 \tag{6}$$

on the cylinder surface and

$$\Psi = v = \Omega = \frac{\partial T}{\partial \theta} = 0 \tag{7}$$

on the lines of symmetry.

Placing a circular line far away from the cylinder to represent the outer boundary, the boundary conditions on the velocity are:

$$v = \frac{\partial \Psi}{\partial r} = 0, \qquad and \qquad \Omega = -\frac{1}{r^2}\frac{\partial^2 \Psi}{\partial \theta^2} \tag{8}$$

The fluid is thus assumed to approach or leave the cylinder in the radial direction, i.e. the streamlines are normal to the outer (artificially imposed) boundary. The specification of the boundary conditions for the temperature poses some difficulties. At a region of inflow ($u < 0$), it appears physically justifiable to assume that the fluid entrained into the flow field is at the ambient value. At an outflow region however, the temperature distribution is not known a priori. The commmonly used boundary condition for outflow is to assume that the temperature gradient normal to the pseudo boundary is zero, thus implying that the heat transfer is dominated by convective movement rather than by conduction[32]. Saitoh[20,21], in his numerical study supposed that the temperature at the outer boundary was equal to the ambient temperature. Although his numerical results were in fairly good agreement with experimental data for surface Nusselt numbers, it appears that the balance of heat flux would not be globally satisfied. In the present computations, the temperature boundary conditions used initially were:

At the inflow region ($u < 0$): $T = 1$ and on the outflow region ($u > 0$), $\partial T/\partial r = 0$. However, when convergence problems were encontered during computations in the critical 'dual flow' region, a more rigorous boundary condition based on a truncated version of equation (3) was used. In effect, it was assumed that at the outer boundary (which is supposed to represent infinity!) $v = 0$ and the Laplacian on the RHS is negligibly small, so that

$$\frac{\partial T}{\partial t} + u\frac{\partial T}{\partial r} = 0.$$

This time dependent "characteristic based" boundary condition could be easily incorporated into the numerical procedure by discretizing it in implicit mixed boundary condition form[26]. As discussed later, this boundary condition avoided temperature oscillations observed when the leading surface of the plume traversed the artificial outer boundary. A detailed discussion of this effect has been reported by Abarbanel et al.[33]. The positive influence of this boundary condition on the convergence and stability of the solution did not however, affect the overall results obtained near the surface of the cylinder. The use of artificial boundaries to limit the computational domain is discussed in some detail in the review article by Givoli[34].

NUMERICAL PROCEDURE

The spline fractional step method (SFSM)[25] was used to generate an algorithm
resulting in a tridiagonal system containing either function values or first deriva-
tives at the grid points. The essential feature of this method is that in each
computational step, the problem is treated in a uni-dimensional implicit fash-
ion so that only one tridiagonal matrix system need be evaluated. The SFSM
schemes representing the governing equations (1) to (3) and the treatment of
the boundary condition imposed at the outer circular limit have been reported
in detail in earlier articles[26,27]. These articles have dealt with the utilisation
of the scheme to treat steady state as well as transient natural convection from
isothermal horizontal cylinders. The behaviour of the solution as a function of
the numerically imposed outer boundary condition and mesh spacing has been
investigated. Excellent agreement between the numerically computed values and
experimental results at transient as well as steady state have been obtained, so
that the details of the technique and of the numerical experimentation performed
need not be elucidated further. In order to verify the consistency of the present
numerical study, the first cases considered were those corresponding to existing
transient and steady state results for cavities with the effect of density inversion
on natural convection. Results for some of the cases studied by Robillard and
Vasseur[15] for different ambient temperatures and Prandtl numbers (for exam-
ple, $A = 4.34 \times 10^9$, $T_{amb} = 4°C$ and $Pr = 11.6$; $T_{amb} = 7°C$ and $Pr = 11.84$,
and $T_{amb} = 10°C$ and $Pr = 11.29$) were obtained. Very close agreement was

found between their results for the flow patterns, isotherms and Nusselt numbers and the present computations thus lending further credence to the present spline technique.

Fig. 1 illustrates the main nonuniform meshes used in the present computation. The nonlinear coupled partial differential equations were solved by considering r, θ grids of 21×31 with $r_{i+1}/r_i = 1.10$ and $\theta_{j+1}/\theta_j = 0.95$ (for $T_{amb} > 4.7°C$)or $\theta_{j+1}/\theta_j = 1.05$ (for $T_{amb} > 5.6°C$). However 41×41 or 61×61 were used at the critical region. Near the cylinder surface and in the plume region, fine grid spacing was used, in order to better define the plume and the inflow - outflow region. The coarsest mesh spacings were used when treating the ambient temperature ranges that resulted in unidirectional flow since these spacings had already been demonstrated[26] to be adequate. The maximum number of mesh points were chosen when computing cases that resulted in the "dual flow" solutions mentioned earlier and to be discussed in detail further on.

The criterion for convergence to a steady-state solution was that the maximum relative change in flow and temperature fields satisfy the following inequality:

$$|\frac{\phi_{i,j}^{n+1} - \phi_{i,j}^{n}}{\phi_{i,j}}|_{\max} < \varepsilon = 10^{-\alpha} \tag{10}$$

where ϕ in turn represents the stream function, vorticity and temperature with α = 5 , 5 and 4 respectively. Increasing the values for α did not result in significant change to the solutions.

As a further verification on whether a steady state had been attained, an energy balance was employed by comparing the heat transfer between each section.

Mathematically,

$$\int_0^\pi -\frac{\partial T}{\partial r} R_0 \mathrm{d}\theta = \int_0^\pi (uT - \frac{\partial T}{\partial r})r\mathrm{d}\theta \tag{11}$$

For a large number of these computations, the energy balance was satisfed to an error of better than 1%. This requirement appeared to ensure the obtention of a steady state. In fact, when $T_{amb} < 4.8°C$ or $T_{amb} > 5.6°C$, convergence was rapid and the rate of convergence for requirements (10) and (11) was of the same order. However, when the ambient water temperature fell within the range of between $4.8°C$ and $5.5°C$, requirement (10) and (11) could never be satisfied. (The difficulties experienced in this range, is associated with the fact that the solution never reaches a well-defined steady state as will be discussed later).

RESULTS AND DISCUSSION

Inversion Temperature

The observation that the water in the boundary layer flows in opposite directions on either side of the isotherm of inversion temperature, was first observed experimentally by Dumoré et $al.$[2]. In fact, if the ambient temperature is just below 4°C, the fluid near the surface of the cylinder will have the lowest density, so that the convective flow created will tend to rise. However, when the ambient temperature is above 4°C, at increasing distances from the surface, the density of the fluid will first increase, pass through its maximum value, and then decrease smoothly to the value corresponding to the ambient temperature. Consequently, the possibility of the presence of two flow regions exists. However, this possibility becomes a reality only after the ambient temperature reaches some critical value. This is because that on the one hand the density variation between 4°C and 5°C is very small compared with the variation in the other temperature regions (this is especially true when $4°C < T_{amb} < 4.6°C$); on the other hand, due to viscous effects, the upward flow near the surface of the cylinder will entrain the neighbouring fluid to rise with it. Thus, when the positive driving force resulting from the viscous coupling with the upward motion in the inner layer is offset by the negative driving force due to the maximum density effect, a stagnation region may occur, at the outside edge of the region with upward flow. Any further increase in the ambient temperature will result in a "dual motion". It is clear therefore, that the dual flow region can exist, only when the ambient temperature is above

this critical value. In the present numerical study, this critical temperature was found to be close to 4.7°C. This value is close to that observed experimentally by Wilson et al.[9] on a vertical ice surface and lies approximately within midrange of the experimental values corresponding to the observations of Dumoré et al.[2] and those of Schenk et al.[5] whose experimental data was about 4.5°C for a sphere. As expected, this dual flow tends to disappear at higher ambient temperatures. Some steady-state flow patterns obtained for different ambient temperatures are given in Fig. 2.

Below 4.7°C

When the temperature of the ambient water is below 4.7°C, the convective behaviour is not essentially different from the "normal" case. The only peculiarity is a negative thermal expansion coefficient that tends to zero as the temperature increases to 4°C. The result of the negative thermal expansion is to induce an initial motion near the surface of the cylinder that is upwards. Furthermore, the numerical results indicate that as soon as the ice cylinder is immersed in water, fluid particles near the surface at $\theta = 90°$ begin moving and follow a path approximately tangential to the surface of the cylinder until they approach the top ($\theta = 180°$) where they separate and gradually form a weak recirculating vortex region. With the progress of time, convective effects become increasingly dominant and cause development of the plume region. This behaviour resembles that observed around a heated horizontal cylinder in a "normal" fluid case[26].

The local Nusselt number comparison between the computational results and the experimental data of Saitoh[20] at steady state is presented in Fig. 3 for $T_{amb} = 4.6°C$ and $A = 4.34 \times 10^9$ and $A = 5 \times 10^{10}$ respectively. The size

parameter A, although different for the two cases studied does not influence the comparison since the Nusselt numbers on the vertical scale have already been normalized for size. The agreement is seen to be very satisfactory.

For a $T_{amb} = 4.7°C$, some interesting behaviour has been observed as shown in Fig. 4 for different values of the parameter A. Compared with the case of $T_{amb} = 4.6°C$, a marked decrease in convective activity occurs. As before, inverted flow is observed just below the cylinder. This downflow (below the zero-streamline) however, is quite weak compared with the upflow so that the streamlines representing the flow downwards cannot be presented in the figure to the same scale. An almost stably stratified lower layer is also noted. Indications are however, that the critical temperature is attained somewhere within this region.

Above 6°C

The experiments of Schenk and Schenkels[5] indicate that at an ambient of above 6°C, the observed flow pattern does not show any notable irregularity. The prevailing positive expansion coefficient causes a downward boundary layer flow separating somewhere ahead of the lower stagnation point, the separation point moving gradually downward with increasing temperature. In the present study, at $T_{amb} = 6°C$ the separation point is at about $\theta = 35°$ to $40°$ which is coincident with the experimental observation[5] for a sphere, and about $\theta = 10°$ for $T_{amb} = 7°C$. When $T_{amb} > 8°C$, no inverse convection occurs and the flow is always downwards. This is in good agreement with the experimental observations of Saitoh[20] using an ice cylinder. The steady state local Nusselt numbers are presented and compared with those of Saitoh[20] in Fig. 5. The agreement here is also very good.

Between 4.8°C and 6°C

This range of temperatures resulted in three types of interesting solutions:
A dual flow region, a region of oscillatory behaviour and a region where multiple
solutions were obtained.

The "Dual Flow"

The dual flow region was observed to occur only in the limited range of values
4.8°C to 8°C for T_{amb}. In fact, at a temperature of 6°C, the dual flow region
although present, was very weak, with only a small region of opposite motion
persisting near the lower stagnation point. As shown in Fig. 2, the subsequent
weakening and disappearance of the dual flow region as a function of ambient
temperature is clearly portrayed. Under conditions of dual flow, the outer flow
behaves as if it is flowing around a cylinder with a distorted shape, defined by
the dividing streamline. With increasing ambient temperature, the inner flow
region becomes thinner and moves towards the lower stagnation point where it
disappears completely when the ambient temperature is set at 8°C. Since the
downward flow steadily occupies more and more space with increasing ambient
temperature, the region with buoyant upward flow is pushed closer and closer to
the surface of the cylinder. At the same time the mean velocity in this layer will
tend to decrease to zero, owing to its proximity with the cylinder surface (which
would increase dissipation effects) and to the effect of the viscous coupling with
the flow in the opposite direction trying to drag it down. At about $T_{amb} = 5.8$°C,
the region of downward flow extends to the cylinder surface forming a rather thick
"boundary layer". The separation point is found numerically to be at about

$\theta = 30°$. This is coincident with Schenk's observation for the case of a sphere[5].

Oscillatory Solution

As mentioned earlier, when the ambient temperature is above a critical value, two flow regions may be present, one at the surface (maintained at 0°C) with an upward motion, the other region being situated some distance away where the motion is predominantly downwards. These two regions are separated by a region of very slow motion. However, this dual flow does not immediately occur at the start of the simulation. At the initiation of convection, the effect of density inversion causes the water near the cylinder surface to rise at first and form a recirculating vortex region that increases gradually and migrates towards the top of the cylinder. For the case of $T_{amb} = 5.3°C$ and $A = 2 \times 10^{10}$, starting at about $t = 0.004$, a second recirculating vortex, now rotating in the opposite direction appears and with the passage of time gradually dissipates. This sequence of events has been inferred from an inspection of the streamline patterns. Due to space considerations the relevant figures are not presented here. Figures 6.1 to 6.20 detail the streamline pattern and isotherms continuing from t=0.062 to t=0.1 at time intervals of 0.002. This sequence of figures documents rather well the unsteady quasi-periodic behaviour. The formation of a plume that grows in size and then diminishes without separating from the cylinder is clearly portrayed. (The appearance of a stronger dual flow region may be seen in Figures 6.5 and 6.6 or in Figures 6.16 and 6.17).

Figures 6.1 to 6.20 cover about two cycles of this oscillatory behaviour. The Nusselt number variation corresponding to this quasi-periodic phenomenon is shown in figure 7. It is important to note that this type of solution was obtained

in the range of $4.8°C < T_{amb} < 5.5°C$. This behaviour was especially evident in the region near the upper stagnation point. Extensive numerical experimentation with different mesh sizes was unable to resolve the problem. An experimentally observed instability in approximately the same range of parameter values has been observed by Saitoh[20], the instability being of a three-dimensional nature.

In order to investigate this region of anamolous behaviour in the solutions, extensive computations, some lasting several days were executed on the personal computer. (It may be mentioned here that generally, a complete transient solution up to steady state could be obtained in under four hours). The type of solution obtained was highly sensitive to the value of the parameter A. For example, when $A = 10^9$, (shown in figure 7) the solution although appearing to have stabilized from a visual inspection, had not reached a true steady state but was undergoing very long period oscillations. This was revealed on examination of the heat balance criterion of equation (11). When however, the values of A were in the range $A > 5 \times 10^{10}$, the solution appeared to reach a quasi-periodic steady state relatively early; the computation was therefore continued in hopes that a steady state might be obtained. The result was completely unexpected. After several days of computation, the solution which had remained bounded suddenly erupted in an explosive instability! At this stage, it was decided to embark on a more ambitious program of computation using first an IBM RISC workstation and then a mainframe computer. These computations were executed in double (64 bit) precision. A very fine grid (41×41 or 61×61) with mesh points concentrated near the plume region was used. [Fig. 1].

In order to further reduce the influence of the outer boundary conditions, its distance was increased from 3 to 7 cylinder radii from the surface. Furthermore,

the modified boundary condition for the temperature, namely $\partial T/\partial t + u\partial T/\partial r = 0$ was also incorporated into the solution procedure. The incorporation of this 'characteristic' type boundary condition into the computations resulted in the disappearance of temperature oscillations which were previously observed in the plume close to the outer limit. It is concluded that these spurious oscillations were the result of numerical reflection from the outer boundary as it was traversed by the plume. A detailed analysis of numerical reflection effects from an artificially imposed outer boundary has been presented by Abarbanel et al.[33] for the case of the oscillatory wake behind a cylinder in a uniform stream.

With these changes, corresponding solutions were obtained for all values of A although some of the solutions were quasi-periodic as before. The solutions were continued upto a dimensionless time of 0.1 compared with 0.06 performed earlier on the PS/2 for $A = 6.72 \times 10^{10}$ at $T_{amb} = 5.3°C$. The time step was 2.5×10^{-6} so that 0.1 represents a total of 40000 time steps. Under these conditions, the catastrophic instability observed earlier did not manifest itself leading to the conclusion that it was probably of numerical origin.

The transient behaviour of the solutions have been studied by plotting the streamlines, isotherms and lines of constant density. At an ambient temperature of between 4.8°C and 5.5°C, a thin layer of fluid close to 0 degrees centigrade is formed in proximity to the cylinder surface. This layer of fluid being buoyant when compared to its ambient, starts to rise slowly, reaches the top, separates and gradually forms into a plume. In this region however, it comes rather quickly into contact with warmer water that results in increasing its temperature towards the 4°C density maximum. At this point the buoyancy force reverses direction rapidly, causing it to slow down, stop and then descend in a layer just outside

the layer of fluid in immediate proximity to the cylinder. This behaviour which is influenced by inertial effects has been clearly observed in the simulation. (The outer region with fluid at maximum density flowing downwards is sandwiched between the outer and next to outer line of iso-density). For example, for $A = 6.72 \times 10^{10}$ and $T_{amb} = 5.3°C$, a second recirculating zone is formed at a point approximately 30 degrees ahead of the upper stagnation point. This recirculating zone serves to feed the plume region with relatively cool and therefore buoyant fluid; however its path into the plume region is blocked since the fluid ahead of it is decelerating due to reversal of the buoyancy force. This results in a ballooning of this fluid into a secondary "hump" which has been observed in the streamline patterns of the simulation. (Again, the figures relevant to this part of the discussion are not presented here due to space limitations.)

Meanwhile, the fluid above separates into a plume, is rapidly warmed by contact with its ambiant, reaches close to maximum density, and plunges downward in a well defined outer layer. The path is then clear for the cooler buoyant fluid below to flow into the space just evacuated and develop into a plume. The process then repeats itself. Sometimes the cooling of the lower fluid is so rapid that the "hump" ruptures into a secondary plume at a point approximately 30 degrees upstream of the upper stagnation region. This is probably the reason why a well-defined periodic state is not attained. The flow field in this case then appears never to repeat itself exactly, so that "hunting" occurs in the solution. (A typical example of this is illustrated by the curve for $A = 6.72 \times 10^{10}$ and $T_{amb} = 5.3°C$ in figure 7). It appears that as for the case of natural convection from a vertical surface under similar conditions, a gap in the range of obtainable solutions probably also exists.

Fig. 7 summarizes the behaviour of the solutions in the critical region with $T_{amb} = 5.3°C$. The increase in oscillatory behaviour as A is increased from 10^9 to 6.72×10^{10} is evident. The amplitude of the oscillations vary from 3% to 15% of the mean value as A is increased. The same figure indicates that when $T_{amb} = 5.8°C$ or when $T_{amb} = 4.6°C$ the steady state is reached rapidly, since these values for the ambient temperature lie outside the critical range.

Multiple Solutions

For 6°C, different mesh sizes were tested starting from initially motionless fluid. It was found impossible to obtain the two completely different converged solutions as reported by Saitoh[20]. However, on both sides of the gap in solutions for temperatures in the range of $5.56°C \leq T_{amb} \leq 5.63°C$, and close to $T_{amb} = 4.75°C$, multiple solutions were obtained. This is consistent with the findings of El-Henawy et al.[11] for horizontal plane flow in cold water, which is that multiple solutions arise when the temperature gap is approached from either side.

Fig. 8a to Fig. 8c are two completely different solutions for $T_{amb} = 5.6°C$ respectively. It is interesting to note that the difference between the two solutions at ambient temperature 5.6°C is not obvious from an inspection of the streamlines and isotherms. However the local Nusselt number and surface vorticity distributions are quite different. When $T_{amb} = 4.75°C$ the flow patterns are also completely different as shown in Fig. 9a. Most interesting is the appearance of three distinct flow patterns in solution II. Very close to the cylinder lies a boundary layer which is sufficiently cooled to generate an upward flow. This flow entrains ambient fluid with it starting from about $\theta = 80°$. Below $\theta = 80°$, there is a region of very slow moving fluid which is close to the ambient temperature.

Finally, between the lower stagnation point and about $\theta = 20°$, there is fluid entrained from the external ambient that however descends in an outer layer some distance away from the cylinder surface. The isotherms and surface vorticity distribution in both cases do not appear to be too different and seem to indicate transfer of heat by conduction. An inspection of Fig. 9b which is a representation of the Nusselt Number distributions indicates significant differences between the two solutions near the lower stagnation point, these differences being compatible with the different flow patterns observed there.

Local and Average Nusselt Numbers

At time $t = 0$, the surface temperature on the cylinder is decreased suddenly from T_∞ to 0°C. Heat is transferred initially by pure conduction to the cylinder, this initial conductive phase being characterized by concentric circles for the isotherms in the axial plane, until a certain critical time is reached as in ordinary natural convection. In general, at the initial stage, the local Nusselt numbers are uniformly distributed since heat is transferred by conduction. With time, convection sets in so that the difference between the Nusselt numbers becomes more and more marked. For a T_{amb} below 4.7°C or a T_{amb} above 6°C, the phenomenon is closely related to the case of natural convection in an ordinary fluid as presented by Wang et al.[26]; a slight "overshoot" effect appears and finally, steady state is reached. However, when $4.8°C < T_{amb} < 6°C$, the convective behaviour is complicated by the appearance of the dual flow effect, as shown in Fig. 10 for $T_{amb} = 5.6°C$ and $A = 6.72 \times 10^{10}$ (in the figure t^* signifies a time close to the steady state). At $t = 0.001$, the Nusselt number is virtually uniform along the surface of the cylinder where heat is transferred by conduction from

the surrounding fluid. The slightly higher value at the lower stagnation point than at the upper one ($\theta = 180°$) is due to the effect of a weak upward motion. This behaviour continues at $t = 0.003$ where the heat transfer is still primarily by conduction. A drop in the Nusselt number is clearly seen and is caused by the fact that the surrounding fluid has been cooled towards 0°C thus inhibiting the heat transfer. Beyond this point, convection effects begin to appear, however near the lower stagnation point the Nusselt number decreases to a local minimum due to accumulation of stagnant fluid. The appearance of the local peak in the Nusselt number near $\theta = 165°$ corresponds to the separation around the plume region. The water in this region is continually being replenished so that the heat transfer to the cylinder is relatively high. Just ahead of this point, at $\theta = 145°$ a local minimum is observed. In this region, descending water that has been cooled, impinges on the cylinder surface giving rise to this minimum. Due to the dual flow characteristic, a region of virtually stagnant fluid adjacent to the cylinder, moving comparatively slowly is formed, resulting in an almost uniform circumferential variation of Nusselt number on the surface of the cylinder. Fig. 11 corresponds to the case for $T_{amb} = 5.8°C$. The remarkable change in behaviour is obvious. Local minima near the lower stagnation point are observed while at the upper end $\theta = 180°$ the minima and maxima have disappeared.

The local Nusselt number distributions for different T_{amb} at steady state for $A = 6.72 \times 10^{10}$ are given in Table 1. The time variation of the mean Nusselt numbers $\overline{Nu}$ at the cylinder surface for different ambient temperatures is presented in Fig. 12. An oscillating solution for $T_{amb} = 5.5°C$ may be noted.

On the Minimum Nusselt number

When the temperature of the surrounding water is within the critical range necessary to exhibit the "dual flow" type behaviour, it is not necessarily implied that the average heat transfer from the cylinder surface (or the average Nusselt number) will reach its minimum value. In fact, within the boundary layer, the region of stagnant fluid appears at a much later time than when the dual flow is apparent. Merk[3] has presented a calculation of free convection in water using the boundary layer assumptions. He found that the minimum average Nusselt number was reached at a $T_{amb} = 5.3°C$. The value of the minimum Nusselt number however was severely underestimated. The discrepancy is not surprising since in this region, the boundary layer assumptions are not valid. Experimentally, by studying the melting of ice spheres Schenk[5] found that the minimum average Nusselt number occurred at 5.3°C. In the present study, for different A: $A = 4.34 \times 10^9$, $A = 5 \times 10^{10}$ and $A = 6.72 \times 10^{10}$, the computational results also indicate that the mean value of the average Nusselt numbers (no steady state results) are reached when the ambient temperature is about 5.25°C - 5.3°C. This is in better agreement with Merk's theoretical prediction[3] and Schenk's experimental data for spheres[5] than with the experiments of Dumore[2], who found that the minimum heat transfer occurred at a critical temperature of 4.7°C. Fig. 13 compares the present results with those of other authors[2,3,5] for the overall value of the Nusselt number as a function of the ambient temperature T_{amb} (in the figure, the present results are for $A = 5 \times 10^{10}$ corresponding to a D of about 4.5cm and the mean value of the average Nusselt numbers was used when $4.8°C < T_{amb} < 5.5°C$). From Schenk's experimental data[5], the diameter

of the ice spheres that he used was evaluated to be about 3.8cm and the constant factor in the expression $\mathrm{Nu} = C(\mathrm{Gr} \times \mathrm{Pr})^{0.25}$ was taken as equal to 0.56, according to Merk's calculations. Dumoré on the other hand, adopted a C of 0.65. The present computational results are in goood agreement with Schenk's experimental data and also with Merk's theoretical results when $T_{amb} \leq 6°\mathrm{C}$.

Variation of Surface Vorticity

Fig. 14 shows the time variation of the vorticity distribution at an ambient temperature of 5.8°C. At low values of time the vorticity variation is smoothly monotonic but then rapidly experiences sign reversals corresponding to the formation of multiple separation lines. Even at the steady state (denoted by t^*) a weak separation line with flow reversal is still evident. (Note that the passage through zero of the vorticity corresponds to a separation line, while positive or negative values indicate the flow direction at the surface). The surface vorticity distribution at steady state for different ambient temperatures are shown in Fig. 15. Above a temperature of 5.8°C, it is seen that steady separation at the cylinder surface is established, the point of separation moving close to the lower stagnation point with increasing temperature. The separation is due to the effect of the density inversion at 4°C. Presumably, at a sufficiently high temperature of the ambient fluid, the separation line will be coincident with the lower stagnation point and the flow will then be entirely downwards.

CONCLUSIONS

The transient natural convection from a horizontal cylinder in water at a temperature near the maximum density point has been studied numerically using spline integration techniques. Good agreement with published experimental and numerical data has been obtained. The appearance of a dual flow region has been documented and studied. The minimum Nusselt number at about 5.3°C has been verified numerically. A more detailed investigation into the behaviour of the solutions in the range of $4.8°C < T_{amb} < 5.5°C$ was undertaken in order to obtain more information on the solution behaviour in this critical region. Quasi-periodic solutions as well as solutions displaying sudden catastrophic instability after a long period of quiescent behaviour were encountered. Additional computations using high precision and a non-reflecting boundary condition resulted in stable solutions, indicating that the instability was probably of numerical origin. In the range of $5.56°C \leq T_{amb} \leq 5.63°C$ and close to $T_{amb} = 4.75°C$, multiple solutions were found. The study has served to underline the importance of using correctly posed infinite boundary conditions as well as high precision in the computations when treating natural convection flows with reversing buoyancy.

REFERENCES

[1] A.J. Ede, Proceeding of the 8th International Congress of Refrigeration, London, 260 (1951).

[2] J.M. Dumoré, H.J. Merk and J.A. Prins, *Nature*, **172**, 460 (1953).

[3] H.J. Merk, *Appl. Sci. Res.*, **4**, 435 (1954).

[4] R.S. Schechter and H.S. Isbin, *A.I.Ch.E Journal*, **4**, 81 (1958).

[5] J. Schenk and F.A.M. Schenkels, *Appl. Sci. Res.*, **19**, 465 (1968).

[6] M.S. Bendell and B. Gebhart, *Int. J. Heat Mass Transfer*, **19**, 1081 (1976).

[7] B.Gebhart and J.C. Mollendorf, *J. Fluid Mech.*, **89**, 673 (1978).

[8] V.P. Carey, B. Gebhart and J.C. Mollendorf, *J. Fluid Mech.*, **97**, 279 (1980).

[9] N.W. Wilson and B.D. Vyas, *J. Heat Transfer*, **101**, 313 (1979).

[10] N.W. Wilson and J.J. Lee, *J. Heat Transfer*, **103**, 13 (1981).

[11] B.Gebhart and J.C. Mollendorf, *J. Fluid Mech.*, **122**, 235 (1982).

[12] I. El-Henawy *et al.*, *Int. J. Heat Mass Transfer*, **29**, 1655 (1986).

[13] V.S. Desai and R.E. Forbes, *ASME Trans. Environmental and*

Geophysical Heat Transfer, 41 (1971).

[14]   A. Watson, *Quart. J. Mech. and Appl. Math.*, **25**, 423 (1972).

[15]   L. Robillard and P. Vasseur, *Can. J. Civ. Eng.*, **6**, 481 (1979).

[16]   N. Seki, S. Fukusako and M. Nakoaka, *J. Heat Transfer*, **97**, 556 (1975).

[17]   T.H. Nguyen, P. Vasseur and L. Robillard, *Int. J. Heat Mass Transfer*, **25**, 1559 (1982).

[18]   P. Vasseur, L. Robillard and B. Chandra Shekar, *J. Heat Transfer*, **105**, 117 (1983).

[19]   R.R. Gilpin, *Int. J. Heat Mass Transfer*, **18**, 1307 (1975).

[20]   T. Saitoh, *Appl. Sci. Res.*, **32**, 429 (1976).

[21]   T. Saitoh and K. Hirose, *J. Heat Transfer*, **102**, 261 (1980).

[22]   C.J. Ho and S. Chen, *Int. J. Heat Mass Transfer*, **29**, 1369 (1986).

[23]   S. G. Rubin and R. A. Graves, *Comput. Fluids*, **3**, 1 (1975).

[24]   P. Wang and R. Kahawita, *Int. J. Computer Math.*, **13**, 271 (1983).

[25]   P. Wang, *Numer. Heat Transfer*, **11**, 95 (1987).

[26]   P. Wang, R. Kahawita and T.H. Nguyen, *Numer. Heat Transfer*, **17**, Part A, 191 (1990).

[27]   P. Wang, R. Kahawita and D.L. Nguyen, *Int. J. Heat Mass Transfer*, **34**, 1429 (1991).

[28] C.R. Vanier and C. Tien, *Chem. Engng Prog. Symp. Ser.*,
      82, 240 (1968).

[29] T. Fujii, *Progress in Heat Transfer Engineering*, **3**, 66 (1974).

[30] B. Gebhart and J. Mollendorf, *Deep-Sea Research*, **124**, 831 (1977).

[31] Landolt-Börnstein, *Zahlenheit und Functionen*, *6th Auf. Springer*,
      Berlin, (1971).

[32] T.H. Kuehn and R.J. Goldstein, *Int. J. Heat Mass Transfer*, **23**,
      971 (1980).

[33] S. S.Abarbanel, W. S. Don, D. Gottieb, D. H. Rudy and J. C. Townsend,
      J. Fluid Mech.,**225**, 557 (1991).

[34] D. Givoli, *J. Comput. Phys.*, **94**, 1 (1991).

Table 1. Local and Average Nusselt Numbers for $A = 6.72 \times 10^{10}$

$$\mathrm{Nu} = (\partial T/\partial r)_w$$

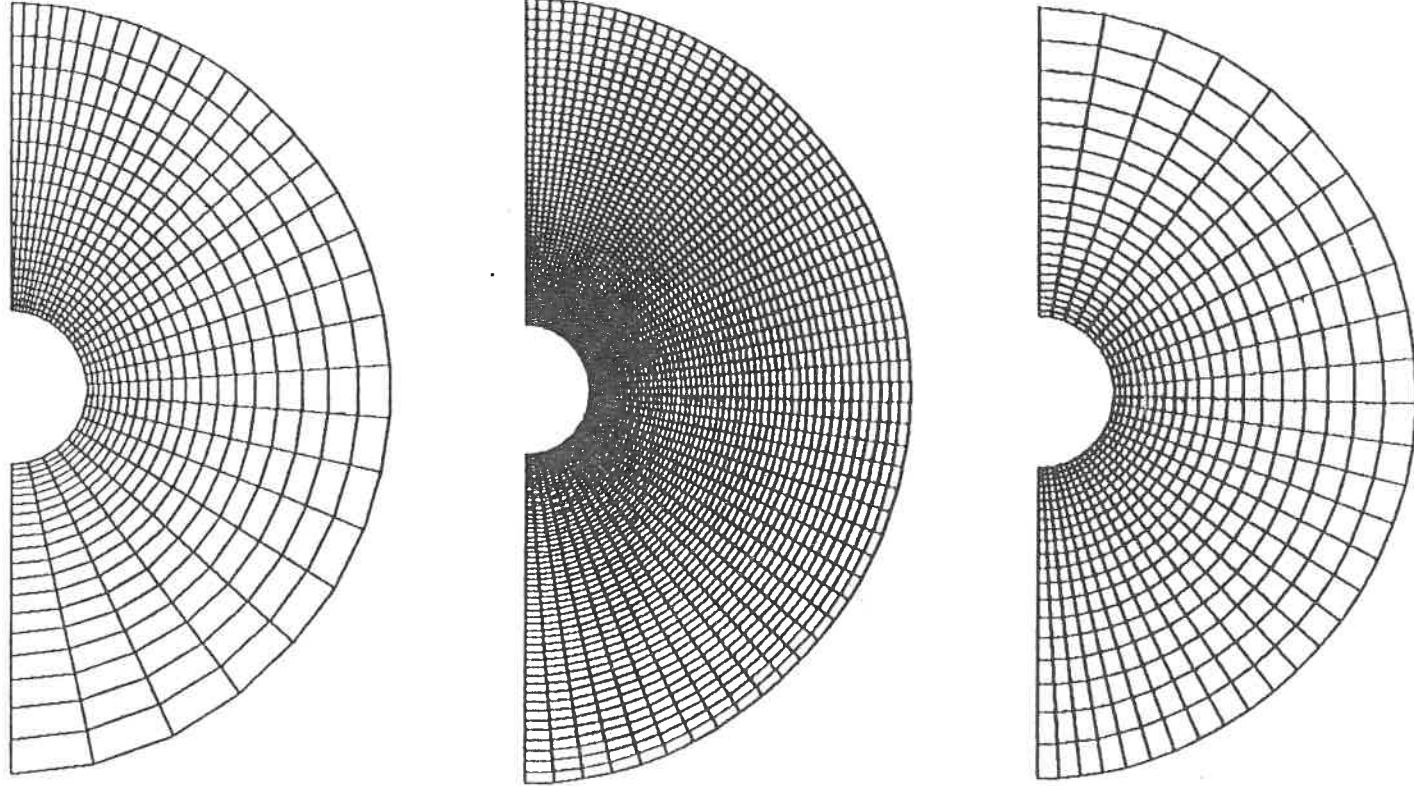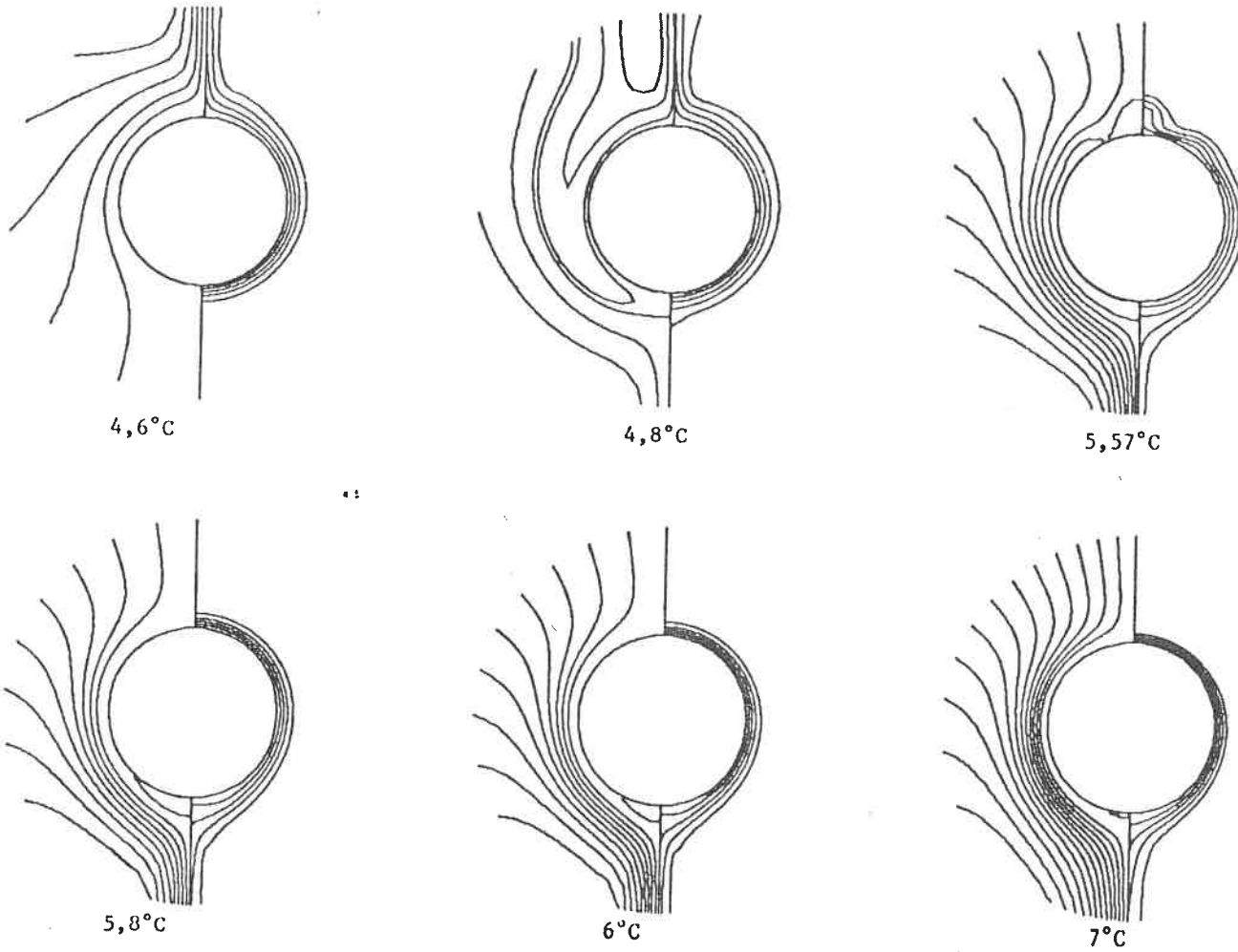|	Nu							
T_{amb}	$\theta = 0°$	30°	60°	90°	120°	150°	180°	$\overline{\mathrm{Nu}}$
2.00 °C	16.61	16.40	15.75	14.37	13.04	10.77	3.03	13.66
2.75 °C	16.86	16.65	15.98	14.91	13.20	10.96	3.05	13.86
3.50 °C	16.44	16.23	15.57	14.51	12.85	10.71	3.03	13.53
4.60 °C	14.09	13.89	13.29	12.28	10.84	8.89	2.90	11.54
5.70 °C	5.67	5.20	8.95	10.09	10.32	10.30	10.25	8.80
5.80 °C	5.61	5.07	10.15	11.41	11.94	12.22	12.31	9.98
6.00 °C	4.88	7.20	11.38	12.55	13.25	13.65	13.78	11.14
7.00 °C	3.54	11.96	15.14	16.40	17.50	18.13	18.36	15.01
8.00 °C	3.44	14.27	17.63	19.04	20.29	20.96	21.18	17.38
10.00 °C	3.76	16.45	20.12	22.62	24.12	25.03	25.13	20.83

LIST OF FIGURES

Fig. 1. Different meshes used;

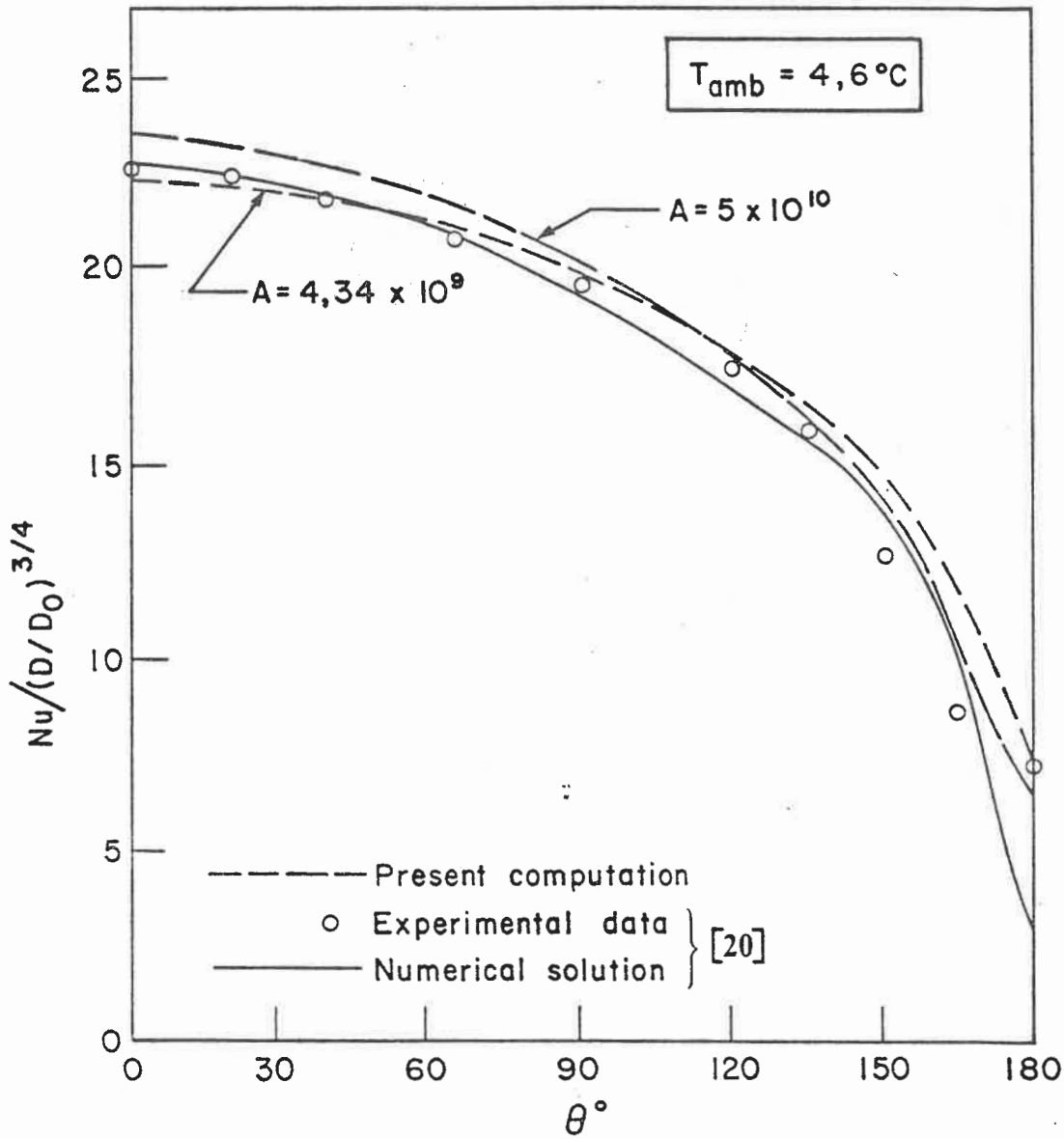Fig. 2. Steady-state isotherms (right) and streamlines (left) for different T_{amb} ($\Delta\Psi = 15$ and $\Delta T = 0.2$);

Fig. 3. Comparison between the present solution and those of [20] at $T_{amb} = 4.6°C$ for local heat transfer coefficients at steady state;
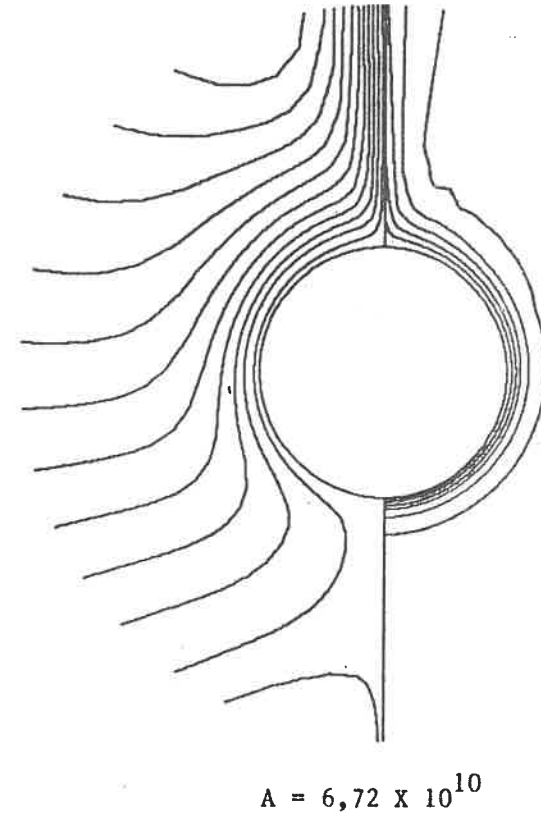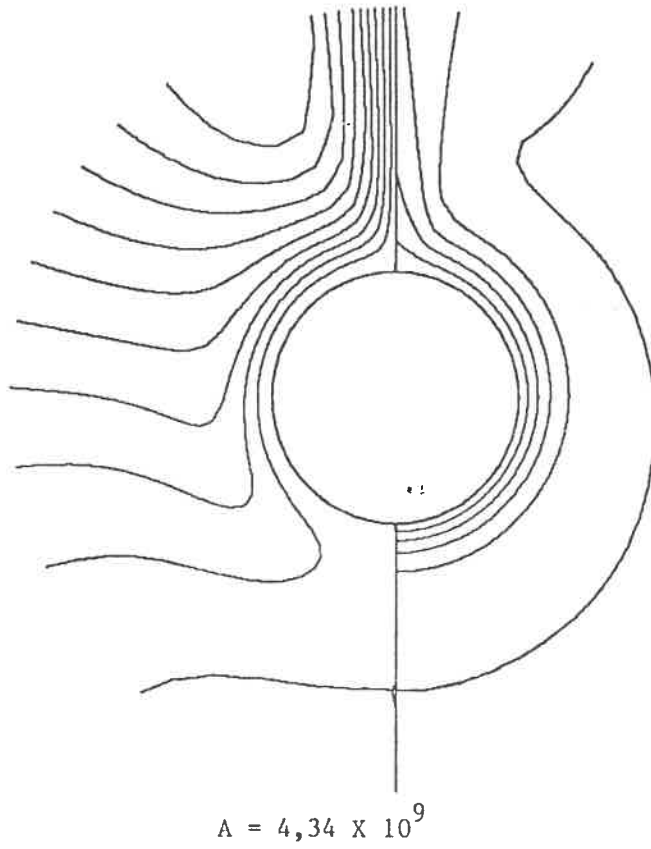
Fig. 4. Steady-state isotherms and streamlines for $A = 4.34 \times 10^9$ ($\Delta\Psi = 3$ and $\Delta T = 0.2$); and for $A = 6.72 \times 10^{10}$ ($\Delta\Psi = 10$ and $\Delta T = 0.2$); and $Pr = 12.4$ at $T_{amb} = 4.7°C$;
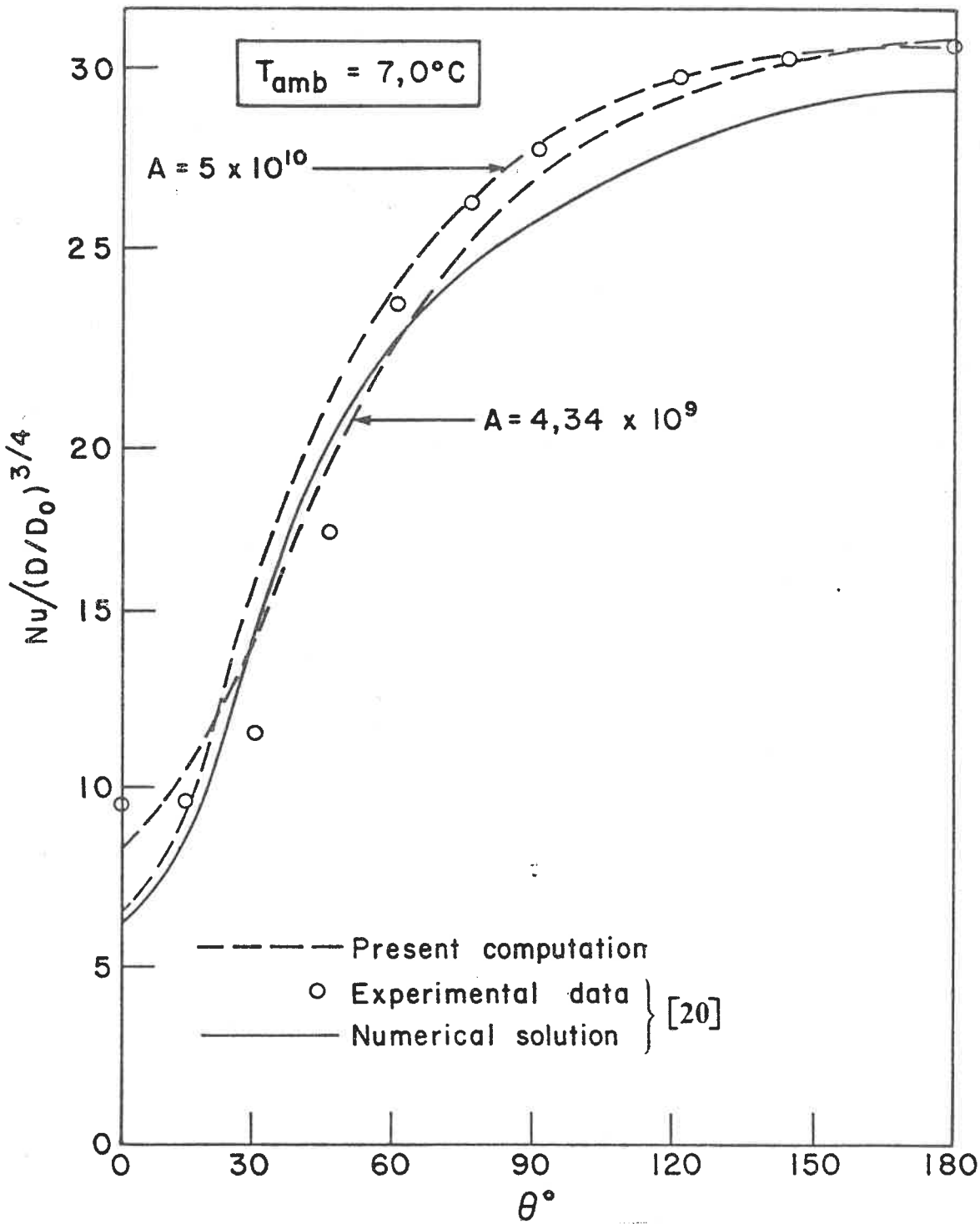
Fig. 5. Comparison between the present solution and those of [20] at $T_{amb} = 7°C$ for local heat transfer coefficients at steady state;
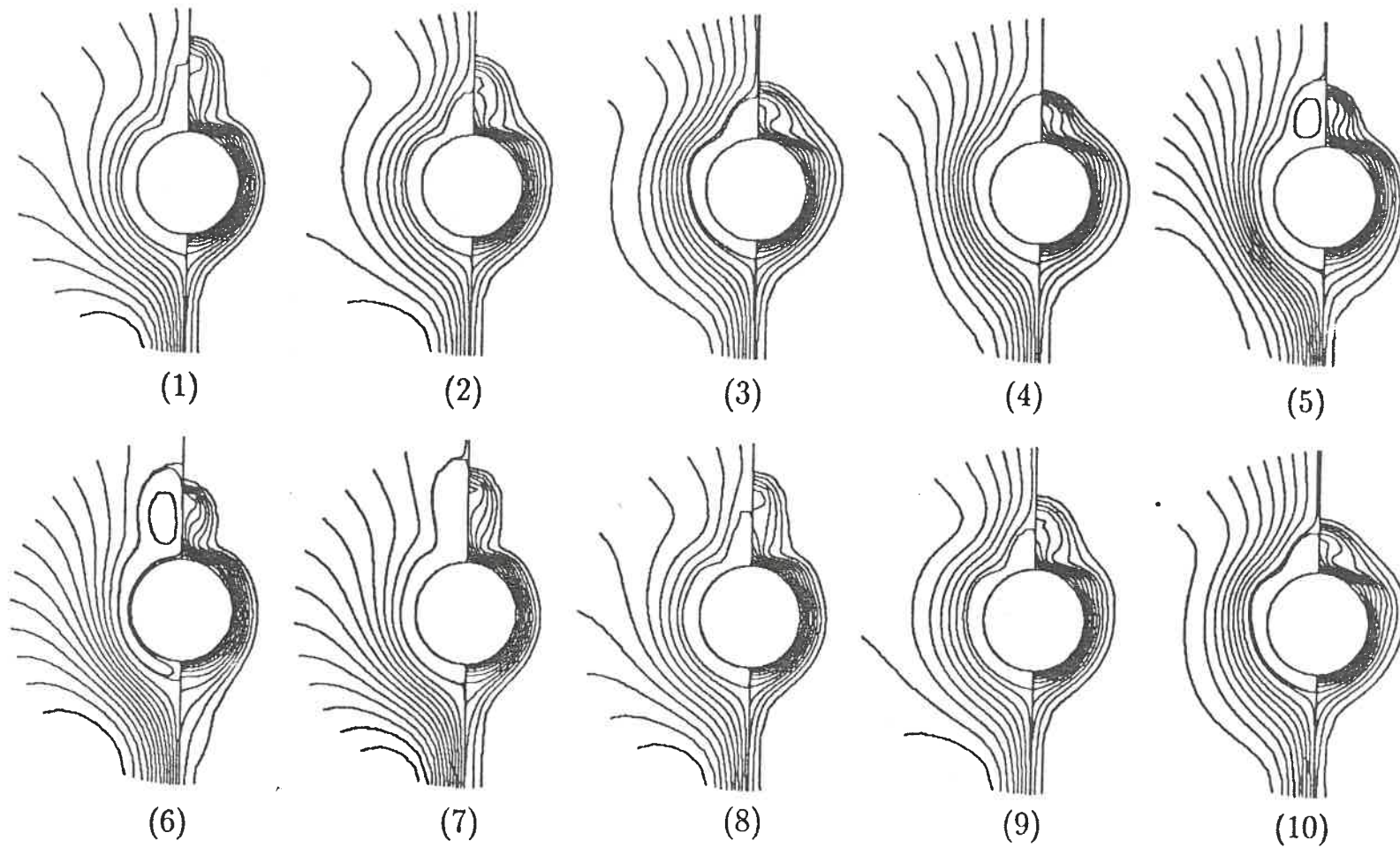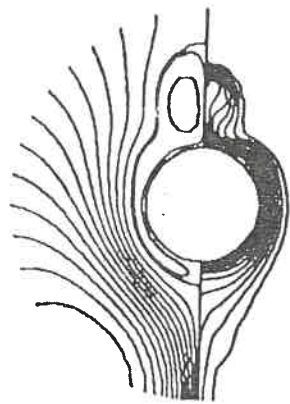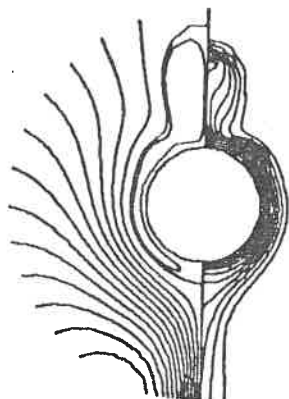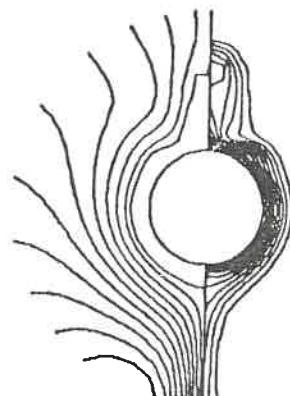
Fig. 6. Quasi-periodic transient isotherms and streamlines for $A = 2 \times 10^{10}$ and $Pr = 12.3$ at $T_{amb} = 5.3°C$ ($\Delta\Psi = 10$ and $\Delta T = 0.2$);

Fig. 7. Time histories of $\overline{Nu}$ for $T_{amb} = 5.3°C$ at different values of A and $Pr = 11.6$;

Fig. 8. Two different solutions for a $Pr = 11.6$ and $A = 6.72 \times 10^{10}$ at $T_{amb} = 5.6°C$:

(a) Steady-state isotherms and streamlines; ($\Delta\Psi = 15$ and $\Delta T = 0.2$);

(b) Steady-state distribution of local Nusselt numbers;

(c) Steady-state surface vorticity distribution;

Fig. 9. Two different solutions for a $Pr = 12.4$ and $A = 6.72 \times 10^{10}$ at $T_{amb} = 4.75°C$:

(a) Steady-state isotherms and streamlines; ($\Delta\Psi = 10$ and $\Delta T = 0.1$);

(b) Steady-state distribution of local Nusselt numbers;

(c) Steady-state surface vorticity distribution;

Fig. 10. Time-varying distribution of local Nusselt numbers for a $Pr = 11.6$ and $A = 6.72 \times 10^{10}$ at $T_{amb} = 5.6°C$;

Fig. 11. Time-varying distribution of local Nusselt numbers for a $Pr = 11.6$ and $A = 6.72 \times 10^{10}$ at $T_{amb} = 5.8°C$;

Fig. 12. Time histories of $\overline{Nu}$ for various T_{amb} at $A = 6.72 \times 10^{10}$ and $Pr = 11.6$;

Fig. 13. Comparison between numerically computed and experimentally measured average Nusselt numbers for different T_{amb};

Fig. 14. Time-varying surface vorticity distribution for a $Pr = 11.6$ and $A = 6.72 \times 10^{10}$ at $T_{amb} = 5.8°C$;

Fig. 15. Steady-state surface vorticity distribution for different T_{amb} at $A = 6.72 \times 10^{10}$ and $Pr = 11.6$;

Fig. 1. Different meshes used

$$\Lambda = 6,72 \times 10^{10}$$

4,6°C
4,8°C
5,57°C

5,8°C
6°C
7°C

Fig. 2. Steady-state isotherms(right) and streamlines(left) for different T_{amb} ($\Delta\Psi = 15$ and $\Delta T = 0.2$)

Fig. 3. Comparison between the present solution and those of [20] at $T_{amb} = 4.6°C$ for local heat transfer coefficients at steady state

A = 4,34 X 10^9

A = 6,72 X 10^{10}

Fig. 4. Steady-state isotherms and streamlines for $A = 4.34 \times 10^9$ ($\Delta\Psi = 3$ and $\Delta T = 0.2$); and for $A = 6.72 \times 10^{10}$ ($\Delta\Psi = 10$ and $\Delta T = 0.2$); and $Pr = 12.4$ at $T_{amb} = 4.7°C$

Fig. 5. Comparison between the present solution and those of [20] at $T_{amb} = 7°C$ for local heat transfer coefficients at steady state

Fig. 6. Quasi-periodic transient isotherms and streamlines for $A = 2 \times 10^{10}$ and $\mathrm{Pr} = 12.3$ at $T_{amb} = 5.3°\mathrm{C}$ ($\triangle\Psi = 10$ and $\triangle T = 0.2$);
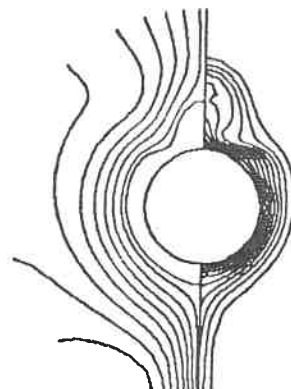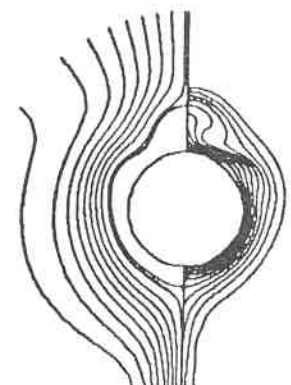
(11)   (12)   (13)   (14)   (15)
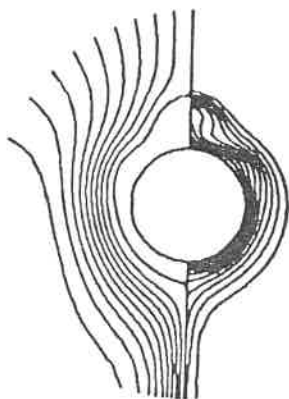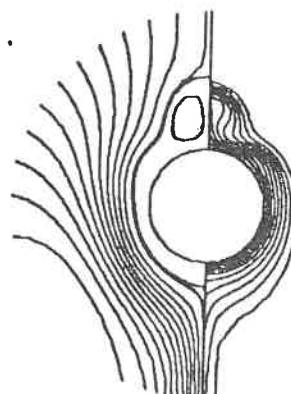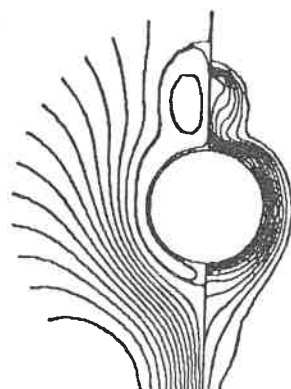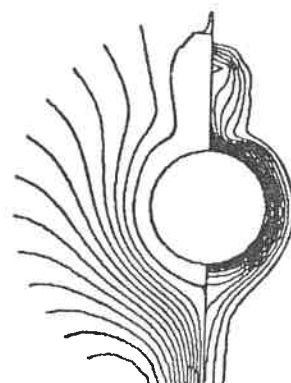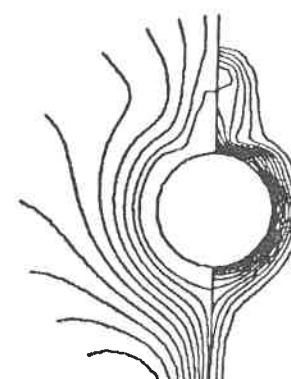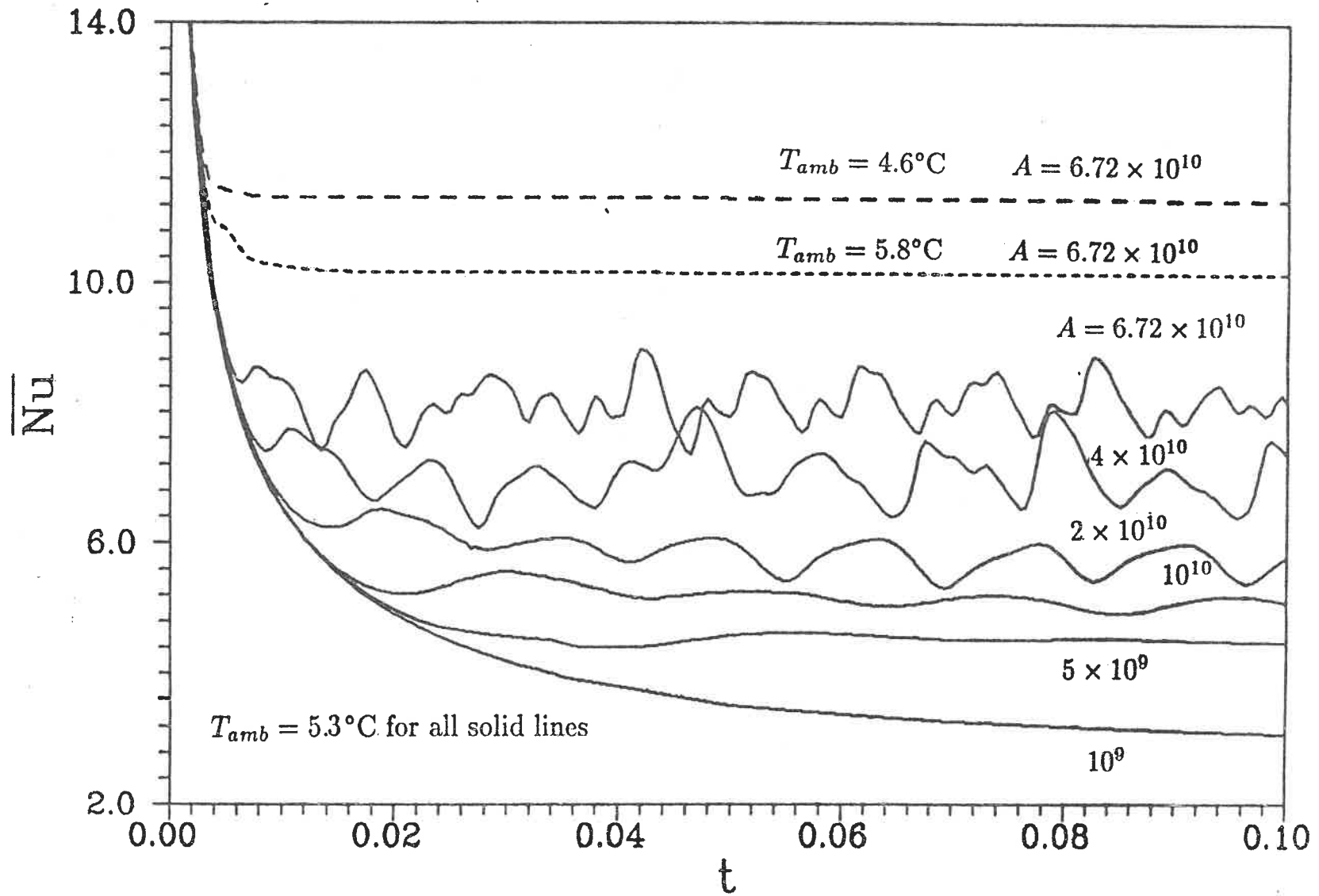
(16)   (17)   (18)   (19)   (20)

Fig. 6. (CONTINUED)

Fig. 7. Time histories of $\overline{\mathrm{Nu}}$ for $T_{amb} = 5.3°\mathrm{C}$ at different values of A and $\mathrm{Pr} = 11.6$

The figure shows curves labeled:
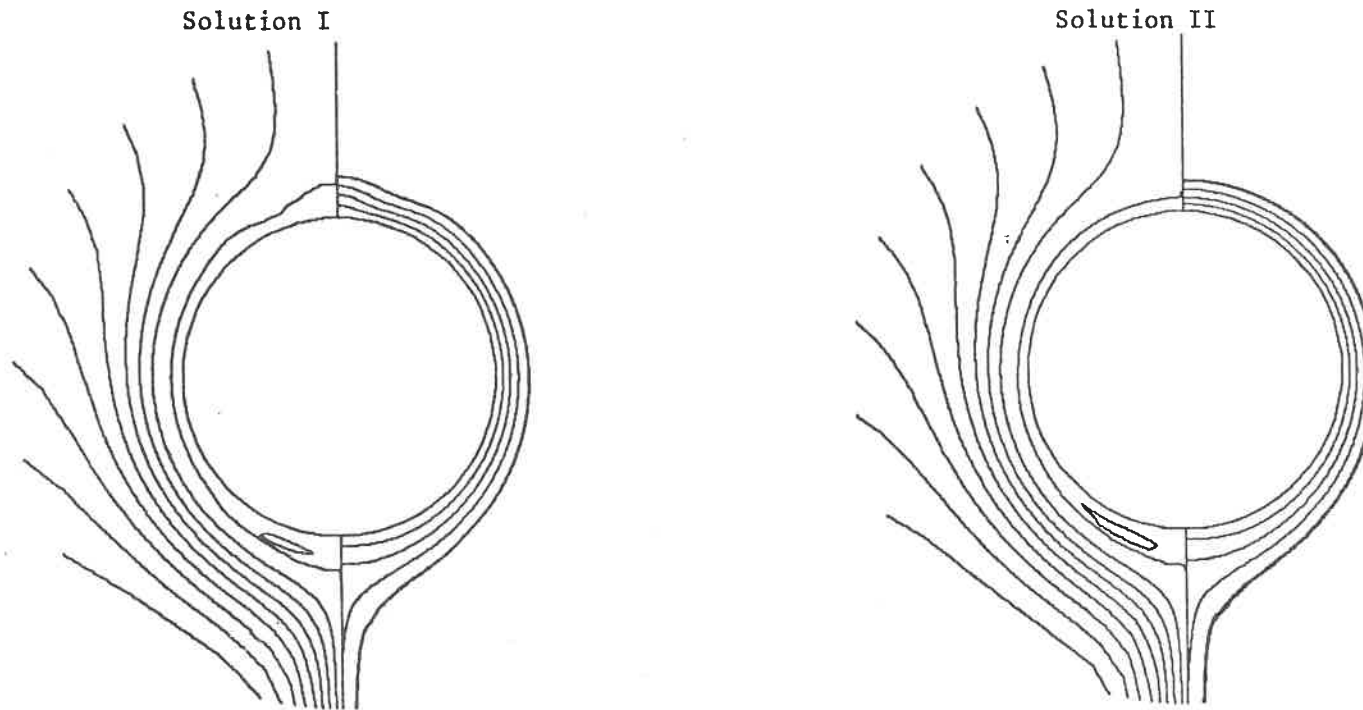
$T_{amb} = 4.6°\mathrm{C}$ $\qquad A = 6.72 \times 10^{10}$

$T_{amb} = 5.8°\mathrm{C}$ $\qquad A = 6.72 \times 10^{10}$

$A = 6.72 \times 10^{10}$

4×10^{10}

2×10^{10}

10^{10}

5×10^{9}

10^{9}

$T_{amb} = 5.3°\mathrm{C}$ for all solid lines

Tamb = 5,6°C

A = 6,72 X 10^{10}

Solution I

Solution II

Fig. 8. Two different solutions for a $Pr = 11.6$ and $A = 6.72 \times 10^{10}$ at $T_{amb} = 5.6°C$:

(a) Steady-state isotherms and streamlines; ($\Delta\Psi = 15$ and $\Delta T = 0.2$)

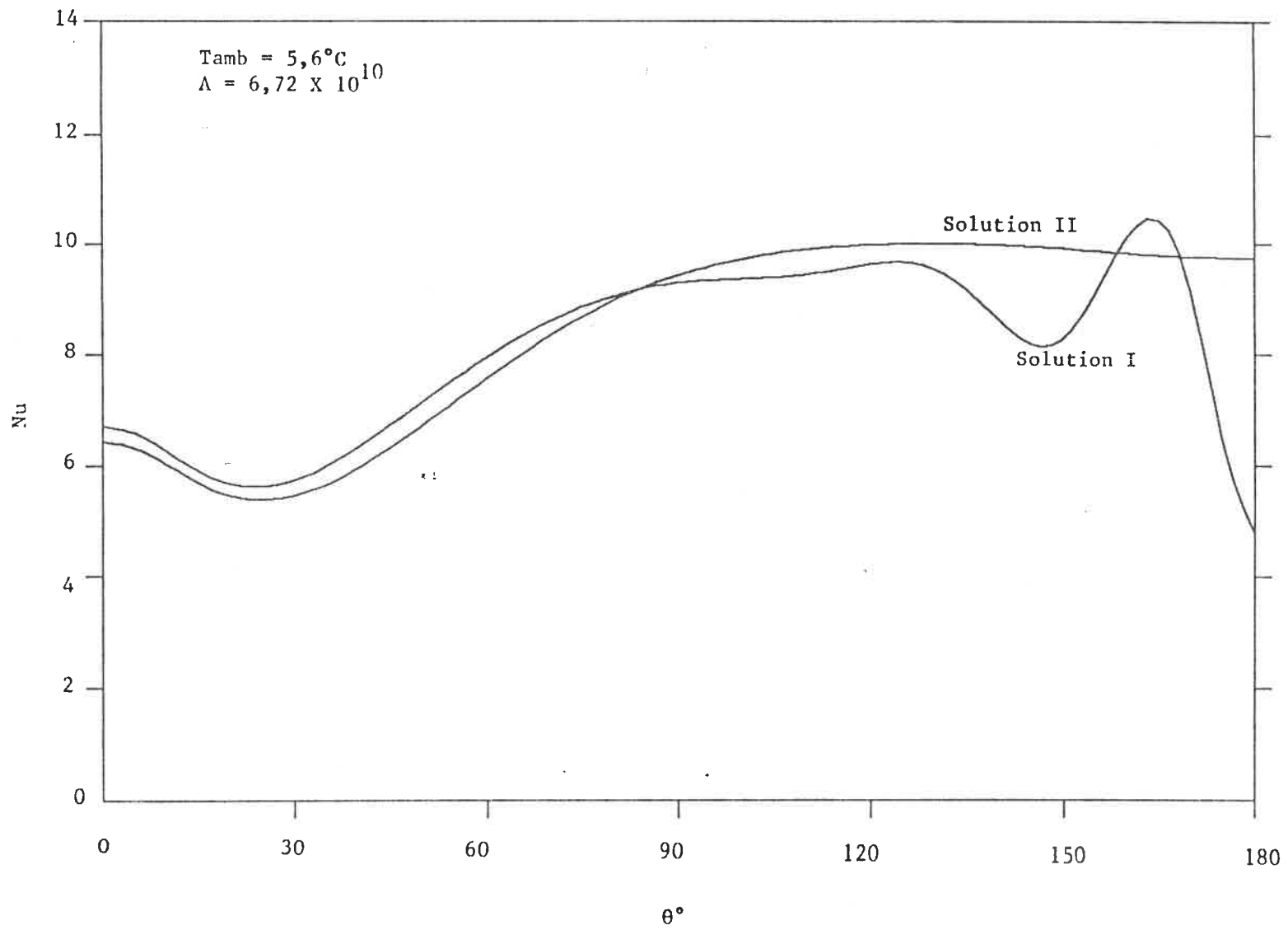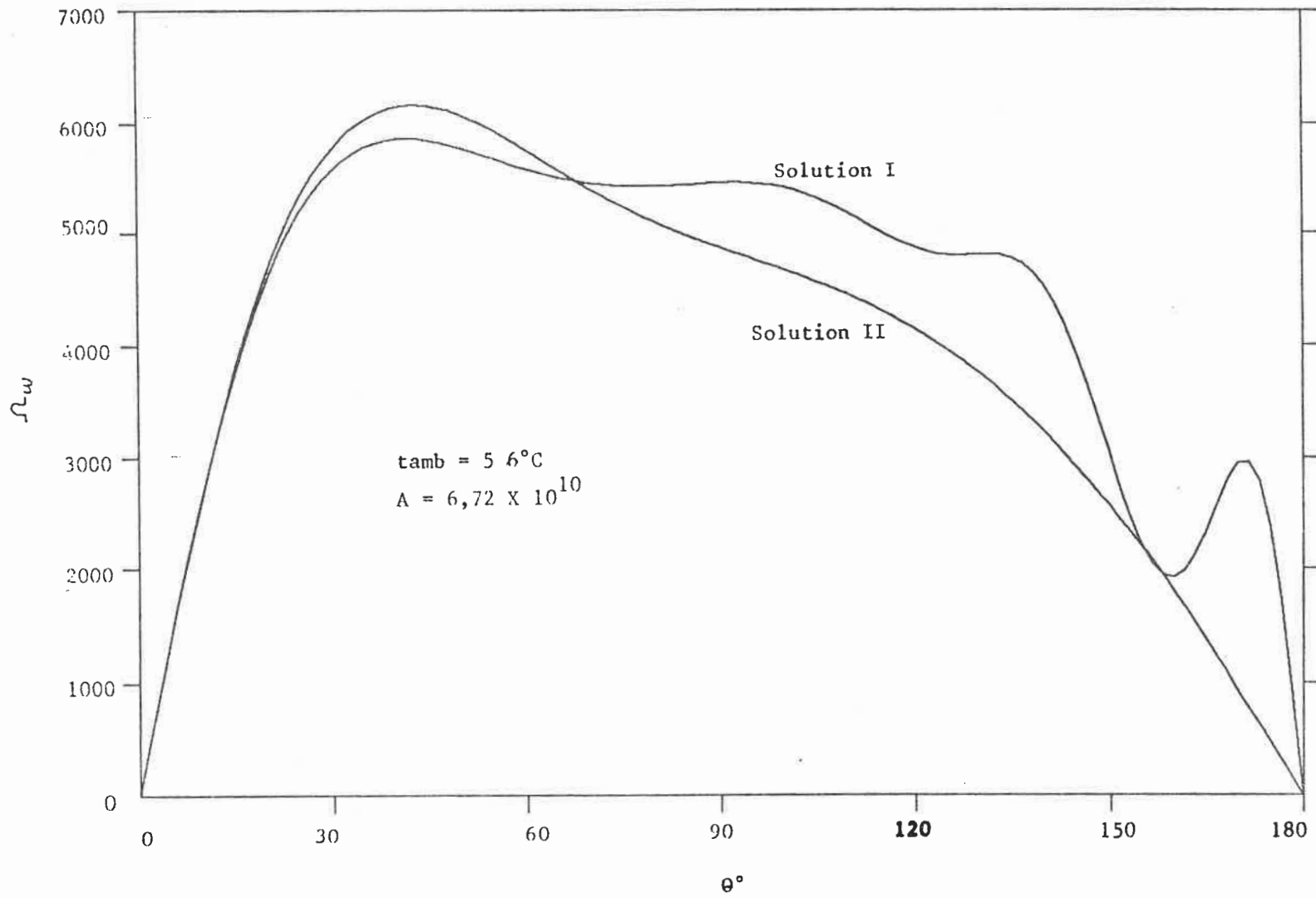Fig. 8. (b) Steady-state distribution of local Nusselt numbers

Fig. 8. (c) Steady-state surface vorticity distribution

Tamb = 4,75°C
A = 6,72 X 10^10

Solution I   Solution II
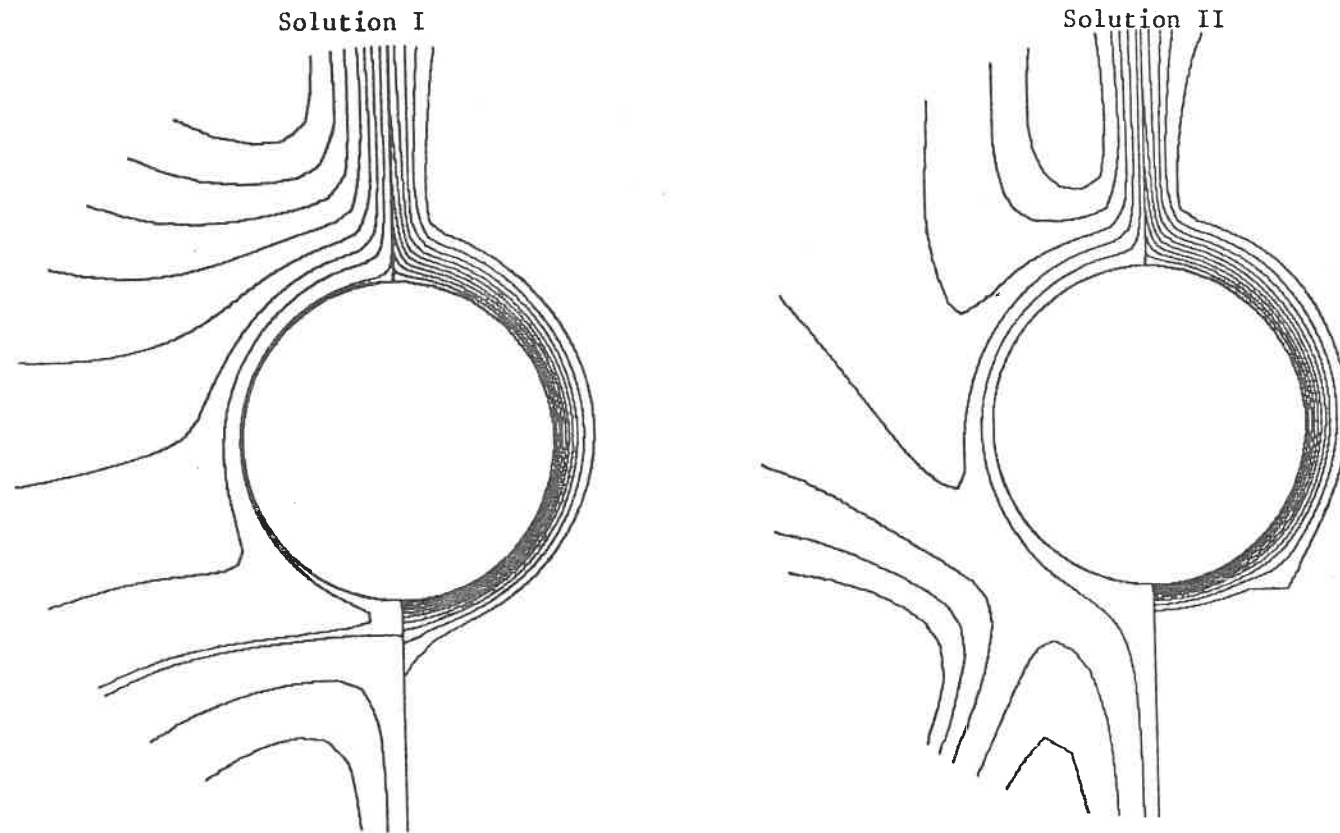
Fig. 9. Two different solutions for a $Pr = 12.4$ and $A = 6.72 \times 10^{10}$ at $T_{amb} = 4.75°C$:

(a) Steady-state isotherms and streamlines; ($\Delta\Psi = 10$ and $\Delta T = 0.1$)
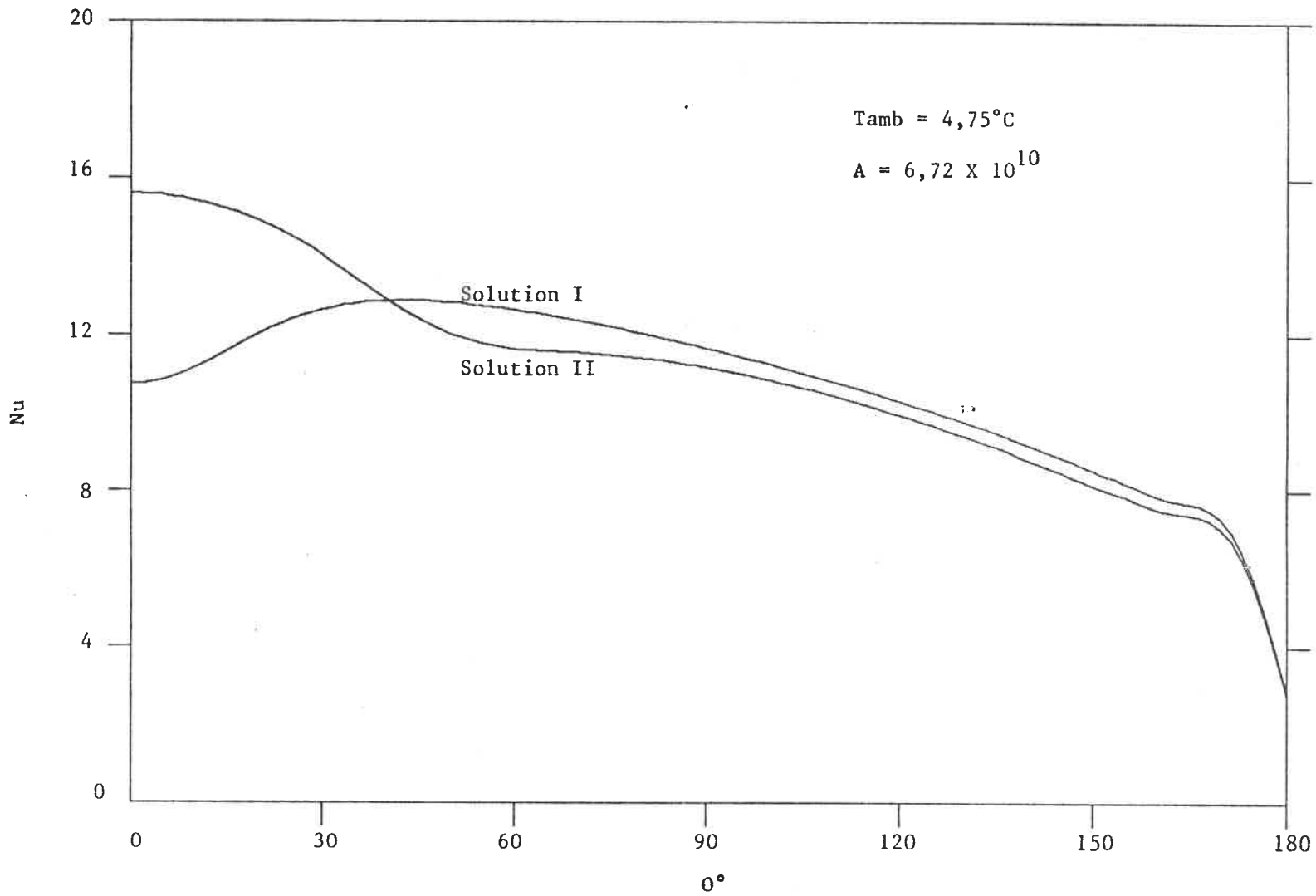
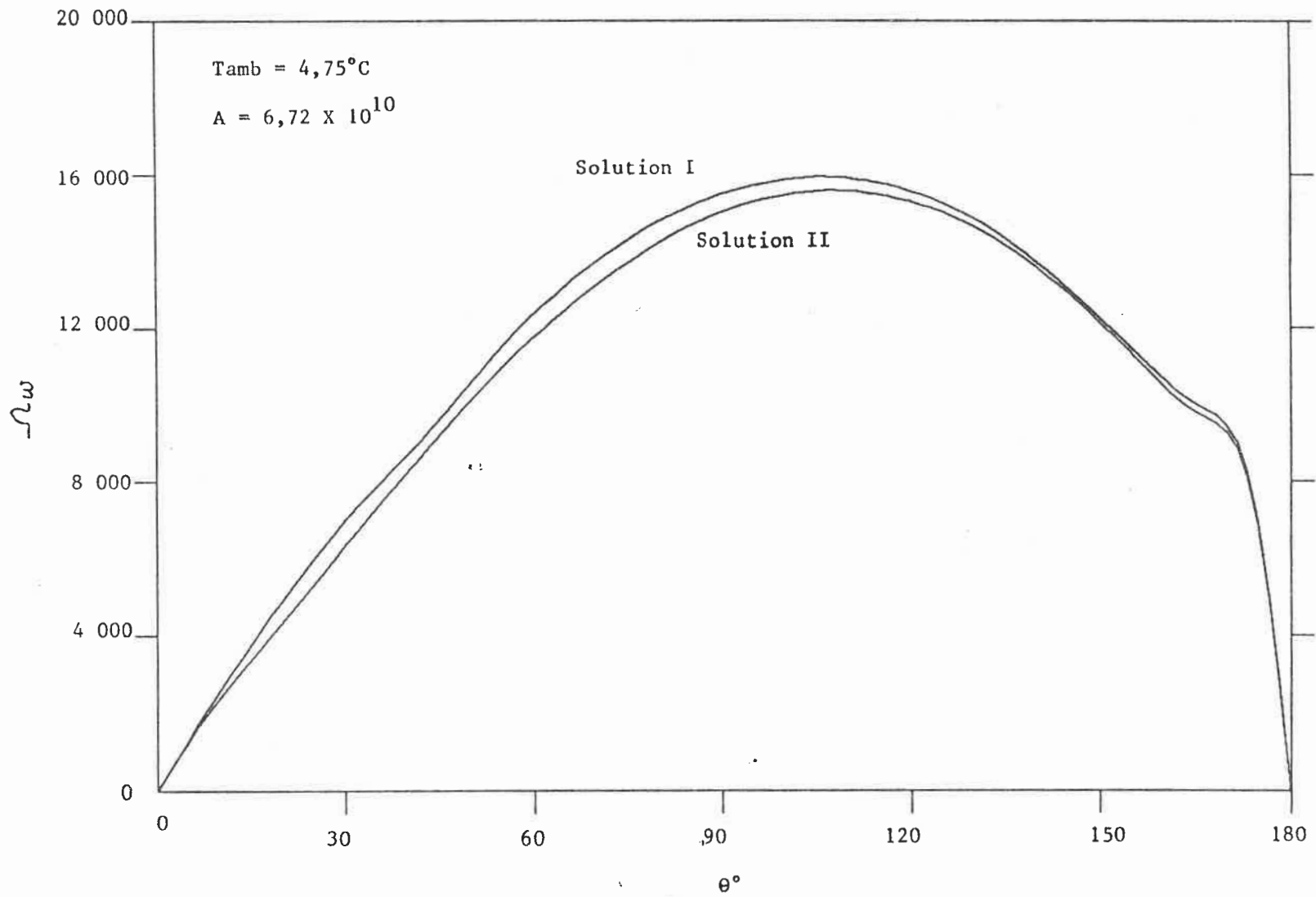Fig. 9. (b) Steady-state distribution of local Nusselt numbers

Fig. 9. (c) Steady-state surface vorticity distribution.

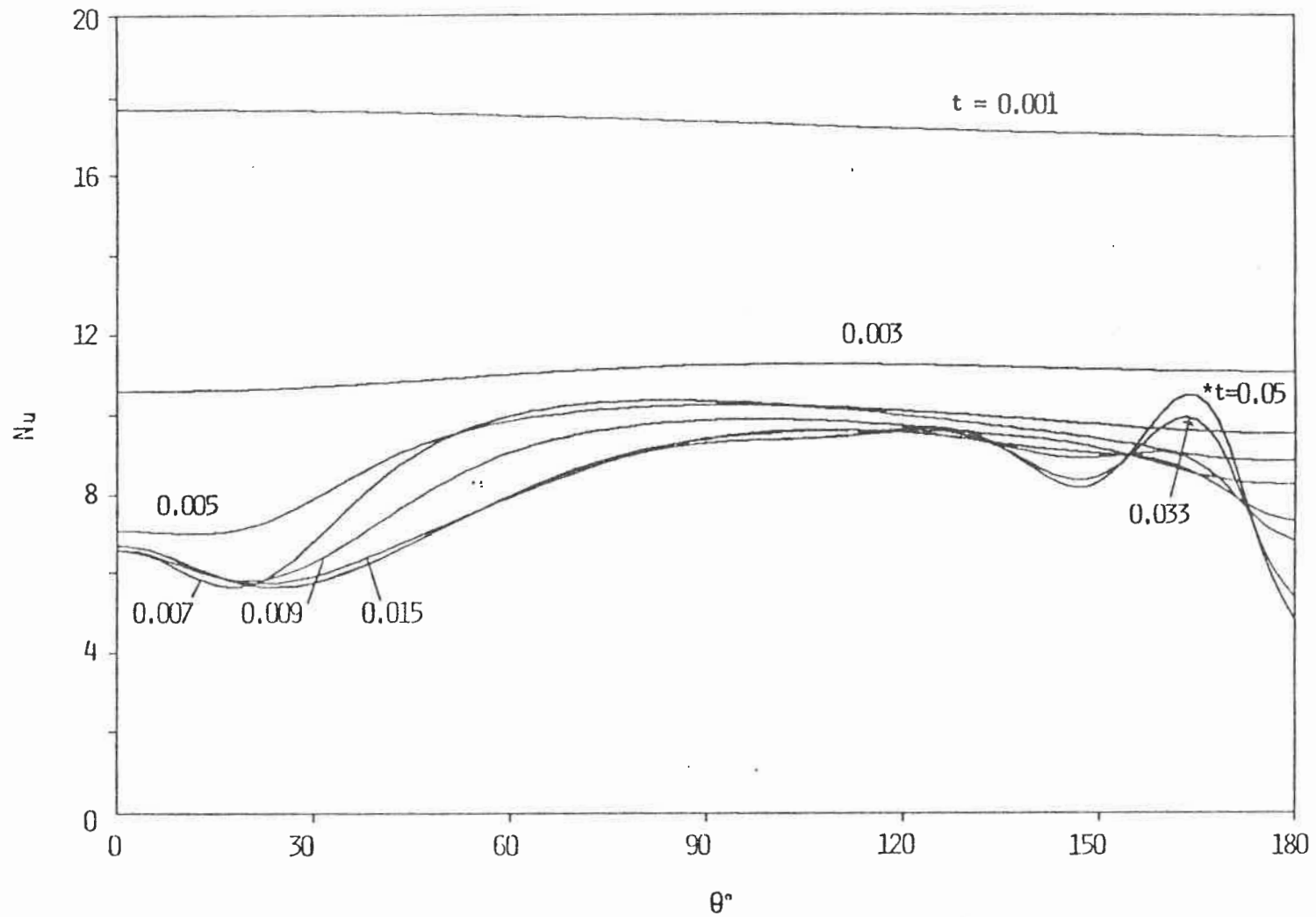Fig. 10. Time-varying distribution of local Nusselt numbers for a Pr = 11.6 and
$A = 6.72 \times 10^{10}$ at $T_{amb} = 5.6°C$
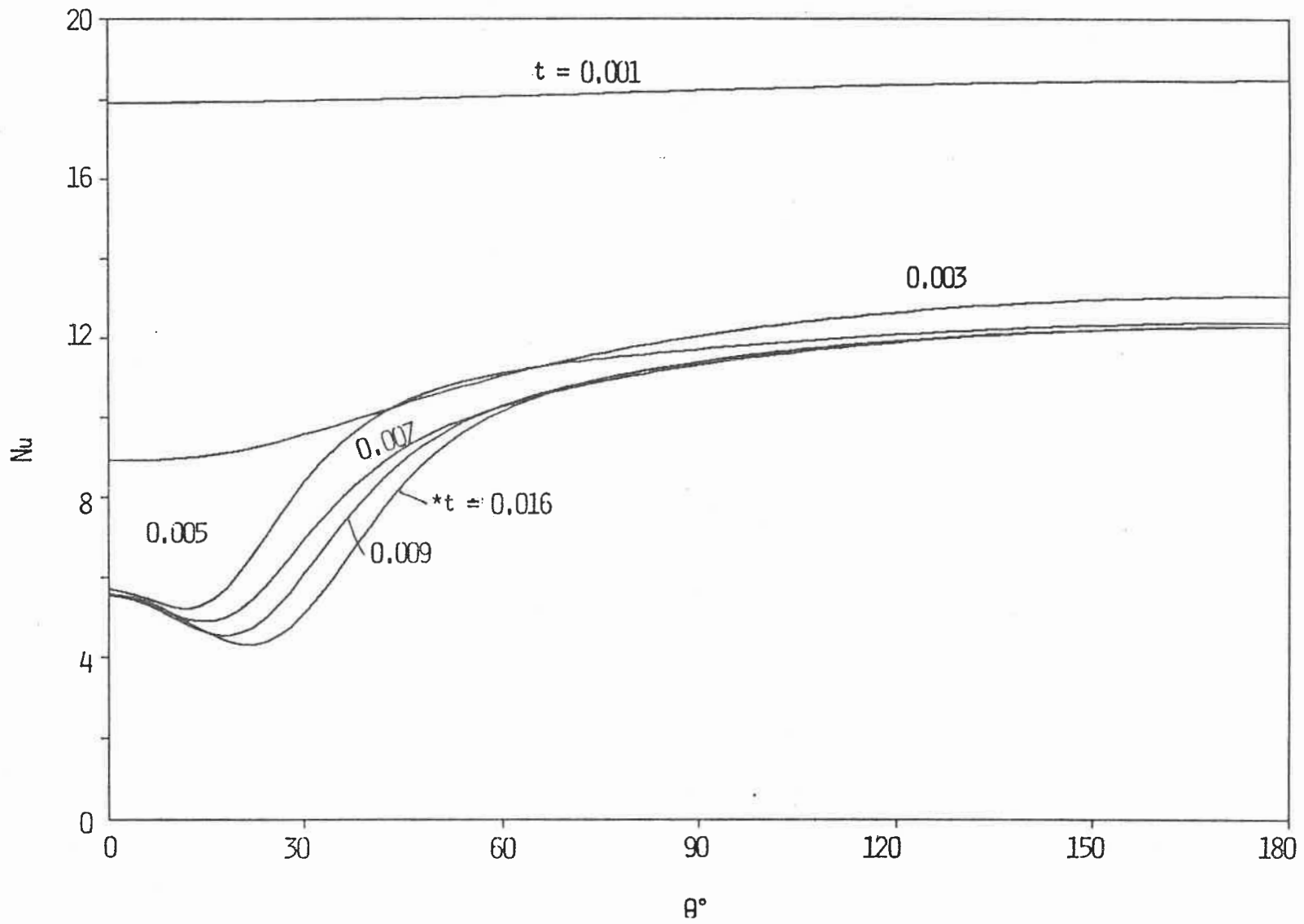
Fig. 11. Time-varying distribution of local Nusselt numbers for a $Pr = 11.6$
and $A = 6.72 \times 10^{10}$ at $T_{amb} = 5.8°C$
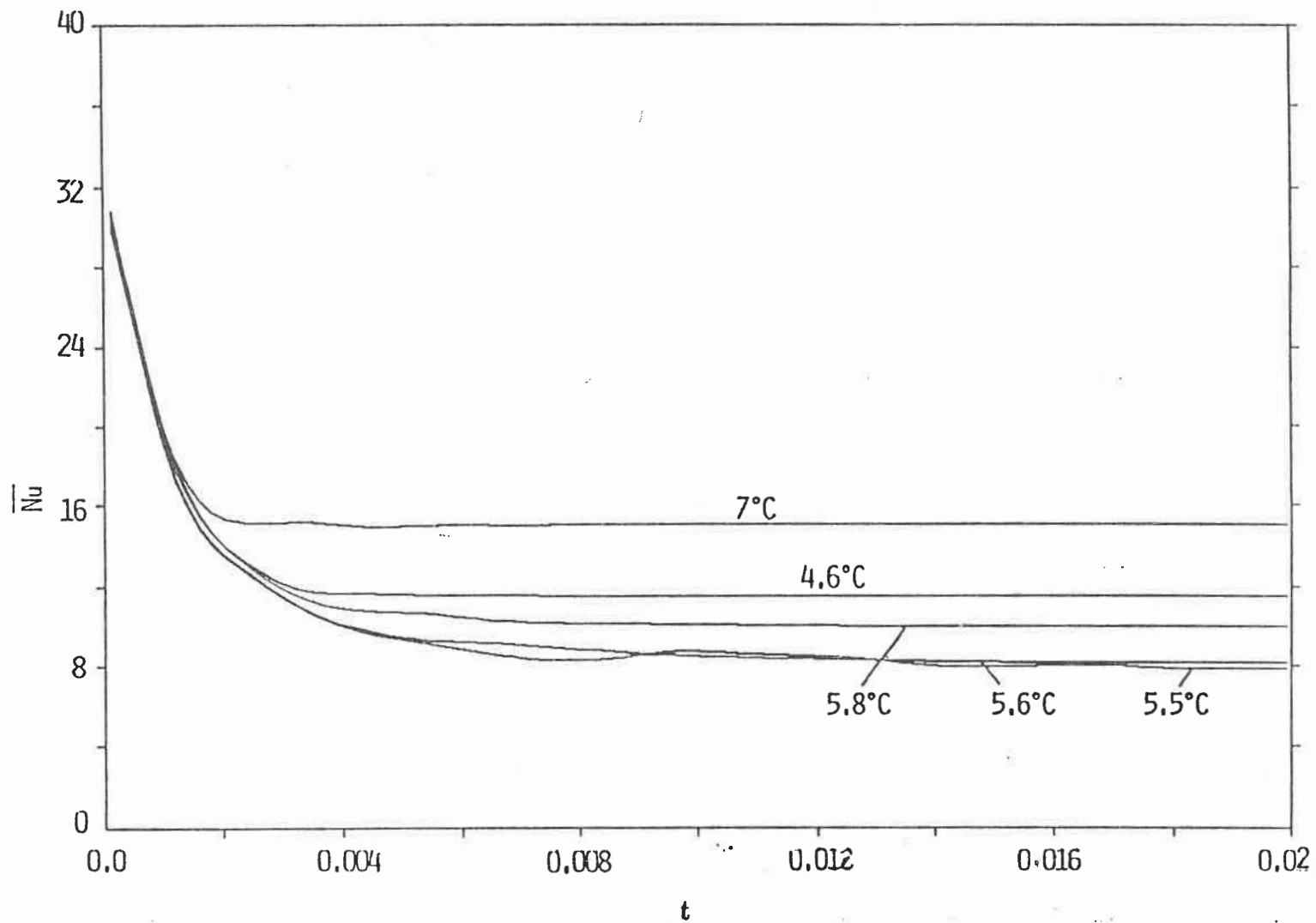
Fig. 12. Time histories of $\overline{Nu}$ for various T_{amb} at $A = 6.72 \times 10^{10}$ and $Pr = 11.6$

Fig. 13. Comparison between numerically computed and experimentally measured average Nusselt numbers for different T_{amb}

Fig. 14. Time-varying surface vorticity distribution for a Pr = 11.6 and
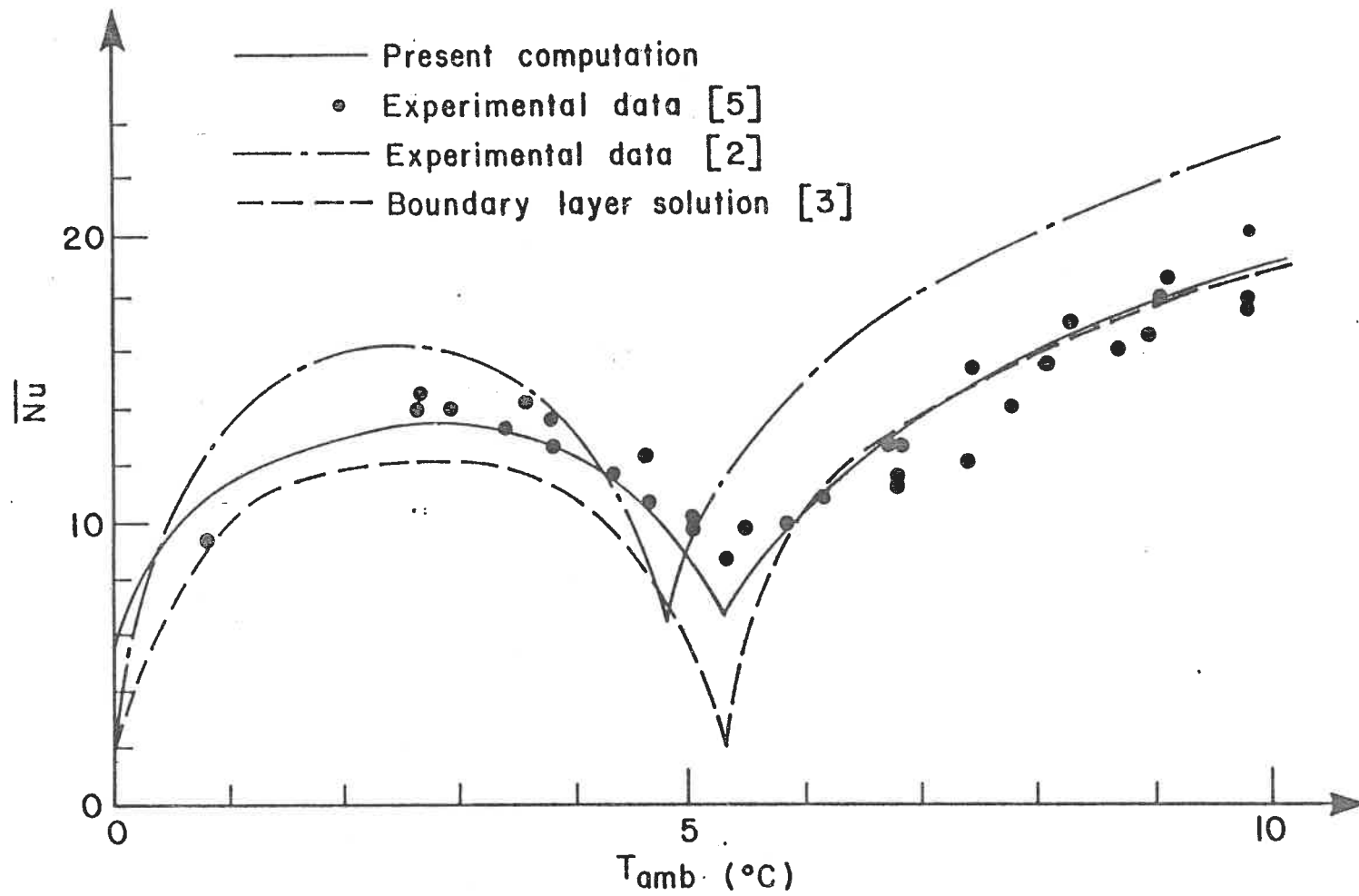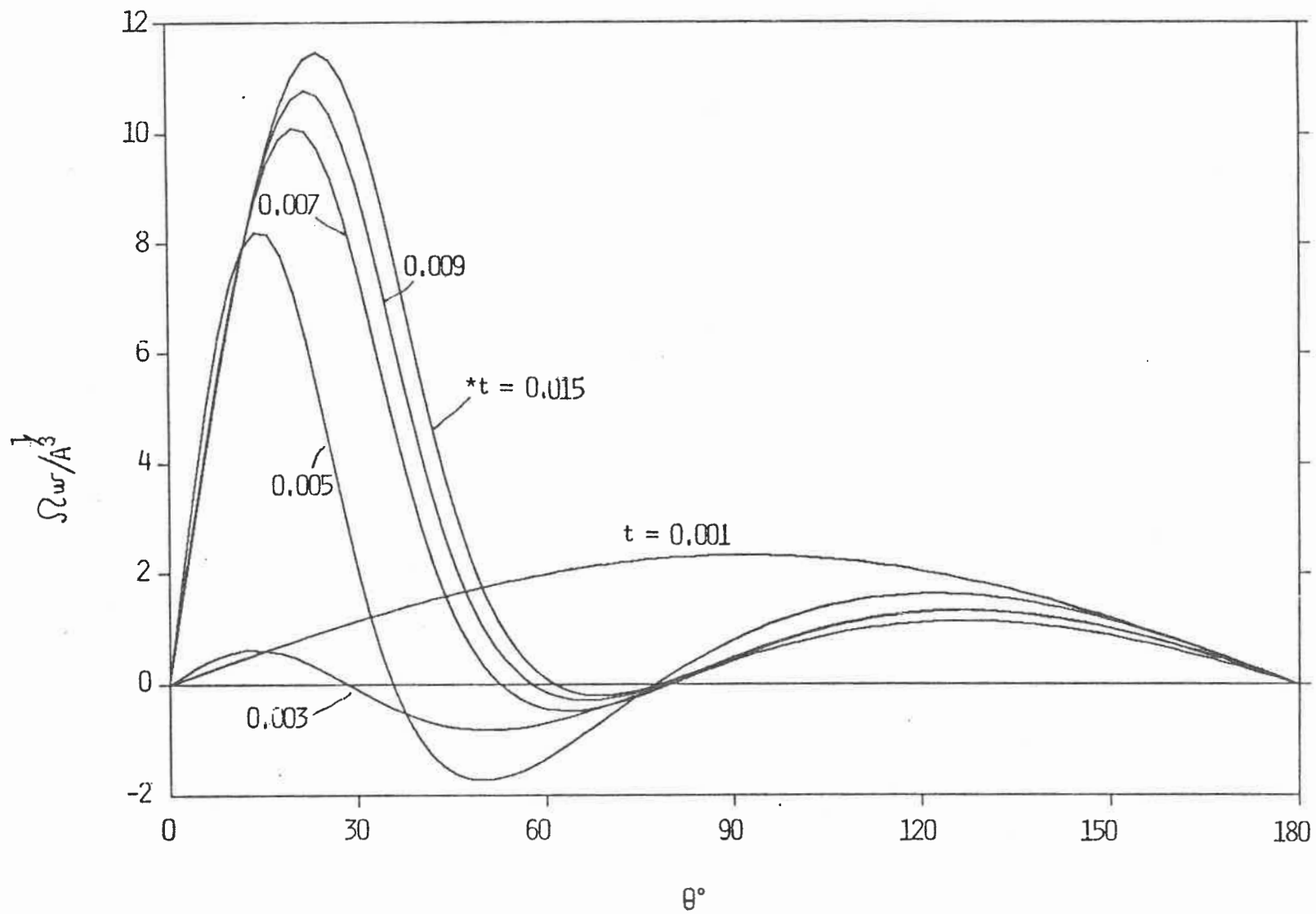$A = 6.72 \times 10^{10}$ at $T_{amb} = 5.8°C$

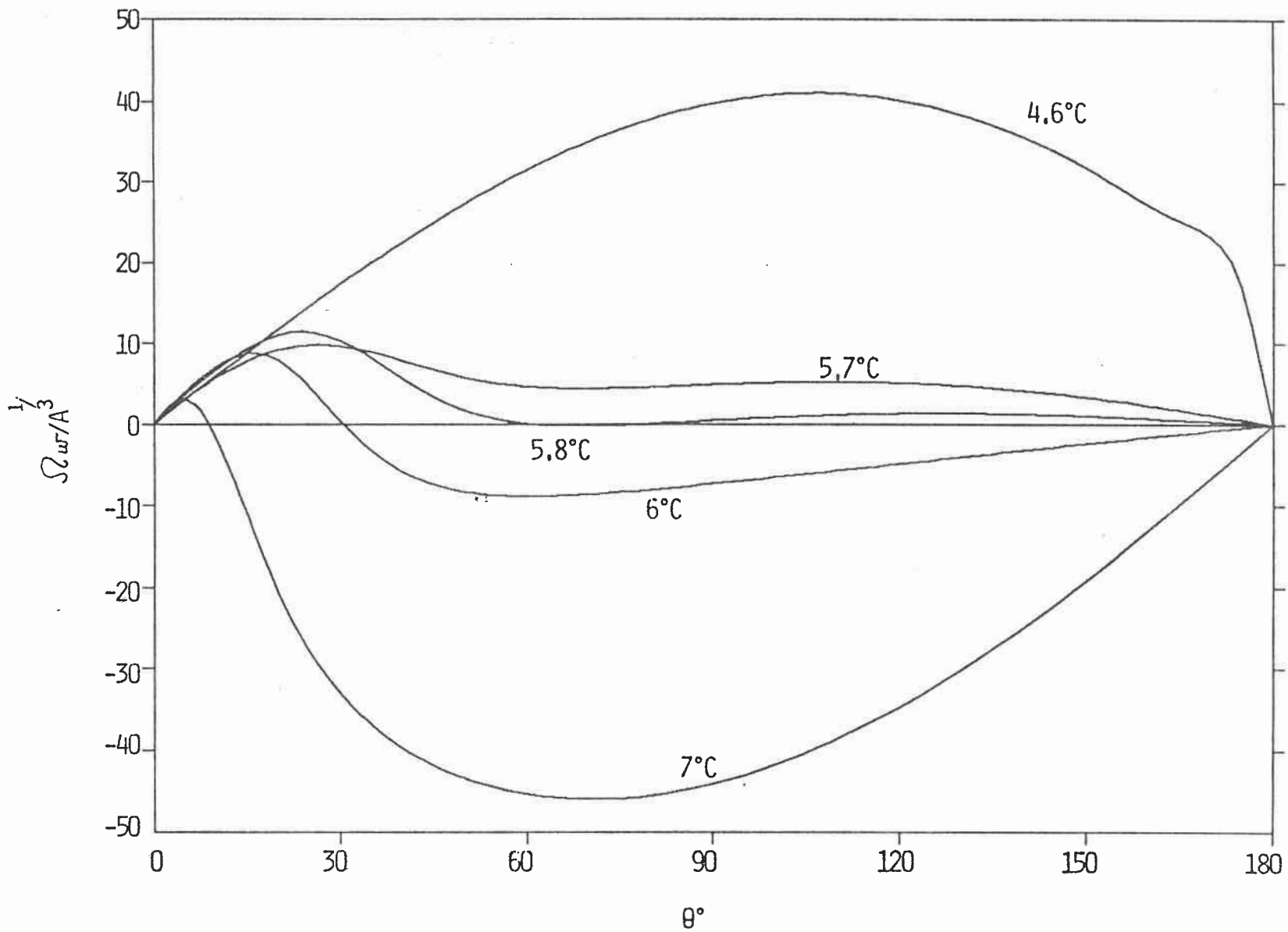Fig. 15. Steady-state surface vorticity distribution for different T_{amb} at
$A = 6.72 \times 10^{10}$ and $\mathrm{Pr} = 11.6$

CONCLUDING REMARKS

The numerical studies of the laminar natural convection flow around a heated (or cooled) horizontal cylinder under diverse surface boundary conditions using a spline fractional step technique have been presented in this thesis. From the results reported , some conclusions may be reached as follows:

Numerical solutions have been obtained by solving the Navier-Stokes and energy equations. For a heated cylinder under steady state conditions, the results for the isothermal boundary condition as well as for the uniform heat flux have general been in good agreement with published experimental data and with other solutions presently available in the literature. Some new computations at very high Rayleigh numbers, have indicated the existence of attached "separation" vortices in the downstream plume region, the appearance of these vortices being dependent on the values of the Biot number. The numerical results also indicate that for $Bi > 500$ the surface temperature variation becomes less than 5% and the mixed and isothermal boundary conditions become equivalent. When $Ra^* * \geq 2 \times 10^7$ and $Bi > 500$, separation vortices in the plume region close to the cylinder surface appear. Detailed computations have led to the conclusion that they originate from the physics of the flow.

The unsteady natural convection from a circular, horizontal cylinder has been presented in Chapter III. Some characteristics of the boundary layer obtained

with a scale analysis have been compared with the numerical results. At small times, the present numerical solutions approach the boundary layer results and are in good agreement with the results from the scale analysis. The development of the plume region as well as the surface heat transfer and local flowfield have been evaluated. Good agreement with published experimental and numerical data has been obtained. Overshoot and oscillatory behaviour of the local Nusselt numbers have been observed which decay as the steady state is approached. This has been associated with fluid inertia effects. At high Rayleigh numbers, the appearance of separation vortices, which are subsequently formed, shed and reformed when $Ra > 5 \times 10^7$, has been noted.

Finally, the transient natural convection from a horizontal cylinder in water at a temperature near the maximum density point has been studied numerically. Good agreement with published experimental and numerical data has been obtained. The appearance of a dual flow region has been documented and studied. The presence of oscillatory solutions when the physical parameters lie within a certain range of values has been reported The minimum Nusselt number at about 5.3°C has been verified numerically. A more detailed investigation into the behaviour of the solutions in the range of $4.8°C < T_{amb} < 5.5°C$ has been undertaken in order to obtain more information on the solution behaviour in this critical region. Quasi-periodic solutions as well as solutions displaying sudden catastrophic instability after a long period of quiescent behaviour have been encountered. Additional computations using double(64 bit) precision and a non-reflecting boundary condition resulted in stable solutions, indicating that the instability was probably of numerical origin. In the range of

$5.56°C \leq T_{amb} \leq 5.63°C$ and close to $T_{amb} = 4.75°C$, multiple solutions were found. The study has served to underline the importance of using correctly posed infinite boundary conditions as well as high precision in the computations when treating natural convection flows with reversing buoyancy.

The numerical scheme presented here appears to be versatile and efficient so that a large range of problems may be computed. Since the spline approximation has high accuracy both for uniform as well as non-uniform grid spacing, significant savings in storage as well as computer time may be achieved so that most of the results presented in this thesis were computed on a personal computer using unequally spaced grids. The applications of this method presented in this thesis, indicate not only that the numerical results obtained are acceptable, but also that the technique is of sufficient flexibility to permit application to a wide variety of engineerring problems.

The intrinsic structure of the spline formulation offers the possibility of directly incorporating boundary conditions containing derivatives into the solution procedure, the discretised accuracy at the boundary points is then the same as for the governing equation. A general formulation to treat mixed boundary conditions using the spline approximation has been presented in Chapter II. This general formulation considerably simplifies the treatement of boundary conditions while computational accuracy is maintained. The time dependent "characteristic based" boundary condition:

$$\frac{\partial T}{\partial t} + u\frac{\partial T}{\partial r} = 0.$$

has been easily incorporated into the numerical procedure by discretizing it in the general form. This boundary condition avoides the temperature oscillations observed when the leading surface of the plume traverses the artificially imposed outer boundary.

REFERENCES

Abarbanel, S.S., Don, W.S., Gottieb, D., Rudy, D.H. and Townsend, J.C. 1991 *Secondary frequencies in the wake of a circular cylinder with vortex shedding, J. Fluid Mech.*, Vol. 225, pp.557–574.

Ahlberg, J.H., Nilson, E.N. and Walsh, J.L. 1967 *The theory of Splines and Their Applications*, Academic Press.

Aihara, T. and Saito, E. 1972 *Measurement of Free Convection Velocity Field around the Periphery of a Horizontal Torus, J. Heat Transfer*, Vol. 94, pp.95–98.

Akagi, S. 1965 *Effect of Curvature on Free Convection Around a Horizontal Cylinder, Trans. JSME*, Vol. 31, pp.1327–1335.

Bendell, M.S. and Gebhart, B. 1976 *"Heat Transfer and Ice-Melting in Ambient Water near Its Density Extremum,"*,Int. *J. Heat Mass Transfer*, Vol. 19, pp.1081–1087.

Carey, V.P., Gebhart, B. and Mollendorf, J.C. 1980 *"Buoyancy Force Reversals in Vertical Natural Convection Flows in Water,"*, *J. Fluid Mech.*, Vol. 97, pp.279–297.

Chen, C.S. 1989 *Solution Approximating Solute Transport in a Leaky Aquifer Receiving Wastewater Injection, Water Recources Research*, Vol. 25, pp.61–72.

Cheng, K.C. and Takeuchi, M. 1976 *Transient Natural Convection of Water in a Horizontal Cylinder with Constant Cooling rate through 4°C*, J. Heat Transfer, Vol. 98, pp.581–587.

Cheng, K.C. and Takeuchi, M. 1978 *Transient Natural Convection in a Horizontal Water Pipe with Maximum Density Effect and Supercooling*, Numerical Heat Transfer, Vol. 1, pp.101–115.

Chiang, T. and Kaye, J. 1962 *On Laminar Free Convection from a Horizontal Cylinder*, Proc. 4th Natl. Cong. Appl. Mech., pp.1213–1219.

Chiang, T., Ossin, A. and Tien, C.L. 1964 *Laminar Free Convection from a Sphere*, J. Heat Transfer, Vol. 86, pp.537–542.

Churchill, S.W. 1974 *Laminar Free Convection from a Horizontal Cylinder with a Uniform Heat Flux Density*, Lett. Heat Mass Transfer, Vol. 1, pp.109–112.

Churchill, S.W. and Chu, H.S. 1975 *Correlating Equation for Laminar and Turbulent Free Convection from a Horizontal Cylinder*, Int. J. Heat Mass Transfer, Vol. 18, pp.1049–1053.

Davenport, L.F. and King, C.J. 1974 *The Onset of Natural Convection from Time-Dependent Profile*, Int. J. Heat Mass Transfer, Vol. 17, pp.69–76.

deBoor, C. and Lynch, R.E. 1966 *On splines and their minimum properties*, J. Math. Mech., Vol .15, pp.953–969.

Desai, V.S. and Forbes, R.E. 1971 *Free Convection in Water in the Vicinity of Maximum Density*, ASME Trans. Environmental and Geophysical Heat Transfer, pp.41–47.

Dumoré, J.M., Merk, H.J. and Prins, J.A.   1953 *Heat Transfer from Water to Ice by Thermal Convection*, Nature, Vol. 172, pp.460–461.

Ede, A.J.   1951 *Heat Transfer by Natural Convection in Refrigerated Liquid*, Proceeding of the 8th International Congress of Refrigeration, London, pp.260.

El-Hennawy, I., Gebhart, B. and Kazarinoff, N.D.   1986 *Multiple Steady-State Solutions for Horizontal Buoyant flows in Cold Water*, Int. J. Heat Mass Transfer, Vol. 29, pp.1655–1667.

El-Hennawy, I., Hassard, B. Kazarinoff, N., Gebhart, B. and Mollendorf, J   1982 *Numerically computed multiple steady states of vertical buoyancy-induced flows in cold pure water* , J. Fluid Mech., Vol. 122, pp.235-250.

Elliott, L.   1970 *Free Convection on a Two-Dimensional or Axisymmetric Body*, Quart. J. Mech. and Math. Vol. 23, pp.153–162.

Evans, L.B. and Stefany, N.E.   1965 *An Experimental study of transient Heat Transfer to Liquids in Cylindrical Enclosures*, AIChE Preprint No.4, Eighth National Heat Transfer Conference, Los Angeles, Calif., pp.209–215.

Fand, R.M., Morris, E.W. and Lum, M.   1977 *Natural Convection Heat Transfer from Horizontal Circular Cylinder to Air, Water and Silicone Oils for Rayleigh Number between $3 times 10^2$ and 2×10^7*, Int. J. Heat Mass Transfer, Vol. 20, pp.1173–1184.

Farouk, B. and Guceri, S.I.   1981 *Natural Convection from a Horizontal Cylinder - Laminar Regime*, J. Heat Transfer , Vol. 103, pp.522–527.

Foster, T.D.   1965 *Onset of Convection in a layer of Fluid cooled from above*, *Physics of Fluids*, Vol. 8, pp.1770–1774.

Foster, T.D.   1968 *Effect of Boundary Conditions on the Onset of Convection*, *Physics of Fluids*, Vol. 11, pp.1257–1262.

Foster, T.D.   1969 *Onset of Manifest Convection in a Layer of Fluid with a Time Dependent Surface Temperature*, *Physics of Fluids*, Vol. 12, pp.2482–2487.

Fujii, T.   1974 *Fundamentals of Free Convection Heat Transfer*, Progress in Heat Transfer Engineering, Vol. 3, pp. 66–67.

Fujii, T., Fujii, M. and Matsunaga, T.   1979 *A Numerical Analysis of Laminar Free Convection Around an Isothermal Cylinder*, Numerical Heat Transfer, Vol. 2, pp.329–344.

Gebhart, B. and Mollendorf, J.   1977 *A New Density Relation for Pure and Saline Water*, *Deep-Sea Research*, Vol. 124, pp.831–848.

Gebhart, B. and J.C. Mollendorf, J.C.   1978 *"Buoyancy-Induced Flows in Water under Conditions in Which Density Extremum May Arise,"*, J. Fluid Mech., Vol. 89, pp.673–707.

Genceli, O.F.   1980 *The Onset of Manifest Convection from Suddenly Heated Horizontal Cylinders*, Warme-und Stoffubertragung. Vol. 13, pp.163–169.

Genceli, O.F. and Onat, K. 1974 *The Onset of Natural Convection in a Horizontal Air Layer Heated from Below*, Warme-und Stoffubertragung Vol. 7, pp.248–256.

Gilpin, R.R. 1975 *Cooling of a Horizontal Cylinder of Water Through its Maximum Density Point at* 4°C, Int. J. Heat and Mass Transfer, Vol. 18, pp.1307–1315.

Givoli, D. 1991 *Non-reflcting Boundary Conditions*, J. Comput. Phys., Vol. 94, pp.1–29.

Gupta, A.S. and Pop, I. 1977 *Effects of Curvature on unsteady Free Convection past a Circular Cylinder*, The Physics of Fluids Vol. 20, pp.162–163.

He, G. and Wang, P. 1987 *Solution of Partial Differential Equations with Spline 4*, Journal of Lanzhou University (in Chinese), Vol. 23, No.1, pp.17–24.

Hermman, R. 1954 *Heat Transfer by Free Convection from Horizontal Cylinders in Diatomic Gases*, NACA TM 1366.

Ho, C.J. and Chen, S. 1986 *Numerical Simulation of Melting of Ice around a Horizontal Cylinder*, Int. J. Heat and Mass Transfer, Vol. 29, pp.1369–1386.

Holladay, J.C. 1957 *Smoothest curve approximation*, Math. Tables Aids Computation, Vol. 17, pp.233–243.

Holster, J.L. and Hale, L.A. 1979 *Finit Element Simulation of Transient Free Convection from a Horizontal Cylinder*, ASME Paper No.79-TH-49.

Hung, C.I., Chen, C.K. and Cheng, P. 1989 *Transient Conjugate Natural Convection Heat Transfer along a Vertical Plate Fin in a High-Porosity Medium*, Numerical Heat Transfer, Vol. 15, pp.133–148.

Jain, M.K. and Tariq Aziz 1981 *Spline Function Approximation for Differential Equations*, Comput. Meths. Appl. Mech. Engrg., Vol. 26, pp.129–143.

Katagiri, M. et al. 1979 *Transient Free Convection from an Isothermal Horizontal Circular Cylinder*, Warme-und Stoffubertragung, Vol. 12, pp.73–81.

Kuehn, T.H 1976 *Natural Convection Heat Transfer from a Horizontal Circular Cylinder to a Surrounding Cylindrical Enclosure Ph.D. thesis, University of Minnesota.*

Kuehn, T.H. and Goldstein, R.J. 1980 *Numerical Solution to the Navier-Stokes Equations for Laminar Natural Convection about a horizontal isothermal circular cylinder*, Int. J. Heat Mass Transfer Vol. 23, pp.971–979.

Lauriat, G. and Altimir, I. 1985 *A New Formulation of the SADI Method for the Prediction of Natural Convection Flows in Cavities*, Computers and Fluids, Vol. 13, pp.141–155.

Levy, S. 1955 *Integral Methods in Natural convection Flow*, J. Appl. Mech., Vol. 22, pp.515–522.

Lin, F.N. and Chao, B.T. 1974 *Laminar Free Convection over Two-Dimensional and Axisymmetric Bodies of Arbitrary Contour*, J. Heat Transfer, Vol. 96, pp.435–442.

Lin, S., Wang, P. and Kahawita, R. 1983 *The Cubic Spline Numerical Solution of the Ablation Problem*, AIAA Paper 83–1556.

Lin, S., Wang, P. and Kahawita, R.   1984 *Cubic Spline Numerical Solution of an Ablation Problem with Convective Backface Cooling*, AIAA Journal, Vol. 22, pp.1176–1177.

Mark, H.J. and Prins, J.A.   1953-1954 *Thermal Convection in Laminar Boundary Layers,I,II and III*, Appl. Sci. Res., Vol. 4A, pp.11–24, pp.195–224.

Merk, H.J.   1954 *The Influence of Melting and Anomalous Expansion on the Thermal Convection in Laminar Boundary Layers*, Applied Science Research, Vol. 4, pp.435–452.

Merkin, J.H.   1976 *Free Convection Boundary Layers on an Isothermal Horizontal Cylinders*, ASME Paper No.76-HT-16.

Merkin, J.H.   1977 *Free Convection Boundary Layers on Cylinders of Elliptic Cross Section*, J. Heat Transfer, Vol. 99, pp.453–457.

Morgan, V.T.   1975 *The Overall Convective Heat Transfer from Smooth Circular Cylinders*, Adv. in Heat Transfer, Vol. 11, pp.199–264.

Mucoglu, A. and Chen, T.S.   1977 *Analysis Combined Forced and Free Convection Across a Horizontal Cylinder*, The Can. J. Chem. Engrg., Vol. 5, pp.265–279.

Nakai, S. and Okazaki, T.   1975 *Heat Transfer from a Horizontal Cylinder Wire at Small Reynolds and Grashof Numbers Pts.I and II*, Int. J. Heat Mass Transfer, Vol. 18, pp.387–413.

Nguyen, T.H. , Vasseur, P. and Robillard, L.   1982 *Natural Convection Between Horizontal Concentric Cylinders With Density Inversion of Water for Low Rayleigh Numbers, Int. J. Heat and Mass Transfer*, Vol. 25, pp. 1559–1568.

Nielsen, R.C. and Sabersky, R.H.   1973 *Transient Heat Transfer in Benard Convection, Int. J. Heat Mass Transfer*, Vol. 16, pp.2407–2420.

Ostrach, S. 1953 *An Analysis of Laminar Free Convection flow and Heat Transfer about a Flat Plate Parallel to the Direction of Generating Body Force, NACA TR 1111.*

Ostroumov, G.A.   1965 *Unsteady Heat Convection Near a Horizontal Cylinder, Soviet Technical Physics*, Vol. 1 pp. 2627–2641.

Paramicheal, N. and Whiteman, J.R.   1973 *A Cubic Spline Technique for the One Dimensional Heat Conduction Equation, J. Inst. Math. Applic.*, Vol. 9, pp.111–113.

Parsons, J.R. and Mulligan, J.C.   1978 *Transient Free Convection from a Suddenly Heated Horizontal Wire, Journal of Heat Transfer*, Vol. 100, pp.423–428.

Pera, L. and Gebhart, B.   1971 *On the Stability of Laminar Plumes: Some Numerical Solutions and Experiments, Int. J. Heat Mass Transfer*, Vol. 14, pp.975–984.

Peterka, J.A. and Richarson, P.D.   1969 *Natural Convection from a Horizontal Cylinder at Moderate Grashof Numbers, Int. J. Heat Mass Transfer* Vol. 12, pp.749–752.

Qureshi, Z.H. and Ahmad, R.   1987 *Natural Convection from a Uniform Heat Flux Horizontal Cylinder at Moderate Rayleigh Numbers*, Numerical Heat Transfer, Vol. 11, pp. 199–212.

Rubin, S.G. and Graves, R.A.   1975 *Viscous Flow Solutions with a Cubic Spline Approximation*, Computers and Fluids, Vol. 3 pp.1–36.

Rubin, S.G. and Khosla, P.K.   1976 *Higher Order Numerical Solutions using Cubic Splines*, AIAA Journal, Vol. 14, pp.851–859.

Rubin, S.G. and Khosla, P.K.   1977 *Polynomial Interpolation Methods for Viscous Flow Calculations*, J. Comput. Phys., Vol. 24, pp.217–244.

Saitoh, T.   1976 *Natural Convection Heat Transfer from a Horizontal Ice Cylinder*, Applied Scientific Research, Vol. 32, pp. 429–451.

Saitoh, T. and Hirose, K.   1980 *Thermal Instability of Natural Convection flow over a Horizontal Ice Cylinder Encompassing a Maximum Density Point*, Journal of Heat Transfer, Vol. 102, pp. 261–267.

Sako, M., Chiba, T., Garza, J.M.S. and Yanagida, A.   1982 *Numerical Solution of Transient Natural Convective Heat Transfer from a Horizontal Cylinder*, Japanese Heat Transfer, pp.27–44.

Saville, D.A. and Churchill, S.W.   1967 *Laminar Free Convection in Boundary Layers near horizontal cylinders and vertical axisymmetric bodies*, J. Fluid Mech., Vol. 29, pp. 391–399.

Schechter, R.S. and Isbin, H.S. 1958 *Natural-convection Heat Transfer in Regions of Maximum Fluid Density,A.E.Ch.E Journal*, Vol. 4, pp. 81–89.

Schenk, J. and Schenkels, F.A.M.   1968 *Thermal Free Convection from an Ice Sphere in Water, Applied Science Research*, Vol. 19, pp. 465–476.

Schoenbeng, I.J.   1946 *Spline interpolation and the higher derivatives, Natl. Acad. Sci. U.S.*, Vol. 51, pp.24–28.

Schorr, A.W. and Gebhart, B.   1970 *An Experimental Investigation of Natural Convection Wakes above a line Heat Source, Int. J. Heat Mass Transfer*, Vol. 13, pp.557–571.

Seki, N., Fukusako, S. and Nakoaka, M.   1975 *Experimental Study on Natural Convection Heat Transfer With Density Inversion of Water Between Two Horizontal Concentric Cylinders, Journal of Heat Transfer*, Vol. 97, pp. 556–561.

Shaw, H.J., Chen, C.K. and Cleaver, J.W.   1987 *Cubic Spline Numerical Solution for Two-Dimensional Natural Convection in a Partially Divided Enclosure, Numerical Heat Transfer*, Vol. 12, pp. 439–455.

Shaw, H.J. and Chen, C.K.   1988 *Natural Convection in a Partitioned Enclosure Heated from Below*, Warme-und Stoffubertragung, Vol. 22, pp. 303–308.

Shee, Y.T. and Singh, S.N.   1982 *Natural Convection from a Horizontal Cylinder at Small Grashof Number*, Numerical Heat Transfer, Vol. 5, pp.479–492.

Song, Y.W.   1989 *Numerical Solution of Transient Natural Convection Around a Horizontal Wire, J. Heat Transfer*, Vol. 111, pp. 574–576.

Takeuchi, M. and Cheng, K.C.   1976 *Transient Natural Convection in Horizontal Cylinders with Constant Cooling rate*, Warme-und Stoffubertragung, Vol. 9, pp. 215–225.

Vanier, C.R. and Tien, C.   1968 *Effect of Maximum Density and Melting on Natural Convection Heat Transfer from a Vertical Plate*, Chem. Engng Prog. Symp. Ser., Vol. 82, pp. 240–255.

Vasseur, P. and Robillard, L.   1980 *Transient Natural Convection Heat Transfer in a Mass of Water Cooled Through* 4°C, International Journal of Heat and Mass Transfer, Vol. 23, pp. 1195–1205.

Vasseur, P., Robillard, L. and Chandra Shekar, B.   1983 *Natural Convection heat Transfer of Water Within a Horizontal Cylindrical Annulus With Density Effects*, Journal of Heat Transfer, Vol. 105, pp. 117–123.

Vest, C.M. and Lawson, M.L.   1972 *Onset of Convection Near a Suddenly Heated Horizontal Wire*, International Journal of Heat and Mass transfer 15, 1281–1283.

Van Der Hegge Zijnen, B.G.   1956 *Modified Correlation Formulae for the Heat Transfer by Natural and by forced Convection from Horizontal Cylinders*, Appl. Sci. Res., Vol. A6, pp.129–140.

Walsh, J.I., Ahlberg, J.H. and Nilson, E.N.   1962 Best approximation of spline fit, *J. Math. Mech.*, Vol. 11, pp.225–234.

Wang, P.   1985a *Numerical Dispersive and Dissipative Effects for Cubic Spline Approximation*, Proceedings of the IASTED International Symposium MODELLING AND SIMULATION, June 24-26, Lugano, Switzerland, pp.5–8.

Wang, P.   1985b *Spline-Lax-Wendroff Scheme and Spline-Leap-Frog Scheme* , Acta Aerodynamica Sinica, (in Chinese), Vol. 3, No.3, pp. 90–95.

Wang, P.   1986 *Variable Time Step Methods using Cubic Splines for the One-Dimensional Stefan Problem with Mixed Boundary Conditions, 1984 Proc. of Chinese National Conference on Heat and Mass Transfer,*(in Chinese), Science Press, pp.38–43.

Wang, P.   1987a *Spline Method of Fractional Steps in Numerical Model of Unsteady Natural Convection Flow at High Rayleigh Number*, Numerical Heat transfer,Vol. 11, pp.95–118.

Wang, P.   1987b *The Method of Fractional Steps for Solving Navier-Stokes Equations using Parametric Splines*, Acta Aerodynamica Sinica, (in Chinese), Vol. 5, No.3, pp.218–225.

Wang, P.   1987c *Spline Simulations of Unsteady Natural Convection Flows in a Square Cavity at Ra=10 with Method of fractional Steps*, Acta Mechanica Sinica, (in Chinese), Vol. 23, No.Supplement, pp.79–86.

Wang, P. and Kahawita, R.   1983a *Numerical Integration of Partial Differential Equations using Cubic Splines*, Int. J. Computer Math., Vol. 13, pp. 271–286.

Wang, P. and Kahawita, R.   1983b *A Two-Dimensional Numerical Model of Estuarine Circulation using Cubic Splines*, Can. J. Civil Eng., Vol. 10, pp. 116–124.

Wang, P. and Kahawita, R. 1983c *Cubic Spline Techniques in Numerical Models of Estuarine Circulation*, Acta Aerodynamica Sinica, (in Chinese), Vol. 1, No.3, pp.17–29.

Wang, P. and Kahawita, R. 1983d *The Numerical Solution of the Natural Convection Flow in a Square Cavity, Proc. of 4th International Conference on Mathematical Modelling in Science and Technology*, Aug. 24-26, Zurich, pp.640–645.

Wang, P. and Kahawita, R. 1984 *The Numerical Solution of Burgers Equation using Splines*, Acta Aerogynamica Sinica, (in Chinese) Vol. 2, No.2, pp.11–18.

Wang, P. and Kahawita, R. 1987 *The Numerical Solution of the Unsteady Natural Convection flow in a Square Cavity at High Rayleigh Number using the SADI Method*, Applied Mathematics and Mechanics, Vol. 8, pp. 219–228.

Wang, P. and Kahawita, R. 1988 *Viscous Flow Solution with a Parametric Spline Method*, International Conference on Computational Methods in Flow Analysis (ICCMFA) , September 2–7, Japon.

Wang, P. and Kahawita, R. 1990 *Hydrodynamic Modelling of Estuarine Circulation using Spline Method of Fractional Steps*, Int. J. Sediment Research, Vol. 5, No.1, pp.67–81.

Wang, P., Kahawita, R. and Nguyen, T.H. 1990 *Numerical Computation of the Natural Convection Flow about a Horizontal Cylinder using Splines*, Numerical Heat Transfer Vol. 17, Part A, pp.191–215.

Wang, P., Kahawita, R. and Nguyen, D.L. 1991 *Transient Laminar Natural Convection from Horizontal Cylinder, Int. J. Heat and Mass Transfer*, Vol. 34, pp.1429–1442.

Wang, P., Kahawita, R. and Nguyen, D.L. 1991 *Transient Natural Convection with Density Inversion from a Horizontal Cylinder*, (to be published in *Physics of Fluids* **A**).

Wang, P., Lin, S. and Kahawita, R. 1985 *The Cubic Spline Integration technique for Solving Fusion Welding Problems, J.* Heat Transfer, Vol. 107, pp.485–489.

Watson, A. 1972 *The Effect of the Inversion Temperature on the Convection of Water in an Enclosed Rectangular Cavity*, Quarterly Journal of Mechanics and Applied Mathematics, Vol. 25, pp. 423–446.

Wilks, G. 1972 *External Natural Convection about Two-Dimensional Bodies with Constant Heat Flux, Int. J.* Heat Mass Transfer, Vol. 15, pp. 351–354.

Wilson, N.W. and Lee, J.J. 1981 *Melting of a vertical Ice Wall by Free Convection with Fresh Water, J.* Heat Transfer, Vol. 103, pp. 13–18.
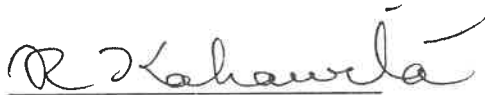
Wilson, N.W. and Vyas, B.D. 1979 Velocity Profiles near a Vertical Ice Surface Melting into fresh Water, *J.* Heat Transfer, Vo;. 101, pp. 313–317.

Yao, L.S. and Chen, F.F. 1980 *Effects of Natural Convection in the Melted Region Around a Heated Horizontal Circular Cylinder, J.* Heat Transfer, Vol. 102, pp.667–672.
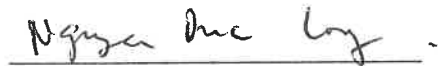
APPENDIX

À qui de droit,

Nous certifions que le travail contenu dans la Thèse de Doctorat de M. Pu Wang intitulée "Numerical Solution of Thermo-Convective Problems using Spline Integration" représente sa propre recherche scientifique.

René Kahawita, Ph.D.

Duc Long Nguyen, Ph.D.

T. Hung Nguyen, Ph.D.

ÉCOLE POLYTECHNIQUE

ÉCOLE D'INGÉNIEURS FONDÉE EN 1873
AFFILIÉE À L'UNIVERSITÉ DE MONTRÉAL

Campus de l'Université de Montréal
Case postale 6079 succursale "A"
Montréal, Québec   H3C 3A7

July 25th, 1983

A T T E S T A T I O N

Mr. Wang Pu visiting scholar from the University of Lanzhou, Lanzhou, Peoples Republic of China has submitted to us a report entitled:

> "Numerical Solution of Second Order Partial
> Differential Equations using a Cubic Spline
> Approximation".

This report summarises his research at the Ecole Polytechnique de Montreal during the years 1981 to 1983. We have examined this report and have attended it's formal presentation by Mr. Wang Pu. We consider his work to be of such high standing as to easily exceed the research requirements for a Doctoral Thesis from our Institution.

Since Mr. Wang Pu was not registered as a student at the Ecole Polytechnique it is unfortunately not possible for him to be officially awarded the Ph.D. degree. We certify however, that during his stay here he has surpassed all the required academic standards for the Ph.D.

Signed:

R. Camarero, Ph.D.   (Professor of Applied Mathematics)

P. Vasseur, Ph.D.   (Professor of Civil Engineering)

R. Kahawita, Ph.D.   (Professor of Civil Engineering)

Dr. Ing. S. Lin   (Professor of Mechanical Engineering, Concordia University - Montreal, Canada).

ECOLE POLYTECHNIQUE

ÉCOLE D'INGÉNIEURS FONDÉE EN 1873
AFFILIÉE À L'UNIVERSITÉ DE MONTRÉAL

Campus de l'Université de Montréal
Case postale 6079, succursale "A"
Montréal, Québec   H3C 3A7

August 8th, 1983

TO WHOM IT MAY CONCERN :

Subject: Mr. Wang Pu visiting scholar at
        Ecole Polytechnique

Gentlemen:

From 1981 to 1983 we had the pleasure of welcoming
Mr. Wang Pu at Ecole Polytechnique in our Civil Engineering
Department. He has conducted research work in the following
subject:
        "Numerical Solution of Second Order Partial
        Differential Equations using a Cubic Spline
        Approximation".

He has published many technical papers on the subject with
Professor René Kahawita of the Ecole Polytechnique. Here are
the titles of three of them :

        "A Two-Dimensional Model of Estuarine Circulation
        using Cubic Splines".
        Canadian Journ. of Civil Eng.

        "Numerical Integration of Partial Differential Equations
        using Cubic Splines".
        Int. Journal of Computer Mathematics.

        "The Cubic Spline Integration Technique for Solving
        Fusion Welding Problems".
        Journal of Heat Transfer.

There is no doubt in our mind that the qualifications
of this person are excellent. It is unfortunate that Mr. Wang Pu
was not able to register as a Ph.D. student in our School when he
arrived in 1981, for he would certainly have obtained his degree.

.../2

ÉCOLE POLYTECHNIQUE

August 8th, 1983
page 2

	We would be pleased if Mr. Wang Pu could come back again
in our School and if then he decided to register in one of our
graduate programs we would facilitate the procedures for him.

	It is with pleasure that I recommend Mr. Wang Pu to your
attention because he is a competent person and because I am
convinced that he will succeed very well in his teaching career.

Director of Studies

Maurice Poupard

MP/tdl
c.c.: Mr. Jacques Cléroux
        Chairman of Civil
        Engineering Department

encl.: Attestation from:
        R. Camarero, Ph.D.
        P. Vasseur, Ph.D.
        R. Kahawita, Ph.D.
        S. Lin, Dr.Ing.